Investigating the Role of Sirtuin 1 in the Pulmonary Vascular Response to Chronic Hypoxia-Induced Pulmonary Hypertension

Mohamad Taha

This thesis is submitted as a partial fulfillment of the Ph.D. program in

Cellular & Molecular Medicine

Submitted on: February 12, 2018

Department of Cellular & Molecular Medicine

Faculty of Medicine

University of Ottawa

Ottawa, ON, Canada

ABSTRACT:

Background: Pulmonary arterial hypertension (PAH) is a devastating disease characterized by increased pulmonary artery pressure, leading to right ventricle hypertrophy and ultimately heart failure and death. Sirtuin 1 (SIRT1) is an NAD^+ dependent protein deacetylase that has been strongly implicated as a crucial link between longevity, stress response and maintenance of vascular health. In this thesis, we investigated the role of SIRT1 in the pulmonary vascular hypoxic response and the pathogenesis of pulmonary hypertension (PH) working under the hypothesis that SIRT1 plays a protective role in the pulmonary vasculature and that lack of SIRT1 would lead to worsening of PH in a model of chronic hypoxia (CH).

Results: We determined that global SIRT1 knockout or SIRT1 catalytic inactivation resulted in a marked increase in right ventricle pressure and remodeling compared to wildtype mice in CH. Furthermore, hypoxia-induced erythrocytosis and pulmonary vascular remodeling were profoundly increased in both SIRT1 mouse lines. Subsequent molecular assessment revealed that SIRT1 knockout, but not inactivation, led to a significant increase in mRNA levels of hypoxia inducible factor (HIF)-1α and significantly higher activity in hypoxia, leading to elevated lactate dehydrogenase A (LDHA) and BCL2/adenovirus E1B 19 kDa protein-interacting protein 3 (BNIP3) in the lungs. Interestingly, both knockout and inactivation of SIRT1 enhanced the activity of HIF2α in the hypoxic lungs and kidneys, leading to increased erythropoietin (EPO) and plasminogen activator inhibitor-1 (PAI-1). Moreover, SIRT1 knockout or inactivation was associated with a trend towards hypoxic-independent increases in HIF3α mRNA in the lungs. Prevention of glycolytic shift using dichloroacetate (DCA) did not result in

improvement in this model, yet resveratrol (RSV), a SIRT1 activator/mimic, partially prevented PH only in absence of SIRT1 activity. Finally, selective endothelial cell SIRT1 deletion was sufficient to cause worse PH in the CH model.

Conclusions: SIRT1 plays a protective role in the hypoxic response through transcriptional and non-transcriptional control of the hypoxia inducible factors, thus protecting against worse hypoxia-induced PH. SIRT1 could be a novel target for future therapies in PAH.

TABLE OF CONTENTS

LIST OF TABLES

LIST OF FIGURES

LIST OF APPENDICES

LIST OF ABBREVIATIONS

ANOVA	analysis of variance
APAH	associated pulmonary arterial hypertension
b-HLH	basic helix-loop-helix domain
BMP	bone morphogenetic protein
BMPR2	bone morphogenetic protein receptor type II
cAMP	cyclic adenosine monophosphate
CCB	calcium channel blockers
cGMP	cyclic guanosine monophosphate
CH	chronic hypoxia
CH+MCT	chronic hypoxia plus monocrotaline
CO	cardiac output
C-TAD	C-terminus transactivation domain
DCA	dichloroacetate
EC	endothelial cell
eNOS	endothelial nitric oxide synthase
EPAS1	endothelial PAS domain containing protein 1
EPO	erythropoietin
ET-1	endothelin-1
ETA	endothelin receptor A
ETB	endothelin receptor B
FIH	factor inhibiting HIF
FMA	fluorescent microangiography

HAPH	high altitude pulmonary hypertension
HAT	histone acetyltransferase
HCT	hematocrit
HDAC	histone deacetylase
HIF	hypoxia inducible factor
HPAH	hereditable Pulmonary Arterial Hypertension
HPV	hypoxic pulmonary vasoconstriction
HRE	hypoxia responsive element
IL	interleukin
IPAH	idiopathic pulmonary arterial hypertension
IRE	iron responsive element
LV	left ventricle
LV+S	left ventricle + septum
MCT	monocrotaline
mmHg	millimeters of mercury
mPAP	mean pulmonary arterial pressure
NO	nitric oxide
N-TAD	N-terminus transactivation domain
ODD	oxygen degradation domain
PAEC	pulmonary artery endothelial cell
PAH	pulmonary arterial hypertension
PAP	pulmonary arterial pressure
PAS	PER-ARNT-SIM

PASMC	pulmonary artery smooth muscle cell
PGI_2	prostacyclin
PH	pulmonary hypertension
PHD	prolyl-4-hydroxylase
PO_2	partial pressure of oxygen
PVR	pulmonary vascular resistance
RSV	resveratrol
RV	right ventricle
RV/(LV+S)	weight ratio of right ventricle to left ventricle plus septum
RVH	right ventricular hypertrophy
RVSP	right ventricular systolic pressure
SIRT1	Sirtuin 1 (protein)
SMA	smooth muscle actin
SMC	smooth muscle cell
SU	SU5416
SU5416	3-(3,5-dimethyl-1H-pyrrol-2-ylmethylene)-1,3-dihydroindol-2-one
SUCH	SU5416 + chronic hypoxia
TXA2	thromboxane A2
VEGF	vascular endothelial growth factor
VEGFR2	vascular endothelial growth factor receptor, type 2
VHL	von Hippel-Lindau

LIST OF PUBLICATIONS

1. Kenny Schlosser, **Mohamad Taha** and Duncan J Stewart. Systematic Assessment of Strategies for Lung-targeted Delivery of MicroRNA Mimics (2018) *Theranostics* 8(5): 1213-1226.
2. Kenny Schlosser, **Mohamad Taha**, Yupu Deng, Duncan J Stewart. Systemic Delivery of MicroRNA Mimics with Polyethylenimine Elevates Pulmonary MicroRNA Levels, But Lacks Pulmonary-Selectivity (2018) *Pulmonary Circulation*, 8(1): 1-4.
3. **Mohamad Taha**, Virgilio J.J. Cadete and Duncan J. Stewart. Macro- and micro-heterogeneity of lung endothelial cells: they may not be smooth, but they got the moves (2017) *Pulmonary Circulation*, 7(4): 755-757.
4. Paola Caruso, Benjamin J. Dunmore, Kenny Schlosser, Sandra Schoors, Claudia C. Dos Santos, Carol Perez-Iratxeta, Jessie R. Lavoie, Hui Zhang, Lu Long, Amanda R. Flockton, Maria G. Frid, Paul D. Upton, Angelo D'Alessandro, Charaka Hadinnapola, Fedir N. Kiskin, **Mohamad Taha**, Liam A. Hurst, Mark L. Ormiston, Akiko Hata, Kurt R. Stenmark, Peter Carmeliet, Duncan J. Stewart, Nicholas W. Morrell. Identification of miR-124 as a Major Regulator of Enhanced Endothelial Cell Glycolysis in Pulmonary Arterial Hypertension via PTBP1 and PKM2 (2017) *Circulation;* 136 (25): 2451-2467.
5. Kenny Schlosser, **Mohamad Taha**, Yupu Deng, Shirley H.J. Mei and Duncan J. Stewart. High circulating angiopoietin-2 levels exacerbate pulmonary inflammation but not vascular leak or mortality in endotoxin-induced lung injury in mice (2017). *Thorax;* doi:10.1136/thoraxjnl-2017-210413

6. Ketul R. Chaudhary, **Mohamad Taha**, Virgilio J.J. Cadete, Rafael S. Godoy, Duncan J. Stewart. Proliferative Versus Degenerative Paradigms in Pulmonary Arterial Hypertension: Have We Put the Cart Before the Horse? (2017) *Circulation Research;* 120:1237-1239.
7. Kenny Schlosser, **Mohamad Taha**, Yupu Deng, Baohua Jiang, Lauralyn McIntyre, Shirley HJ Mei, Duncan Stewart. Lack of elevation in plasma levels of proinflammatory cytokines in common rodent models of pulmonary arterial hypertension: questions of construct validity for human patients (2017). *Pulmonary Circulation*, 7(2): 476–485.
8. Baohua Jiang, Yupu Deng, Colin Suen, **Mohamad Taha,** Ketul Chaudhary, David W. Courtman, Duncan J Stewart. Marked Strain-specific Differences in the SU5416 Rat Model of Severe Pulmonary Arterial Hypertension (2015). *American Journal of Respiratory Cell and Molecular Biology*; 54(4):461-8.
9. Heather Goldthorpe, Jin-Yi Jiang, **Mohamad Taha**, Yupu Deng, Tammy Sinclair, Cindy Ge, Paul Jurasz, Kursad Turksen, Shirley H. J. Mei, & Duncan J. Stewart. Occlusive Lung Arterial Lesions in Endothelial-targeted, Fas-Induced Apoptosis Transgenic Mice (2015). *American Journal of Respiratory Cell and Molecular Biology;* 53(5): 712-718.
10. Kenny Schlosser, **Mohamad Taha**, Yupu Deng, Baohua Jiang, Duncan J. Stewart. Discordant regulation of microRNA between multiple experimental models and human pulmonary hypertension (2015). *Chest*; 148(2): 481-490.

CONTRIBUTIONS OF COLLABORATORS & FUNDING AGENCIES

I would like to acknowledge the contributions of people who participated in the work presented in Chapters 2 and 3*.

- Dr. Duncan J. Stewart: Supervised the project including contribution to experimental design, data interpretation and thesis revisions
- Dr. Michael McBurney: Provided the SIRT1 mutant and knockout mice as well as experimental suggestions
- Dr. Yupu Deng: RSVP measurement and RV dissection
- Dr. Ken Schlosser: Collected blood for plasma and hematocrit assessment
- Danielle Dewar-Darch: Performed breeding, weaning and tagging of SIRT1 mice
- Karen Jardine: Performed all genotyping for *Sirt1*$^{-/-}$ and *Sirt1*$^{Y/Y}$ mice
- Dr. Shirley Mei: Provided experimental suggestions, facilitated work for project
- Dr. David Courtman: Provided experimental suggestions

* Additional technical assistance is mentioned in detail at corresponding material and methods sections

I would like to acknowledge the following contributions of funding agencies for the student and project:

Funding for **Mohamad Taha**: Ontario Graduate Scholarship; University of Ottawa Excellence Scholarship; Canadian Vascular Network Scholar Award

Funding for **Duncan J Stewart**: Canadian Institute for Health Research

Funding for **Michael McBurney**: Canadian Institute for Health Research (Grant partially based on data presented in this thesis)

ACKNOWLEGMENTS

Having started this journey in the summer of 2011, I find it somewhat refreshing that it is about to end. Throughout this experience, I was able to develop both personally and professionally into a whole new person. However, that wouldn't be possible without the support of those surrounding me, all of whom deserve a shout out. This acknowledgement will forever be a record for our encounter and exchange of personal, professional or scientific expertise.

I would like to start by acknowledging my supervisor and mentor, **Dr. Duncan John Stewart**. You took me into your lab as an international student, while many others wouldn't/couldn't. I was quickly mesmerized by your charisma and took the plunge into scientific research. Your humble attitude, modesty and desire to learn even with your vast knowledge were a strong motivation for me throughout my studies and continue to surprise me everyday. There are no words that can describe my gratitude towards you. Dr. Stewart, please accept my HUGE thanks.

Next, I would like to acknowledge the second in command in our lab, **Dr. Shirley Mei**. I don't think things would have progressed the way they did without your constant support. Your advice and presence for me and for students/staff in the lab helped create a healthy and productive work environment and allowed our efforts to move forward. You always had my best interest at heart, so thank you for that.

Two more people should be acknowledged at this point. I don't think I will ever forget the great debt I have for **Dr. Baohua Jiang**. You were the one who gave me confidence to do surgery and to become an independent scientist. Your desire to teach and dedication to science made me enjoy scientific studies and animal work. Your

teachings will forever be itched in my head. **Dr. Ken Schlosser**, my greatest collaborator in this lab and my great friend. Thank you for never looking down on me and always treating me as an equal. Our names will forever be associated with each other through our numerous publications.

Following, I would like to acknowledge several people who directly contributed to this work, which would have stalled without their continuous efforts. I thank **Dr. Yupu Deng**, for his continuous and skillful surgical prowess. **Dr. Ken Schlosser**, for his support in plasma collection and hematocrit assessment. **Danielle Dewar-Darch** for her support in animal breeding and transfers. **Karen Jardine** for her genotyping efforts, and **Anli Yang**, for her assistance during surgeries and endpoint assessments. I would also like to thank my collaborator, **Dr. Michael McBurney**, for his great support, advice and knowledge about SIRT1 biology and function. As well, a huge thank you to **Dr. David Courtman**, for his "easygoing and chill attitude", including his help in looking at things from a new and unexpected perspective. I would also like to thank my PhD thesis advisory committee for their continuous support and advice, including **Dr. Bernard Thebaud**, **Dr. Alex Mackenzie**, **Dr. David Alan** and **Dr. Kyle Cowan**.

Now, for the good stuff: friends and colleagues at the Stewart lab. **Dr. Ketul Chaudhary**, my travel buddy, thank you for the many conversations and advice, coffee breaks and fun times. **Samantha Hodgins**, since you did not make me your sons godfather, I don't see any point in mentioning our friendship, our fun chats and our hangouts. Yup, not going to bring them up at all. **Katelynn Rowe:** You are the only friend I like *and* terrified of at the same time! Just remember, its leviOsa, not leviosA! **Nicholas Johnson Cober**, indeed, ever since you told me you want to do a PhD and I

just…. Can't …. Put … it… into … words… Thank you so very much for proofreading my thesis. **"Dr." Rafael Godoy**: Please drive safely! Seriously, I beg you! And remember, before you speak, ask yourself: would mother Teresa say this? **Dr. Virgillio Jesus Cadete**: I hope your life is full of fission, but not fusion – or the other way around, I can never remember which one is good and which is bad. **Casey Lansdell**: because of you, I will never be able to look at my ninja blender the same! And that's for life! **Mirabelle and Miriel**: thank you for being awesome; **Chen-Jiang**: easy on the basketball; **Mahmoud**: happy mice, happy life! **Maria**: thank you for being you, your hard work and dedication has always been an inspiration to me. **JiaPey**: I don't now why we get along, but I think its your no-BS attitude. Thank you for all your support. **Sophie**, thank you for being there for our lab and dealing with ordering drama. **Yuan**: I hope one day you will be able to awaken the haoshoku haki. **Andrea**: I bet you wish you got your CPA! **Saad**: I don't know how you do it, but I wish I could just be as care-free as you! I think it would improve my life dramatically. New lab members: **Villie and Luci**, your presence had a significant positive outcome on the last few months of my PhD. No, for real, thank you!

I would also like to thank other GMP facility staff including **Lilly, Ashley, James, I-m-funny-so, Justine, Hiren, Bahati and Melissa**. As well as previous colleagues **Colin, Heather, Jessie, Yifan and Dhiya**. **William Foster**, my student and my mentee, thank you for being my friend. Don't forget this acknowledgement when you're a big shot lawyer charging 300$/hr!!!

It is also important to acknowledge the assistance and efforts of the University of Ottawa animal care facility staff, including animal technicians **Josh, Pascal, Kim,**

Eileen, Melissa, Rebecca, Caro, Catharine as well as office staff **Michelle and Windy**. They all contributed large efforts for the progress of this work and were great people to work with. I would like to thank the many OHRI support staff, who facilitated everyday life and meetings, including **Jennifer, Lisa, Melanie, Adrienne, Deb** the delivery lady, **Charles, Gary** the gas guy, and **Jenn Ganton**. A shout out to my friends who started their PhD with me, **Rose** and **Emily**, as well as colleagues in other labs, including **Marissa**, **XuMai**, **Arul**, **Sohair**, **Akram**, and **Nina**. Of course, I cannot forget my ultimate frisbee friends: **Pascal, Khalid, Lauren, Tom, David R.** and **Ben.** I would also like to thank my friends overseas who were always there during this journey, including **Yang Xu, Mohamad Marie, Mohamad Tag and Husni AlNaji**. Finally, without my close friends, I don't think I would have made it. Thank you, **Abdullah, Ahmed, Fawaz and Majeed,** for always being there to vent, eat, play cards and have fun.

I don't think this PhD would have been possible without the support of my family members. My father for his financial and emotional support, my mother for her attentiveness and excellent cooking, my oldest sister for her positive attitude, my oldest brother for his wisdom and support, my second oldest sister for her economical view and my youngest sister for teaching me how to argue. Finally, to my roommate and sister **Mariam Taha**!!! No comment!!!

Sorry if I missed your name and thank you all for being there for me. Without you, I would not become the person I am today. Every good, bad or ugly experience helped me grow further into the person I am today, which is something I will never forget.

CHAPTER 1: GENERAL INTRODUCTION

1.1 The Pulmonary Circulation

The pulmonary circulation is a high-flow, low-resistance, low-pressure system, which allows efficient re-oxygenation of the blood. Deoxygenated blood, propelled into the lungs by the right ventricle (RV), is distributed through pulmonary arteries and arterioles to the alveolar capillaries. Once oxygenated at the alveolar-capillary level, the blood travels back through the pulmonary venous system to the left ventricle for distribution to the rest of the body. Hemodynamically, the lungs exhibit a mean pulmonary artery pressure (mPAP) of ~13 mmHg (normal range: 8-20 mmHg) with a characteristic low pulmonary vascular resistance (PVR) of ~0.7 wood units (normal range: 0.15-1.25 wood units) (Naeije, 2015), (Ochs & Weibel, 2008).

The low impedance of the pulmonary vasculature is a function of its unique structure, which is distinct from systemic vascular beds, and is essential for the lung to perform its vital function of blood oxygenation. In the lungs, only larger arteries and arterioles (i.e. diameter >100μm) have the distinct 3 layers which characterize all systemic arteries: the inner most layer of endothelial cells (ECs, intimal layer), a middle layer of smooth muscle cells (SMCs, medial layer) and a surrounding layer of collagen and fibroblasts (adventitial layer). These layers are separated by an elastic lamina; the internal elastic lamina separates the endothelium from the medial layer, and the external elastic lamina separates the medial and adventitial layers. In arterioles between 100μm and 50μm in diameter, there is a progressive decrease in the medial SMC layer which becomes discontinuous with SMCs “cork-screwing” around arterioles and eventually petering out in vessels <50μm in diameter, well before the precapillary level. Consequently, in the normal lung, the distal arterioles are unique in that they are devoid

of a distinct medial layer (Ochs & Weibel, 2008). This difference in anatomy between pulmonary and systemic vascular beds reflects their very distinct physiology and function. In systemic beds, the distal arterioles determine resistance and blood distribution to various organs, whereas the lung must accommodate the entire cardiac output (CO), whether at rest or peak exercise, and maintain pressures only slightly above venous. The lungs accomplish this feat by virtue of the vast extent of the pulmonary vasculature, with a surface area equivalent to a tennis court (Qureshi & Mustafa, 2018). Yet, only a minority of the lung microvasculature is needed to maintain the normal low arteriolar pressures at rest, and progressively more vascular capacity can be recruited to accommodate increases in CO during exercise, thereby maintaining low pressure and resistance at all times in the normal pulmonary circulation. The thin walled nature of pulmonary arterioles also allows mural cells to sense changes in oxygen partial pressure, which is critical for the lung vasculature to respond to low oxygen by vasoconstriction. This is another unique pulmonary circulation property that is opposite to the typical vasodilation response in the systemic bed. Despite its physiological advantages, the lack of medial cell support makes the distal lung arterioles uniquely fragile and vulnerable to injury, making the lung more susceptible to vascular injury at the arteriolar level than other vascular beds (Naeije, 2015), (Ochs & Weibel, 2008).

1.1.1 Hypoxic Pulmonary Vasoconstriction (HPV)

Oxygen comprises 20.9% of atmospheric air at sea level, which corresponds to an oxygen partial pressure (PO_2) of 159 mmHg of the total 760 mmHg air pressure. As the air enters the lungs, oxygen rapidly diffuses from the inspired air into the alveolar

capillary blood (**Table 1-1**). Since the oxygenation of blood is one of the main functions of the lungs, matching perfusion to ventilation is critical to allow for efficient gas exchange. This is achieved by vasoconstriction of arterioles in areas of reduced alveolar PO_2, or hypoxia, thus redirecting the deoxygenated blood towards better ventilated regions of the lung, leading to optimized ventilation/perfusion matching. This mechanism is called hypoxic pulmonary vasoconstriction (HPV) and is highly dependent on delicate sensing of PO_2 and subsequent SMC contraction. HPV is unique to pulmonary vasculature, while systemic vasculature usually dilates in response to lower PO_2 in order to allow for better tissue oxygen delivery (Sylvester, Shimoda, Aaronson, & Ward, 2012), (Kylhammar & Rådegran, 2016).

Table 1-1: Oxygen partial pressure in human lungs

	Oxygen Partial Pressure - PO_2	
	mmHg	**%**
Air (760 mmHg, 100%)	159	20.9
Air, trachea	150	19.7
Air, alveoli	110	14.5
Blood, lungs, deoxygenated	40	5.3
Blood, lungs, oxygenated	80-100	10.5-13.2

Adapted from (Sylvester et al., 2012) and (Carreau, El Hafny-Rahbi, Matejuk, Grillon, & Kieda, 2011)

HPV is highly dependent on the PO_2 sensory mechanism and the subsequent SMC contraction mechanism (Sylvester et al., 2012), (Dunham-Snary et al., 2017). The literature is contradictory about the exact PO_2 sensory mechanism in the lungs and whether it lies within the ECs or SMCs, while the contraction mechanism is less controversial. Indeed, several lines of evidence point to increased concentrations of intracellular calcium (Ca^{2+}), or increased Ca^{2+} sensitivity, or both, as the driving

mechanism behind SMC contraction in hypoxia. Decreased PO_2 can lead to increased release of Ca^{2+} from within internal cellular stores (e.g. sarcoplasmic reticulum) as well as increased uptake through voltage gated Ca^{2+} channels. Calcium binds calmodulin leading to a cascade of events including activation of the myosin light-chain kinase leading to phosphorylation of myosin light-chain 20 and subsequent conformational change and sliding of actin past myosin. This leads to contraction, since actin is anchored to the cytoskeleton and sarcolemma (Sylvester et al., 2012). Increased sensitivity to Ca^{2+}, as opposed to increased concentrations, can also lead to contraction of SMCs. While HPV can optimize ventilation/perfusion matching in cases of localized alveolar hypoxia, sustained and/or global decrease in PO_2 (e.g. high altitude, hypoxia) leads to sustained vasoconstriction and adverse pulmonary vascular remodeling, increasing pulmonary artery pressure (Sylvester et al., 2012), (Dunham-Snary et al., 2017).

1.1.1.1 Endothelial Vasomotor Factors:

Nitric oxide: In the lungs, nitric oxide (NO) is produced by oxidation of L-arginine to L-citrulline by endothelial nitric oxide synthase (eNOS); a reaction that requires oxygen. Release of NO from ECs promotes vasodilation through activation of soluble guanylate cyclase (sGC) in SMCs, leading to generation of cyclic guanosine monophosphate (cGMP) and subsequent cGMP mediated decrease in Ca^{2+} concentrations or sensitivity. Cyclic GMP is hydrolyzed by phosphodiesterases (PDEs), which limits the activity of this pathway (Wharton et al., 2005). Overall, NO acts as a vasodilator that dampens the HPV response and plays a role as an anti-mitogenic factor for SMCs, most likely preventing their presence in the capillary level of the pulmonary vasculature.

Decreased NO production, as occurs in endothelial dysfunction, would result in loss of vasodilator tone which would potentiate SMC response to vasoconstrictor stimuli (Garg & Hassid, 1989), (Sylvester et al., 2012), (Kylhammar & Rådegran, 2016).

Endothelin-1: Endothelin-1 (ET-1) is a potent EC-produced vasoconstrictor and SMC mitogen (Alberts, Peifley, Johns, Kleha, & Winkles, 1994). ET-1 can be released systemically, but is mainly released abluminally, where it binds ET-1 receptor A (ETA) or ET-1 receptor B (ETB) on SMCs, causing increased sensitivity or concentration of intracellular Ca^{2+} and subsequent SMC contraction. ECs can carry the ETB receptor, but binding of ET-1 to the endothelial ETB receptors leads to ET-1 clearance and vasodilation, in large by increasing NO release (Fukuroda et al., 1994). Decreased PO_2 is a driver for ET-1 production, both in isolated perfused lungs and pulmonary artery ECs (PAECs), making ET-1 a potential mediator of sustained vasoconstriction in response to maintained hypoxia (Sylvester et al., 2012), (Kylhammar & Rådegran, 2016).

Prostaglandins (Prostacyclin & Thromboxane): Prostaglandin H2 is a product of arachidonic acid catalysis by cyclooxygenases (COX). It is further converted to prostacyclin (PGI_2) or thromboxane A2 (TXA_2) by PGI_2 synthase or TXA_2 synthase, respectively. PGI_2 is released from the endothelium and causes vasodilation via binding to the prostacyclin receptors on SMCs, stimulating adenylate cyclase and increasing production of cyclic adenosine monophosphate (cAMP). Accordingly, PGI_2 is an inhibitory modulator of HPV, which can exert anti-proliferative effects on SMCs (Fetalvero, Martin, & Hwa, 2007). TXA_2 has opposite effects to PGI_2, by binding thromboxane receptors, TXA_2 can cause vasoconstriction and proliferation of SMCs (Nakahata, 2008). Prostaglandins do not appear to elicit as a strong response in the

pulmonary vasculature as NO or ET-1, but are still important for HPV (Sylvester et al., 2012), (Kylhammar & Rådegran, 2016).

1.1.1.2 Hypoxia Inducible Factors:

At the molecular level, hypoxia results in initiation of a unique transcriptional response pathway through activation of the hypoxia inducible transcription factors (HIFs). HIFs are basic helix-loop-helix (bHLH) heterodimeric transcription factors from the PER-ARNT-SIM family (PAS) (**Figure 1-1**). The heterodimers consist of a constitutively expressed beta subunit (known as HIF1β or ARNT) and an oxygen sensitive alpha subunit (HIFα). Their shared bHLH domain is necessary for DNA binding, while their PAS domain is needed for heterodimerization. They also have an N- and C-terminal transactivation domains (N-TAD and C-TAD), which are needed for target selectivity. The alpha, but not beta, subunits have an oxygen-dependent degradation (ODD) domain, which is responsible for their degradation in presence of higher PO_2 (**Figure 1-1**), (Ortmann, Druker, & Rocha, 2014), (Dengler, Galbraith, & Espinosa, 2008).

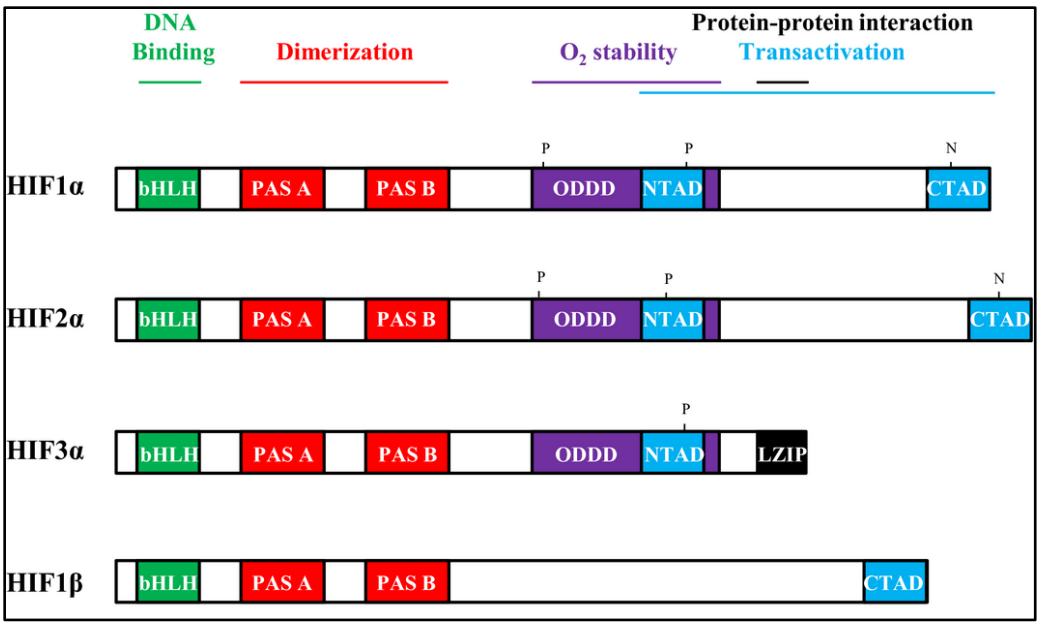

Figure 1-1: **Structure and functional domains of the HIF isoforms**. HIF1α, HIF2α and HIF3α are oxygen-sensitive α subunits while HIF1β is oxygen-insensitive. The HIF3α variant displayed is the full length. bHLH: basic helix–loop–helix domain for DNA binding. PAS: Per–ARNT–Sim domain for heterodimerization. ODD: oxygen-dependent degradation domain for oxygen stability. N-TAD: N-terminal transactivation domain; C-TAD: C-terminal transactivation domain for target selectivity. LZIP: leucine zipper domain in HIF3α for protein–protein interaction. HIF1β lacks ODD, N-TAD and LZIP domains. P: proline residue. N: asparagine residue. Adapted from (Ravenna et al., 2016), with permission

HIF pathway regulation: In normoxic conditions, the HIFα subunits are hydroxylated at key proline or asparagine residues within their ODD or C-TAD domains through the actions of the prolyl-4-hydroxylases (PHD1-4) or the Factor Inhibiting HIF (FIH) (**Figure 1-2**). The hydroxylation reaction, which requires oxygen and iron, of HIFα by PHDs leads to creation of a binding site for the E3 ubiquitin ligase von Hippel-Lindau (VHL). The interaction of the HIFα with VHL results in ubiquitination and proteasomal degradation of the HIFα. Alternatively, hydroxylation by FIH does not lead to degradation but does not allow recruitment of transcriptional co-factors to the HIF dimer in the nucleus, thereby preventing transcription. Consequently, activity of PHDs and FIH is markedly reduced in hypoxic conditions, resulting in stabilization of the HIFα subunits,

relocation to the nucleus and dimerizing to HIF1β and transcriptional co-factors (**Figure 1-2**). The TAD domain of the HIFα subunits confers selectivity for that subunit to specific DNA sequences dubbed as hypoxia responsive elements (HRE – 5'(A/G)GGTG-3'), usually located in the proximal promoters of the target genes. Binding to these HREs within the promoter and/or enhancer region leads to recruitment of RNA Polymerase II and transcriptional initiation. This results in activation of a specific cellular hypoxic adaptive response, including pathways that decrease cellular need for oxygen and improves oxygen delivery to organs (Ortmann et al., 2014), (Dengler et al., 2008).

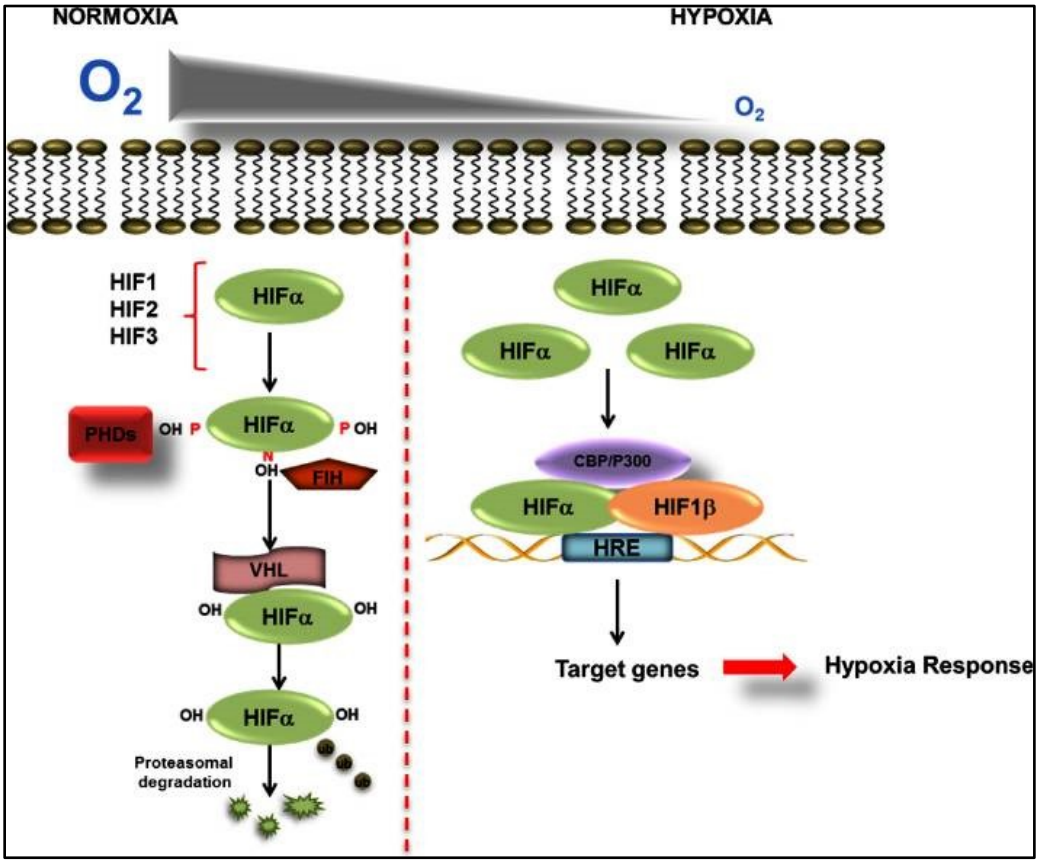

Figure 1-2: HIF pathway regulation. In normoxia, the alpha subunits are hydroxylated and degraded while in hypoxia, they are stabilized, translocate to the nucleus and initiate transcription. Adapted from (Ortmann et al., 2014) with permission.

The first and most studied IHF alpha isoform is HIF1α, which is ubiquitously expressed in all tissues and cells. The second member, HIF2α or endothelial PAS domain-containing protein 1 (EPAS1), is more restricted to specific cell types, most notably, ECs. While both members share high homology in their domains, several studies have shown that each can transcribe unique targets. HIF1α is predominantly responsible for transcription of genes responsible for the glycolytic metabolism shift in hypoxia (Keith, Johnson, & Simon, 2012), (C. J. Hu, Wang, Chodosh, Keith, & Simon, 2003), while HIF2α governs a unique set of targets responsible for erythrocytosis, vascular remodeling and cell cycle control (Tan et al., 2013). Based on searches for bHLH-PAS sequence homology, it was determined that there is a third member of this family, HIF3α, which appears to have a large number of splice variants (Duan, 2016). HIF3α has more limited transcriptional activation ability, due to lack of bHLH or C-TAD in most splice variants (P. Zhang et al., 2014), (Duan, 2016), and HIF3α is not regulated in the same way by oxygen levels as are HIF1α/2α, as evidenced by a lack of ODD domain in some splice variants (Ravenna, Salvatori, & Russo, 2016), (Duan, 2016). Instead, it is believed that HIF3α acts as a dominant negative inhibitor of both HIF1α and HIF2α through either sequestering of HIF1β or direct binding to alpha subunits leading to inactivation (Ravenna et al., 2016), (Y Makino et al., 2001), (Duan, 2016). Overall, as master regulators of the adaptation to hypoxia, normal HIF function is crucial for appropriate HPV response while their dysfunction can lead to pathological implications.

1.2 Pulmonary Hypertension

Pulmonary hypertension (PH) defines a group of diseases with the common hemodynamic feature of increased mPAP at rest ≥ 25mmHg, assessed by right heart catheterization. PH can arise due to lung vasculature dysfunction or as a complication of other diseases, such as left heart disease or thromboembolism. The increased pulmonary pressures leads to increased RV pressure, RV remodeling by hypertrophy and ultimately decompensation and failure (Taichman et al., 2015). The most updated World Health Organization (WHO) classification divides PH into five main categories based on the pathological and genetic origins of the disease, as well as the type of associated disease (**Table 1-2**) (Simonneau et al., 2013).

Group 1 PH, or pulmonary arterial hypertension (PAH), is associated with structural abnormalities in the pre-capillary pulmonary arterioles. Group 2 PH presents with left heart disease and is due to elevation in pulmonary venous pressures leading the passive elevation of PAP. Group 3 PH occurs as a result of lung disease and/or hypoxia, caused by chronic obstructive pulmonary disease (COPD), emphysema or chronic exposure to high altitude. Group 4 PH is caused by repeated thromboembolism, causing obstruction of large and small pulmonary arteries, impeding blood flow and resulting in elevations in PAP. Finally, Group 5 PH is attributed to by unclear and often multifactorial mechanisms, which could include hematological or metabolic disorders (Simonneau et al., 2013). PH classification changed dramatically over the past three decades as our understanding of pathogenesis developed (**Table 1-2**). Each PH group can present with its unique hemodynamic and pathological characteristics resulting in need for unique therapeutic approaches based on these characteristics.

Table 1-2: Updated Classification of Pulmonary Hypertension

1. Pulmonary Arterial Hypertension
1.1 Idiopathic PAH
1.2 Heritable PAH
1.3 Drug and toxin induced PAH
1.4 Associated PAH
1' Pulmonary veno-occlusive disease
1'' Persistent pulmonary hypertension of the newborn
2. PH due to left heart disease
2.1 Left ventricular systolic dysfunction
2.2 Left ventricular systolic dysfunction
2.3 Valvular disease
3. PH due to lung disease and/or hypoxia
3.1 Chronic obstructive pulmonary disease (COPD)
3.2 Interstitial lung disease
3.3 Other pulmonary diseases
3.4 Sleep-disordered breathing
3.5 Alveolar hypoventilation disorders
3.6 Chronic exposure to high altitude
3.7 Developmental lung diseases
4. Chronic thromboembolic pulmonary hypertension
5. Pulmonary hypertension with unclear multifactorial mechanisms
5.1 Hematologic disorders
5.2 Systemic disorders
5.3 Metabolic disorders
5.4 Others

Adapted from (Simonneau et al., 2013).

1.2.1 Pulmonary Arterial Hypertension (PAH)

PAH is a complex disease of the pulmonary vasculature that presents with increased PVR due to extensive pulmonary vascular remodeling characterized by degenerative and proliferative changes leading to loss of the distal arteriolar microvascular bed (Chaudhary, Taha, Cadete, Godoy, & Stewart, 2017). PAH symptoms include dyspnea, fatigue, chest pain, palpitation, syncope, or edema (Austin, Loyd, & Phillips, 1993). Hemodynamically, PAH is defined as mPAP ≥ 25mmHg at rest, accompanied by both pulmonary capillary wedge pressure (PCWP) ≤15mmHg and PVR >3 woods units on right heart catheterization (Taichman et al., 2015), (Lau,

Giannoulatou, Celermajer, & Humbert, 2017). Histologically, PAH presents with narrowing of arterioles due to muscularization in previously non-muscular arterioles or hyperplasia of the media in medium size arterioles. PAH can also present with obliterative complex pulmonary vascular lesions that can disrupt normal vessel anatomy and lead to vascular occlusion. These complex lesions, referred to as plexiform lesions, are a hallmark of PAH pathology (Chaudhary et al., 2017), (Jurasz, Courtman, Babaie, & Stewart, 2010).

The updated classification further subdivides PAH into 4 subgroups (**Table 1-2**). PAH is considered idiopathic, IPAH, when it appears from an unknown cause. In families with two or more members developing PAH, it is classified as hereditable PAH (HPAH). Around 70% of hereditable PAH cases have been linked to heterozygous, loss-of-function mutations in the bone morphogenetic protein receptor 2 gene (*Bmpr2*), a member of the transforming growth factor-β (TGF-β) receptor family (International et al., 2000), (Austin et al., 1993). PAH can also be caused by exposure to specific drugs, such as selective serotonin reuptake inhibitors (SSRIs) or appetite suppressants such as fenfluramine, and more recently amphetamines and cocaine, in which case PAH is classified as drug or toxin induced (Simonneau et al., 2013). The fourth subtype is associated PAH, APAH, in which PAH appears in association with other diseases such as connective tissue disease, HIV infection, congenital heart disease or schistosomiasis infection (Simonneau et al., 2013).

Based on current registries, PAH is considered to be a rare disease, with a prevalence of 15-50 cases per million (Lau et al., 2017). Furthermore, the prevalent subgroup of PAH can differ greatly depending on the continent or even the country. For

example, in the western world, IPAH accounts for 30-50% of all PAH cases, followed by connective tissue disease associated PAH (15-30%), then congenital heart disease associated PAH (10-23%), (Lau et al., 2017). In the Chinese PAH registry, it was reported that over 40% of PAH cases were associated with congenital heart disease, while in Brazil, where there are high levels of schistosomiasis infection, schistosomiasis-associated PAH accounts for 20% of all cases (Lau et al., 2017). Yet, in almost all registries, there appears to be a sex bias in PAH, with women accounting for 62-80% of all cases, making female sex a risk factor for development of PAH (Lau et al., 2017).

PAH survival rates have improved in the past two decades. The national institute of health (NIH) registry in the 80s reported the 5-year survival rate at 34%, while recent data from the REVEAL registry (Registry to Evaluate Early And Long-term PAH Disease Management) from 2006-2009 have reported a 5-year survival rate of 57% (Lau et al., 2017). Unfortunately, the improvements appear modest when taking into account the large advancement in development of PAH therapeutics during the 1990s (**Section 1.2.3**). Currently, there are no PAH registries in Canada, thus limiting our knowledge about the Canadian PAH population. A retrospective analysis study of PAH patients treated in Ontario between 2010 and 2011 provided limited information about only 326 PAH patients, in which 75% were female and over 95% suffered from other cardiovascular comorbidities (Vaid et al., 2016).

1.2.1.1 Pathogenesis of PAH

Early EC injury and apoptosis is believed to act as an initiating mechanism for PAH. As described below, the initial apoptosis is believed to lead to vascular dropout, EC

dysfunction as well as emergence of hyper-proliferative and apoptosis-resistant ECs and SMCs, accompanied with immune system activation in some cases. These pathological changes result in remodeling of the pulmonary vasculature, increased PVR and PAH (**Figure 1-3**).

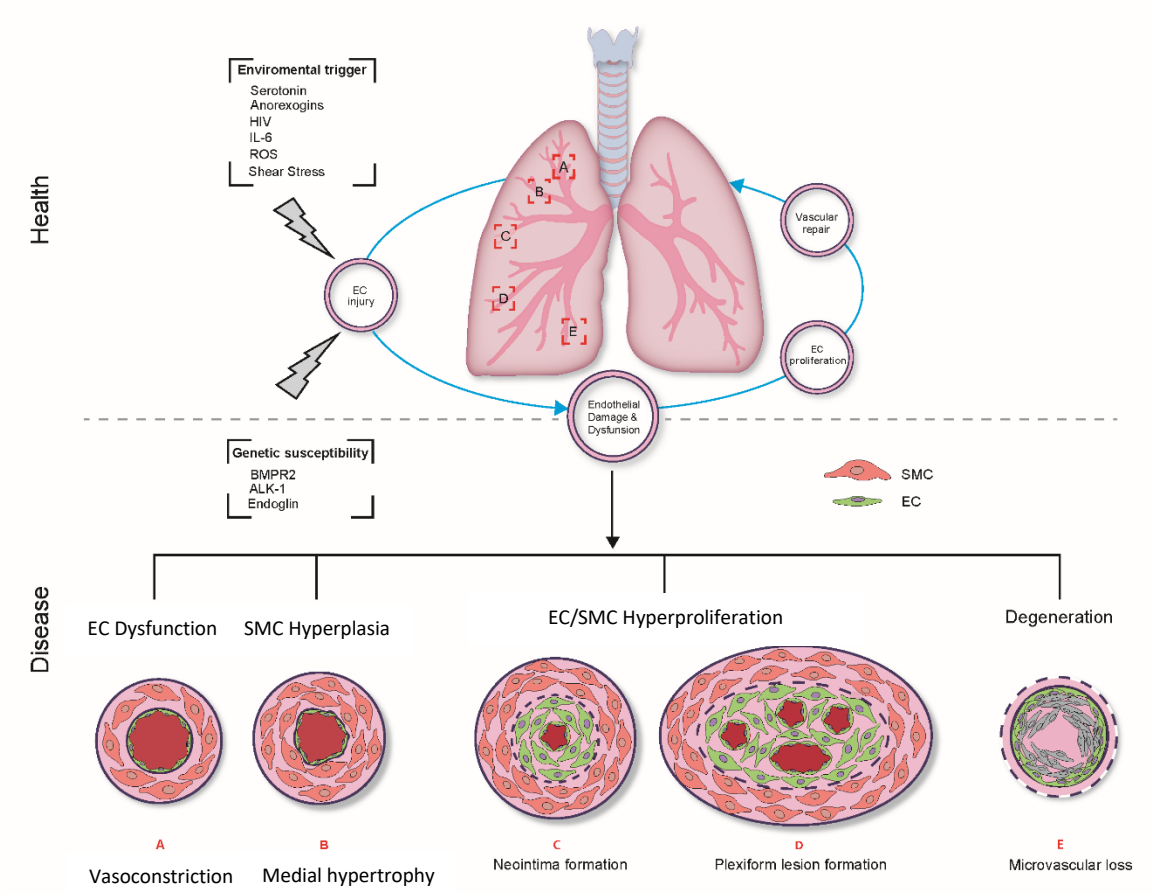

Figure 1-3: Pathogenesis of pulmonary arterial hypertension (PAH). Endothelial cell (EC) injury can occur due to exposure to a variety of environmental insults. Physiological repair mechanisms are able to restore normal lung function after injury and EC damage. However, in cases of genetic susceptibility or great injury, pulmonary EC damage contributes to development of EC dysfunction leading to vasoconstriction (A); SMC hyperplasia leading to medial hypertrophy (B); unregulated EC and SMC hyperproliferation leading to neointimal and plexiform lesion formation (C-D); and, finally, the degeneration of fragile vessels leads to microvascular loss (E). Combined, these pathological changes contribute to increased PVR and development of PAH. ROS: reactive oxygen species; EC: endothelial cells, SMCs, smooth muscle cells. Adapted from (Foster, Suen, & Stewart 2014) with permission.

EC Injury and Vascular Dropout: As discussed earlier, the more distal lung arterioles are made of only a thin layer of ECs, and the occasional supporting cells, leading to fragility and increased susceptibility to injury from environmental or genetic stress. EC apoptosis, as a result of EC injury, can trigger a number of consequences that are believed to lead to functional and structural changes in the lung vasculature that contribute to PAH. In the absence of genetic predisposition, or in cases of acute or limited injury, the lungs are able to recover through efficient repair of the damaged microvasculature. In PAH, however, presence of genetic susceptibility or sustained and widespread microvascular injury can overwhelm the natural repair mechanism, leading to pathological consequences (Jurasz et al., 2010) (**Figure 1-3**).

The evidence implicating EC apoptosis as an initiating mechanism of PAH came from studying animal models and human PAH. Indeed, current animal models of PAH are based on induction of EC apoptosis (See **section 1.2.4** for detailed model description). Briefly, one model combines delivery of a vascular endothelial growth factor (VEGF) receptor 2 inhibitor (SU5416, SU; semaxinib) in conjunction with three-week exposure to chronic hypoxia (CH) (Taraseviciene-Stewart et al., 2001). The inhibition of VEGF signaling results in loss of EC survival signaling, which is necessary to maintain endothelial integrity in the microcirculation (Taraseviciene-Stewart et al., 2001). Widespread lung EC apoptosis is followed by pulmonary arterial remodeling and the development of complex lesions that resemble the hallmark plexiform lesions of clinical PAH (Taraseviciene-Stewart et al., 2001). Notably, both the remodeling and hemodynamic effects in this model were prevented by inhibition of EC apoptosis using a broad spectrum caspase inhibitor, Z-ASP (Taraseviciene-Stewart et al., 2001).

Subsequent studies have shown that induction of EC apoptosis using SU5416 alone is sufficient for development of severe PAH in a "hyper-sensitive" rat sub-strain (Jiang et al., 2016). EC apoptosis has also been described in other experimental models of PAH, including the monocrotaline (MCT) model in rats (Jurasz et al., 2010) (**Section 1.2.4**). Interestingly, MCT-induced PAH can also be prevented by the caspase inhibitor Z-VAD, suggesting a direct role of EC apoptosis in the development of MCT-induced PAH (Jurasz et al., 2010). Further evidence of the role of EC apoptosis as an initiating mechanism of PAH has been demonstrated in experimental models which use targeted EC death and showed development of PH (Goldthorpe et al., 2015). Studies of human cells from control and PAH lungs provide further support to the role of EC apoptosis in PAH. In human PAECs, BMPR2 signaling plays a similar protective role to VEGF signaling, thus mediating EC survival; while loss of BMP signaling leads to increased EC apoptosis (Teichert-Kuliszewska et al., 2006). Consequently, it has been proposed that mutations in the *Bmpr2* gene confers susceptibility of lung ECs to apoptosis, and in combination with a second environmental or genetic "hit", predispose to the development of PAH (Jurasz et al., 2010), (Morrell, 2006). Overall, the evidence supports EC apoptosis as a necessary trigger for the functional and structural arterial changes leading to PAH.

While the precise mechanisms by which EC apoptosis results in the functional and structural vascular abnormalities of PAH is a hotly debated topic in the field, there is general agreement that widespread loss (or pruning) of functional lung microvasculature is the end result which causes progressive increases in vascular resistance and pressures (Chaudhary et al., 2017). Essentially, there are two potential pathways by which EC

apoptosis can cause vascular pruning; the first is a degenerative process in which EC apoptosis leads directly to arteriolar "drop-out", and the second is a proliferative process, in which vascular loss results indirectly by the emergence of apoptosis-resistant, hyperproliferative ECs and SMCs which can lead to complex intimal arterial remodeling with occlusion or obliteration of small arterioles. By far, the greatest interest has been focused on the "proliferative hypothesis" (see below), while the direct role of EC apoptosis in microvascular loss has been largely overlooked (Chaudhary et al., 2017). This is due, in part, to the difficulty in visualizing the complex 3-dimensional architecture of the lung microvasculature. While it is relatively easy to appreciate proliferative arterial remodeling and complex plexiform lesions using standard light microscopy in thin lung sections, the degenerative loss of microvessels requires much more sophisticated imaging approaches, including 3-dimensional imaging of the lung vasculature using high-resolution computed-tomography (HRCT) or novel techniques, such as fluorescent microangiography (FMA), pioneered by our group (Dutly et al., 2006). Using these methods, pruning of the pulmonary vasculature can be demonstrated in both animal models (Y. D. Zhao et al., 2006), (Kugathasan et al., 2009), (Dutly et al., 2006), (Ritman, 2005) and human lungs (Moledina et al., 2011). Indeed, a massive dropout of pulmonary vasculature could lead directly to increased vascular resistance within the pulmonary circulation, thus providing a simple and elegant pathway from EC apoptosis to PAH (Chaudhary et al., 2017).

Vasoconstriction, Vascular Cell Proliferation and Inflammation: A possible pathological consequence of EC apoptosis, observed in PAH, is the rise of dysfunctional ECs (**Figure 1-3**), which exhibit an imbalance in the production of endothelium

vasodilators, such as PGI_2 (Tuder et al., 1999) and NO (Kaneko et al., 1998), and an increase in the release of vasoconstrictors, such as TXA_2 (Christman et al., 1992) and ET-1 (Stewart, Levy, Cernacek, & Langleben, 1991), (Giaid et al., 1993). These changes are accompanied by a decreased level or activity of enzymes responsible for the production of vasodilator factors, including decreased eNOS in plexiform lesions of PAH patients (Giaid & Saleh, 1995), (Hall, Davie, Klein, & Haworth, 2011) or decreased PGI_2 synthase in the pulmonary vasculature and plexiform lesions of PAH patients (Tuder et al., 1999). Furthermore, an increase in ET-1 ligand binding (Davie et al., 2002) or ETB receptor expression on SMCs from PAH patients is possible (Hall et al., 2011). This imbalance favors pulmonary arterial vasoconstriction and remodeling, contributing to increases in PVR. In addition, while PGI_2 and eNOS are known to elicit anti-mitogenic effects on SMCs, ET-1 induces SMC proliferation (Alberts et al., 1994), (Wedgwood, Dettman, & Black, 2001), leading to increased proliferation of SMCs and further narrowing and remodeling of the pulmonary vasculature.

In combination with EC dysfunction, EC apoptosis can trigger reactive changes in vascular cell growth and survival in the distal pulmonary arterial bed that leads to the development of complex, obliterative arteriopathy - i.e. the “proliferative hypothesis” (Chaudhary et al., 2017) (**Figure 1-3**). This cell growth leads to thickening and narrowing of the pulmonary arteries and arterioles, which is a nearly universal histopathological feature in PAH, appearing as medial and adventitial hyperplasia in the mid-sized arteries and arterioles or as extension of SMCs into normally non-muscular, peripheral pulmonary arterioles (Humbert, Morrell, et al., 2004), (Jeffery & Morrell, 2002). Some of the cellular processes leading to this hyperplasia involves increased SMC proliferation in

the medial layer, proliferation of intermediate cells lying inside the internal elastic lamina and recruitment of interstitial fibroblasts from the surrounding lung parenchyma in the distal capillary arterioles, which subsequently take on a SMC-like phenotype and contribute to the muscularization process (Jeffery & Morrell, 2002). Additionally, in the small peripheral muscular arteries, fibroblast hyperplasia and increased production of extracellular matrix components have been reported (K R Stenmark & Mecham, 1997). Collagen deposition and elastin synthesis in the adventitial layer leads to further narrowing of the vascular lumen and contributes to the increased PVR (K R Stenmark & Mecham, 1997), (Tozzi, Christiansen, Poiani, & Riley, 1994).

Appearance of complex plexiform lesions in the lungs of PAH patients has fascinated researchers in this field for a long time. Plexiform lesions are found in the lungs of many PAH patients, particularly in the late stages of the disease (Stacher et al., 2012). However, they are not a universal feature and are sometimes absent in biopsy or autopsy material of patients dying of severe PAH, and when they do occur, they show little correlation with the severity of the disease (Stacher et al., 2012), raising questions about their role in the pathogenesis of PAH. Complex lesions contain a large variety of cell-types including EC, SMC, fibroblast-like, as well as inflammatory cells, including macrophages and T-cells (Jonigk et al., 2011). It has been hypothesized that plexiform lesions are related to a failed and dysfunctional angiogenic process (E D Michelakis, Wilkins, & Rabinovitch, 2008). Indeed, ECs within these lesions have been found to over-express markers of angiogenesis, such as VEGF and its receptors, and to be supported by a stroma comprised of matrix proteins and α-smooth muscle actin-expressing myofibroblasts (Cool, Groshong, Oakey, & Voelkel, 2005). It has also been

suggested that these lesions may be a consequence of the emergence of apoptosis-resistant and hyper-proliferative SMCs and ECs triggered by EC injury and apoptosis (Masri et al., 2007), (Tuder, Groves, Badesch, & Voelkel, 1994). In fact, PAECs and pulmonary artery SMCs (PASMCs) isolated from PAH patients display an abnormal hyper-proliferative, anti-apoptotic phenotype in culture, which is accompanied by a shift in metabolism from oxidative phosphorylation (aerobic) to glycolysis (anaerobic), the so-called "Warburg effect" that is commonly found in neoplastic cells (Rehman & Archer, 2010). Another feature of the cells within the complex arterial lesions is the reduced expression of PGI_2 synthase (Tuder et al., 1999), eNOS (Giaid & Saleh, 1995), and increased expression of ET-1 (Giaid et al., 1993), as well as presence of somatic mutations in apoptosis and proliferation regulating genes, such as BAX and TGF-β type II receptor (Richter et al., 2004), (Yeager, Golpon, Voelkel, & Tuder, 2002). These features of plexiform lesion cells were used as support for the proliferative hypothesis of PAH, however, the importance of these lesions as a contributor to the pathogenesis of PAH is still a matter of debate in the field (Chaudhary et al., 2017).

Immune system dysregulation adds another layer of complexity to PAH pathogenesis, where some patients display increased inflammatory cell infiltrates in lung tissue and plexiform lesions, such as T-cells and macrophages, and increased lung and circulating pro-inflammatory cytokines, such as TNFα, IL-6 and MCP-1 (Groth et al., 2014), (Jonigk et al., 2011), (Schlosser et al., 2017). This is highly prevalent in cases of PAH associated with diseases with inflammatory and autoimmune component, such as connective tissue disease, as well as diseases with dysregulated immune function, such as HIV infection (Lau et al., 2017). Therefore, immune dysregulation is important for some

forms of APAH, but plays a more limited, or yet to be identified, role in other PAH subgroups.

Genetic Predisposition: Around 70% of HPAH cases have been linked to heterozygous, loss-of-function mutations in *Bmpr2* gene, which now includes over 300 different identified mutations linked to PAH (Garcia-Rivas, Jerjes-Sánchez, Rodriguez, Garcia-Pelaez, & Trevino, 2017), (Machado et al., 2015). BMPR2 has been shown to mediate EC survival (Teichert-Kuliszewska et al., 2006), (Morrell, 2006) and thus the association of *Bmpr2* mutations with PAH further strengthens the critical role of EC apoptosis in this disease. Interestingly, mutations in *Bmpr2* were found to be associated with early onset of PAH, associated with more severe clinical and hemodynamic features at diagnosis (Machado et al., 2015).

In addition to *Bmpr2*, diverse heterozygous mutations in other genes encoding members of the TGF-β signaling pathway have been shown to be associated with PAH. These include mutations in the activin A receptor like type 1 (*ACVRL1*) gene, the endoglin (*ENG*) gene, the BMP type I receptor protein (*BMPRIB*) gene, and the Smad family member 9 (*SMAD9*) gene, all of which play an important role in the BMP/TGF-β signaling pathway (Garcia-Rivas et al., 2017). As well, mutations in the ET-1 (*EDN1*) gene have been previously identified in PAH patients (Garcia-Rivas et al., 2017). Interestingly, less frequent mutations have also been identified in other pathways linked to calcium homeostasis (*KCNA5, KCNA3, TRPC6*), mitochondrial metabolism (*SIRT3*) and vasodilation (*PTGIS, NOS2*) (Garcia-Rivas et al., 2017), (Machado et al., 2015). Identification of genetic mutations in PAH, and the development of new and improved genetic tools, helps in our understanding of the mechanism of PAH pathogenesis.

Conclusion: The relative importance of each of the aforementioned mechanisms in the pathogenesis of this disease has yet to be clearly defined. Indeed, it may be that PAH is a heterogeneous condition which can result from multiple mechanisms, and the balance of processes that result in disease may vary in any individual patient.

1.2.2 High Altitude Pulmonary Hypertension (HAPH)

PH due to chronic exposure to high altitude (HAPH) is categorized as Group 3 under the WHO classification, i.e. PH due to lung disease and/or hypoxia (**Section 3.6 in Table 1-1**). The decreased PO_2 at high altitude (**Table 1-3**) leads to activation of a global HPV response, leading to increased PVR and mPAP (Mirrakhimov & Strohl, 2016). In susceptible individuals, persistent exposure to high altitude can lead to HAPH with persistent elevation in PAP and pulmonary vascular remodeling, RV hypertrophy (RVH) and can eventually lead to right heart failure (Mirrakhimov & Strohl, 2016), (Sylvester et al., 2012), (León-Velarde & Mejía, 2008). A strong correlation between HAPH and the magnitude of HPV response suggests that HPV contributes significantly to HAPH; yet, relocation to normal altitude does not always lead to resolution of HAPH. Clinically, HAPH patients present with symptoms similar to PAH and management of HAPH usually involves relocation to lower altitudes or similar treatment options to those used for PAH (Mirrakhimov & Strohl, 2016).

Table 1-3: Oxygen partial pressure at different heights

	Air Pressure	Oxygen Partial Pressure - PO_2	
	mmHg	**mmHg**	**%**
0m (sea level)	760	160	21
1609m (Denver)	633	133	17.5
2500m	570	120	15.8
3100m (Leadville)	530	111	14.6
5959m (Mount Logan)	371	78	10.3
8848 (Everest)	253	53	7.0
Chronic hypoxia model	--	68-76	9-10

1.2.2.1 Pathogenesis of HAPH

Histologically, HAPH is characterized by medial and adventitial thickening due to hypertrophy and proliferation of SMCs, fibroblasts and myofibroblasts. This is accompanied by increased extracellular matrix production and distal extension of SMCs to normally non-muscularized vessels (Mirrakhimov & Strohl, 2016), (Kurt R. Stenmark, Fagan, & Frid, 2006). At the molecular level, persistent HPV leads to maintained high levels of Ca^{2+} inside SMCs, increased and maintained production of vasoconstrictors, such as ET-1 and TXA_2, and reduced levels of NO and PGI_2 (Mirrakhimov & Strohl, 2016).

Genetic predisposition: Several studies in human patients and animal models identified potential genetic variants associated with susceptibility or resistance to HAPH. These variants were mostly in genes involved in the expression and function of components of the oxygen-sensing pathway, mainly the HIFs. In cattle, whole-exome sequencing implicated a mutation in the *HIF2A* gene in the pathogenesis of HAPH. A double variant in HIF2α causing two nonsynonymous amino acid substitutions in the ODD domain was found in 75% of cattle with elevated mPAP (>50 mmHg) and in all high-altitude cattle with HAPH (mPAP > 94 mmHg) studied. It is hypothesized that this

double variant is a gain of function mutation causing increased HIF2α activity (Newman et al., 2015). Human populations also display genetic variations at altitude, associated with different levels of HAPH. Native Tibetans, who have lived for millennia at altitudes higher than 4000m, exhibit minimal HAPH and absence of erythrocytosis (the increase in red blood cell (RBC) production). In contrast, HAPH is prevalent in native Quechua Indians living at altitudes of 3500 to 4000m. Similarly, children living in Leadville, Colorado at 3100m commonly exhibit HAPH. Therefore, it is believed that heritable genetic factors are responsible for HAPH adaptation and correlate with the duration of living at high altitude (25000 years for Tibetans, ~13000 years for Quechua, <100 years for Colorado) (Dunham-Snary et al., 2017). Further genomic studies of Tibetan highlander populations show variations in HIF2α (*HIF2A*) and PHD2 (*EGLN1*) genes, which were associated with normal levels of blood hemoglobin, absence of HPV response and normal PVR (Sylvester et al., 2012). As well, point mutations in the eNOS (*NOS3*) gene, leading to an increase in NO production, in populations residing at altitude, have been recorded (León-Velarde & Mejía, 2008). Overall, there appears to be a strong link between HPV, HAPH development and hypoxic and vasoconstriction response genes.

1.2.3 Therapeutic Interventions for PAH/HAPH

There are currently no therapies approved specifically for HAPH, but a similar treatment is applied to that of PAH patients if relocation to normoxia is ineffective or not possible (Mirrakhimov & Strohl, 2016). Therapeutic agents currently in clinical use for PAH are designed to address endothelial dysfunction by either enhancing vasodilation or

reducing vasoconstriction. These include calcium-channel blockers, prostanoids, PDE5 inhibitors and ET-1 receptor antagonists.

Calcium-channel blockers (CCBs): Initial assessment of PAH patients includes a challenge with inhaled NO or IV prostacyclin in order to assess sensitivity to vasodilators (Medarov & Judson, 2015). Patients who show a strong vasodilatory response in this test, considered vasodilator responsive, will usually respond to long-term therapy with CCBs. However, the use of CCBs is limited in PAH to this population of patients and has limited efficacy in patients who are vasodilator non-responsive, and can even be detrimental, contribiuting to RV dysfunction and hypotension (Medarov & Judson, 2015), (Langleben & Orfanos, 2017).

Prostanoids: Epoprostenol, a prostacyclin analog, was the first FDA-approved therapy for PAH. Continuous IV infusion of Epoprostenol not only can produce symptomatic and hemodynamic improvement in IPAH patients, but also associates with improved survival in New York Heart Association (NYHA) functional class III or IV PAH patients (Nagaya, 2004), (Barst et al., 1994), (Barst et al., 1996). Ever since, several newer prostacyclin analogs with longer half-life have been introduced. Treprostinil is delivered IV or subcutaneously by a smaller mechanical pump with less demanding storage requirements than Epoprostenol (Skoro-Sajer & Lang, 2008). Another prostacyclin analog, Iloprost, is available as an inhaled medication, which was approved in 2004 by the FDA for patients with WHO functional class III or IV symptoms (Mubarak, 2010). Similarly, Treprostinil has also been available as an inhaled medication since FDA approval in 2008 (Skoro-Sajer & Lang, 2008). More recently, Selexipag, an oral prostacyclin receptor agonist, has been approved by the FDA and Health Canada and

demonstrated good efficacy in reducing pulmonary hemodynamics and improving CO (Sitbon et al., 2015).

ET-1 Receptor Antagonists: Bosentan, a dual ETA and ETB receptor antagonist, was found to decrease PVR and improve exercise capacity in a large-scale clinical trial (Channick et al., 2001). Ambrisentan, an ETA specific receptor antagonist, has also led to improvements in hemodynamics and exercise capacity in PAH patients (Galie et al., 2008). Recently, Macitentan, a novel dual ETA and ETB antagonist, has been approved for the treatment of PAH (Iglarz et al., 2008).

PDE5 Inhibitors: Oral administration of the PDE5 inhibitor, Sildenafil, has been shown to lead to pulmonary vasodilation and improve exercise capacity and pulmonary hemodynamics in PAH patients following long-term administration (E D Michelakis et al., 2003). More recently, a longer-acting PDE5 inhibitor, Tadalafil, has been introduced for PAH management (Galie et al., 2009).

Despite the availability of these various therapies and the increasing use of combination therapy to target different pathways involved in PAH pathogenesis, nearly all PAH patients continue to progress and prognosis remains poor (Humbert, Sitbon, & Simonneau, 2004), with recent estimates of the 5-year survival for newly diagnosed PAH patients at 61% (Farber et al., 2015). A significant limitation of pharmacotherapy is the mechanism of action, which is aimed primarily at restoring pulmonary endothelial function by restoring imbalances in vasoactive factors rather than reversing the primary pathological process of lung arterial remodeling. Fears have also been raised that the use of such treatments may result in inhibition of HPV, impairment of pulmonary gas exchange and deterioration of arterial oxygenation, which may negate the potential

benefit of reduced RV afterload. Therefore, it is not surprising that current pharmacotherapy options only provide modest improvements in pulmonary hemodynamics and are non-curative, thereby warranting the need for more effective treatment strategies.

1.2.4 Rodent Models of PAH/HAPH

1.2.4.1 The Chronic Hypoxia (CH) Model

Chronic exposure to hypoxia is mainly used as a surrogate experimental model to study PAH, although by definition it is a model of Group 3 PH, not Group 1 (i.e., PAH) (see **Table 1-2** and **Table 1-3**). In this model, rodents are exposed to low oxygen, i.e., hypoxia, for an extended period of time (3-5 weeks; PO_2 68-76 mmHg; 9-10% O_2). As an experimental model, CH leads to initial vasoconstriction in pulmonary arteries, marked muscularization of pulmonary arterioles and RV remodeling (Kurt R Stenmark, Meyrick, Galie, Mooi, & McMurtry, 2009), (Kurt R. Stenmark et al., 2006), (J. Gomez-Arroyo et al., 2012). Degenerative changes leading to loss of the distal arteriolar microvascular bed, or vascular pruning, have also been noted in rat (Howell, Preston, & McLoughlin, 2003) and mouse (Chandra et al., 2011), (Abdalla et al., 2015) CH models. Similar to human HAPH, and in the absence of genetic predispositions, the CH model is reversible upon relocation of wildtype rodents to normoxic conditions and does not lead to formation of complex intimal remodeling or plexiform lesions. During normoxic recovery from CH, mPAP rapidly decreases, followed by a gradual decrease requiring as long as 6 - 12 weeks to achieve normoxic baseline values in rats (Sylvester et al., 2012) or 2 weeks in mice (Weisel et al., 2014). Since the nature of this model makes it a better representative for HAPH than PAH, other chemical and surgical induced models were developed to

better represent PAH.

1.2.4.2 The Monocrotaline (MCT) Model

MCT is a plant alkaloid derived from the seeds of *Crotalaria spectabilis* and was first shown to induce PAH in rats in 1967 (Kay, Harris, & Heath, 1967). MCT can be delivered subcutaneously or intraperitoneally and leads to rapid development of PAH, usually within 2 to 3 weeks. MCT requires enzymatic activation by cytochrome P450 enzyme CYP3A4 in the liver, to form MCT pyrrole (MCTP), a direct endothelial toxin (Kurt R Stenmark et al., 2009). MCTP causes EC injury and apoptosis through caspase-3 activation *in vitro* (Nakayama Wong, Lamé, Jones, & Wilson, 2010). This was confirmed *in vivo* in the rat model by Jurasz *et al.* who showed apoptotic ECs in the lung from day 3 to 21 after MCT administration (Jurasz et al., 2010). Furthermore, blockade of caspase-3 using Z-ASP significantly attenuated the response to MCT, suggesting that apoptosis through the caspase-3 pathway is an integral mechanism for the MCT-induced PAH (Jurasz et al., 2010). The MCT model is characterized by progressive pulmonary vascular changes, including marked medial hypertrophy in pulmonary arteries and arterioles, associated with increases in PVR and PAP, leading to significant RVH and RV dysfunction by three weeks (J. G. Gomez-Arroyo et al., 2012). This model is also characterized by marked inflammation, with the accumulation of mononuclear cells in the pulmonary adventitia of small intra-acinar vessels (Wilson, Segall, Pan, & Dunston, 1989). The MCT model is the most widely utilized animal model of rat PAH. A distinct technical advantage of this model is the lack of need for specialized equipment, such as hypoxia chambers, to induce PAH; however, MCT(P) can lead to off target toxicity due

to direct toxic effects on other organs, including the liver and kidney (Akhavein, St-Michel, Seifert, & Rohlicek, 2007). Indeed, injury to these "off target" organs appears to be an important contributor to the high mortality seen in the MCT model, in addition to RV failure resulting from PAH (J. G. Gomez-Arroyo et al., 2012). The high mortality beyond 3 weeks also limits the utility of the MCT model for studying the long-term effects of therapeutic agents in treatment (i.e. reversal) studies. Strong differences in the response to MCT among different animal species have been noted, and while MCT readily induces a PAH phenotype in rats and some other species (e.g. dogs, pigs, sheep), mice are relatively resistant to its pulmonary vascular effects, due to the lack of the enzyme CYP3A4 (J. Gomez-Arroyo et al., 2012).

1.2.4.3 Two Hit Models: The SU5416 plus Chronic Hypoxia (SUCH) Model

Besides the MCT and CH models, surgical models of PAH were developed including pneumonectomy, to increase flow through the remaining lung, as well as pulmonary artery banding, to provide a controlled RV afterload (Kurt R Stenmark et al., 2009). However, none of these models exhibit complex vascular occlusive remodeling or plexiform-like lesions, a hallmark of PAH (Kurt R Stenmark et al., 2009). Consequently, "two-hit" animal models have been developed and some are able to reproduce some of these pathological findings. In a seminal report, Taraseviciene-Stewart *et al.* demonstrated that rather than inhibiting hypoxia-induced PH, the administration of the VEGFR2 inhibitor SU5416 potentiated both PAP and arterial remodeling (Taraseviciene-Stewart et al., 2001). SU5416 was originally developed as an anti-angiogenic agent for cancer therapy (Ryan, Marsboom, & Archer, 2013) and in this model, SU plus CH

resulted in lung EC apoptosis, emergence of apoptosis-resistant, hyperproliferative vascular cells and appearance of complex intimal lesions (Taraseviciene-Stewart et al., 2001). Abe *et al* later showed that this model was progressive, even upon relocation to normoxia, and at later stages, beyond 5 weeks, the complex vascular lesions exhibited a close resemblance to the human PAH lesions in type and morphology (Abe et al., 2010). Currently, the model is simplified to a single injection of SU5416 at 20 mg/kg followed by 3 weeks of CH (10% O_2) and a return to normoxia for an additional 2-9 weeks (Ryan et al., 2013). Unlike the MCT model, the SUCH model is generally well tolerated, depending on the background strain, with low mortality in normal Sprague-Dawley rats even beyond 12 weeks (Jiang et al., 2016). Despite the requirement for hypoxia chambers, the SUCH model is well suited for the study of PAH, and has been reproduced by many groups. Moreover, unlike the MCT model, mortality in the SUCH model is attributable to right heart failure, making it ideal for the study of therapeutic agents in treatment of established PAH.

1.2.4.4 Two Hit Models: The MCT plus CH (MCT+CH) Model

Recently, several groups have combined low-dose MCT and CH in order to obtain a more severe, progressive PAH model of the disease. Combination of the two stimuli leads to severe, progressive PAH in rats (Lan, Hayama, Kawaguchi, Furutani, & Nakanishi, 2015), (Morimatsu et al., 2012), yet further work is needed to better understand this model and compare its usefulness in understanding PAH pathology to the SUCH model.

1.2.4.5 Two Hit Models: Genetically Manipulated Models

Mice respond very differently than rats to stimuli, such as CH, MCT, SU5416 or any combination of thereof. CH leads to development of a mild PH phenotype in mice, which is not worsened when combined with multiple injections of high doses of SU5416 during hypoxia (J. Gomez-Arroyo et al., 2012), (Taha, Jiang, Deng, & Stewart, 2012). Although some groups have reported a severe PAH phenotype in the mouse SUCH model (Ciuclan et al., 2011), (Vitali et al., 2014), this is not accompanied by occlusive arterial remodeling and there is considerable debate about whether this truly represents a progressive and irreversible disease model. Similarly, MCT fails to produce a robust and reproducible PAH phenotype in mice due to their inability to metabolize MCT to MCTP (J. Gomez-Arroyo et al., 2012). Despite these significant limitations, transgenic mouse models are commonly used to better understand the molecular mechanisms which underlie PAH. Since the vast majority of such transgenic mouse models fail to show a spontaneous PH phenotype, CH is often used to unmask the role of different genes in the development of PH *in vivo*. Indeed, plexiform pulmonary vascular lesions have been observed in very few transgenic mouse models, specifically, the constitutive over-expression of IL-6 under the lung-specific Clara cell 10-kDa promoter after CH treatment (Steiner et al., 2009), and the more recent EC-specific knockout of PHD2 (Dai, Li, Wharton, Zhu, & Zhao, 2016), (Kapitsinou et al., 2016), (Wang et al., 2016), (Tang et al., 2017).

Over the past twenty years alone, over 40 different transgenic mouse models were used to study PH, many of which using CH (J. Gomez-Arroyo et al., 2012), (Dai & Zhao, 2017). Those include complete knockout models, overexpression models, targeted

transgenic models and cell specific knockout models. Several of these models focused on the BMPR2 pathway, due to its link to hereditary PAH. Some groups generated BMPR2 transgenic mice carrying the same point mutations as human patients or developed haploinsufficient or conditional knockout mice for BMPR2 (Burton et al., 2011). Great insight into the role of BMPR2 and EC apoptosis was gained from these models *in vivo*, and some of these models even develop spontaneous PH, similar to human PAH (J. Gomez-Arroyo et al., 2012), (Morrell, 2006). Further insight into the cell specific role of BMPR2 was established from studies using targeted BMPR2 knockout and transgenic mice. For example, EC-specific BMPR2 knockout mice develop spontaneous PH at low penetrance, establishing a role for BMPR2 signaling in ECs in PAH *in vivo* (Hong et al., 2008).

In addition to BMPR2, several crucial pathways involved in PAH pathogenesis were manipulated *in vivo* in order to better understand PH pathology and the hypoxic response. Those include pathways involved in vasodilation, vasoconstriction and the molecular hypoxic response. For example, eNOS (*NOS3*) knockout mice, which develop higher PH in response to milder hypoxia exposure, helped establish a role of eNOS in PH (Fagan et al., 1999). On the other hand, PGI_2 synthase overexpressing mice, which are protected against development of CH-induced PH, helped establish a role for prostacyclin in PH (Geraci et al., 1999). The use of selective genetic manipulation, usually in combination with hypoxia, provides a great tool for understanding HAPH and PAH development and the *in vivo* hypoxic response, which can provide future insight into novel therapeutic intervention development.

1.2.5 Hypoxia Inducible Factor 1α in PH

HIF1α, the first discovered member of the HIF family, has been shown to regulate the expression of a wide range of genes in response to hypoxia (Dengler et al., 2008). Yet, it appears that one of the main functions of HIF1α is to mediate the acute hypoxic response through a metabolic shift from oxidative phosphorylation to glycolysis (Dengler et al., 2008). This involves increased transcription of pro-glycolytic genes such as lactate dehydrogenase (*LDH*) or inhibitors of oxidative phosphorylation, such as pyruvate dehydrogenase kinase (*PDK*) (Dengler et al., 2008). A shift in mitochondrial metabolism is becoming increasingly recognized as a potential mechanism of growth dysregulation in lung vascular SMCs, contributing to the pathogenesis of PAH (Bonnet et al., 2006), (W. Xu et al., 2007).

In PAH, PAECs and PASMCs display an abnormal hyper-proliferative, anti-apoptotic phenotype, which has been implicated in hyperplasia and hypertrophy of the SMC layer in the pulmonary arterioles as well as development of complex vascular lesions (W. Xu et al., 2007), (Rehman & Archer, 2010). Assessment of these cells in culture reveals a shift in metabolism from oxidative phosphorylation (aerobic) to glycolysis (anaerobic), known as the "Warburg Effect" (Rehman & Archer, 2010). Even though HIF1α plays a physiological role in the shift from aerobic to anaerobic metabolism as an adaption to hypoxia; under protracted exposure to hypoxia or in the context of normoxic HIF1α activation, it can contribute to dysregulation of SMC growth (Bonnet et al., 2006). HIF1α can promote abnormal proliferative and apoptosis resistant phenotypes, in part by decreased expression of Kv1.5 potassium channels, leading to a hyperpolarized mitochondrial state (Rehman & Archer, 2010). HIF1α can also lead to

transcription of pro-survival genes (*VEGF*, *PDGF*, *EGF*, etc.), as well as increase the expression of PDK/LDHA, causing a shift to glycolytic metabolism (Rehman & Archer, 2010). Small molecule inhibitors have been used to normalize inappropriate HIF1α activation in PAH and other disorders. For example, dichloroacetate (DCA), a PDK inhibitor can partially prevent and reverse CH- and MCT-induced PH (McMurtry et al., 2004), (Evangelos D Michelakis et al., 2002) and has shown some efficacy in improving human PAH in a recent clinical trial (Evangelos D. Michelakis et al., 2017).

Data from transgenic animal models supports a potential role for HIF1α in pathogenesis of PH. For example, heterozygous HIF1α knockout mice are protected from development of PH in the CH model (A. Y. Yu et al., 1999). SMC deletion of HIF1α led to a slight decrease in development of CH-PH (Ball et al., 2014), while EC-specific deletion of HIF1α did not affect the degree of development of CH-PH (Cowburn et al., 2016), suggesting that HIF1α plays a larger role in the hypoxic response in SMCs than ECs. Indeed, PASMCs isolated from PAH patients showed clear normoxic activation of HIF1α, which was not observed in lung ECs from the same patients (Tang et al., 2017). Fawn hooded rats, which spontaneously develop PH and mild polycythemia with age, appear to exhibit constitutive normoxic activation of HIF1α reflected by genetic abnormalities, leading to aberrant mitochondrial oxygen sensing (Sato et al., 1992), (Bonnet et al., 2006). Overall, a normoxic-activated HIF1α-mediated shift in mitochondrial metabolism is becoming increasingly recognized as a potential mechanism of growth dysregulation in lung vascular cells, mainly SMCs, contributing to the pathogenesis of PAH.

1.2.6 Hypoxia Inducible Factor 2α in PH

Unlike HIF1α, which is ubiquitously expressed, HIF2α protein is detectible in a more limited number of cells in hypoxia including: ECs, renal interstitial cells, hepatocytes, epithelial cells and cardiomyocytes, while *HIF2A* mRNA is highly expressed in lung and heart (Patel & Simon, 2008). Compelling evidence indicates that erythropoietin (EPO), the first identified hypoxic-induced target and main driver of erythropoiesis, is a HIF2α target (Rankin et al., 2007). Interestingly, HIF1α and HIF2α have somewhat distinctive roles in the hypoxic response, which is dependent on cell type, level of hypoxia and length of hypoxic exposure. In particular, HIF2α activation is associated with a chronic response to hypoxia (Patel & Simon, 2008).

Much of our knowledge about the role of HIF2α in PH comes from mouse knockout and overexpression models. Overexpression of a human HIF2α active mutant in mice results in development of severe PH, associated with increased erythrocytosis and high degree of penetrance (Tan et al., 2013). Additional studies have shown that heterozygous global HIF2α knockout mice (Brusselmans et al., 2003) or EC specific HIF2α knockout mice (Cowburn et al., 2016) are protected from development of severe PH in the CH model. Recent evidence from EC specific PHD2 knockout models from four independent groups have implicated abnormal EC-HIF2α activation, but not HIF1α, in development of severe PH in mice (Dai et al., 2016), (Kapitsinou et al., 2016), (Wang et al., 2016), (Tang et al., 2017). The EC-PHD2 knockout led to activation of all HIFs specifically in ECs, which resulted in severe PH, progressing to right heart failure, accompanied by appearance of complex plexiform-like lesions similar to the complex lesions seen in human PAH. Further crossings with EC-specific HIF1α and HIF2α

knockout mice confirmed that the PAH phenotype was abrogated when PHD2 deficiency was combined with EC-HIF2α deletion, but not HIF1α, suggesting that HIF2α activation in ECs was the main driver of the phenotype. This clearly implicates increased activation of endothelial HIF2α in development of PAH. Further evidence was obtained from recent work assessing normoxic ECs and PASMCs isolated from PAH patients, which present with normoxic HIF2α activation in ECs, but not PASMCs (Tang et al., 2017). Overall, abnormal activation of HIF2α, especially in ECs, plays a potential role in vascular remodeling in the lungs, which appears to contribute to the pathogenesis of PAH.

1.2.7 Lysine Acetylation and Deacetylation in PH

Lysine (Lys, K) is an essential amino acid and its acetylation is an important post-translational modification that can affect both transcription and protein activity. There are more than 6,800 acetylation sites known in the mammalian proteome, affecting a wide range of proteins, including histones, enzymes and transcription factors (Choudhary et al., 2009), (Rauh et al., 2013). Lysine acetylation involves the addition of an acetyl group, from the cofactor acetyl-CoA, while deacetylation is the removal of that acetyl group. The acetylation reaction is mediated by two families of enzymes with opposing roles, the histone acetyltransferases (HATs) and histone deacetylases (HDACs). Acetylation of histone tail lysine, a tightly regulated process by HATs/HDACs, leads to enhanced transcription by weakening the interaction between the histone tail and DNA, thus increasing access of the transcriptional machinery. On the other hand, histone tail deacetylation favors transcriptional repression through chromatin compaction. Acetylation of non-histone targets, such as transcription factors, nuclear receptors or other enzymes, can lead to activation or repression of their function, depending on the

target and site of acetylation, and appears to be less stringently regulated compared to histone acetylation (Yoshida, Kudo, Kosono, & Ito, 2017), (Verdin & Ott, 2015).

While the name suggests they can only modify histones, it is very clear now that HATs/HDACs have both histone and non-histone targets (Yoshida et al., 2017). HATs are divided into two main types: type A are nuclear HATs and type B are cytoplasmic (Wapenaar & Dekker, 2016). Type B HATs are responsible for acetylation of cytoplasmic histones before their relocation to the nucleus and their integration into the DNA. Type A HATs are more abundant and are divided into five families based on their homology and function. These nuclear HATs are responsible for acetylation of nuclear proteins, including histones, as well as act as co-factors for some transcription factors. Some extensively studied HATs include p300, CREB (cAMP response element-binding protein), CBP (CREB-binding protein), and PCAF (p300/CBP associated factor) (Wapenaar & Dekker, 2016). On the other hand, HDACs are divided into four classes based on their homology to the yeast transcriptional repressors (**Table 1-4**). Classes I, II and IV are metal (zinc)-dependent deacetylases, while class III, the sirtuins, are dependent on NAD^+ hydrolysis to catalyze lysine deacetylation (Yoshida et al., 2017). Development of large numbers of HAT/HDAC inhibitors allowed better understanding of the role of acetylation on cell function.

Table 1-4: Histone deacetylase families and members

Class	Yeast Orthology	Mammalian Members
I	RPD3	HDAC1, HDAC2, HDAC3, HDAC8
IIa	HDA1	HDAC4, HDAC5, HDAC7, HDAC9
IIb	HDA1	HDAC6, HDAC10
III	Sir2	Nuclear: SIRT1, SIRT6, SIRT7 Cytoplasmic: SIRT2, Mitochondrial: SIRT3, SIRT4, SIRT5
IV	-	HDAC11

Adapted from (Yoshida et al., 2017), (Stratton & McKinsey, 2015)

Abnormal HDAC levels and activity have been identified in human PAH and rodent models. In IPAH patient lungs, HDAC1, 4 and 5 were elevated, while HDAC2 was decreased and HDAC3 and 7 levels were unchanged (L. Zhao et al., 2012), whereas recent work found that HDAC6 levels are elevated in human PAH lungs (Boucherat et al., 2017). Similar to human PAH, in the rat CH model, HDAC1, 5 were elevated in the lungs and RV of animals after 2 weeks of CH, while HDAC7 was elevated in the lungs and HDAC3 was decreased (L. Zhao et al., 2012), (Cavasin et al., 2012). HDAC1 levels were also elevated in lung tissue in the MCT + CH model (Lan et al., 2015). Assessment of HDACs class I & II activity revealed an overall decreased HDAC activity in the lungs of rats in the MCT and SUCH models, accompanied by an overall increase in RV HDAC activity in all models of PH (De Raaf et al., 2014). A recent assessment of HDAC6 revealed their elevation in rat distal pulmonary arteries in the SUCH and MCT models (Boucherat et al., 2017).

Several groups have modulated HDAC function in PH models in order to correct HDAC dysfunction and elicit a therapeutic effect (**Table 1-5**), with variable degrees of success. Assessment of the pan-HDAC inhibitor Trichostatin A (TSA) in the SUCH model showed no effect of TSA treatment on prevention or development of severe PAH (De Raaf et al., 2014), while use of another pan-HDAC inhibitor, suberoylanilide hydroxamic acid (SAHA), led to modest improvement in the CH rat model (L. Zhao et al., 2012) (**Table 1-5**). Studies conducted with more selective HDAC inhibitors showed some promise compared to pan-HDAC inhibitors. Treatment with the class I inhibitor valporic acid (VPA) resulted in reductions in the severity of the CH rat model (L. Zhao et al., 2012) and some effectiveness in reducing severity of the MCT model, though

pulmonary hemodynamics were assessed only by echocardiography (Cho et al., 2010). While more recent work shows efficacy for VPA in the MCT + CH model (Lan et al., 2015), the use of two different selective HDAC class I inhibitors, MGCD0103 and MS-275, led to great improvement in the CH model (Cavasin et al., 2012). Recently, assessment of the role of HDAC6 in PAH pathology determined that inhibition of HDAC6 using Tubastatin A leads to improved hemodynamics in the SUCH rat model and HDAC6 knockout mice developed milder CH-induced PH (Boucherat et al., 2017).

It should be noted that not all HDAC classes contribute similarly to PH pathology. Studies assessing Sirtuin 3 (SIRT3), a mitochondrial specific class III HDAC, implicated its absence in development of spontaneous PH in mice associated with hyper-acetylation of mitochondrial specific proteins (Paulin et al., 2014), while others found its absence had no effect on CH-induced PH (Waypa et al., 2013). Of note, a recent manuscript described that the class III HDAC Sirtuin 1 (SIRT1) knockout leads to exaggeration in RVSP, RVH and muscularization in response to CH, implicating SIRT1 in playing a protective role in CH-PH (Zurlo et al., 2018). Other studies have attempted activation of SIRT1 using resveratrol (RSV), a natural small polyphenol, or SRT1720a, a synthetic small molecule. Both were initially reported to directly enhance the catalytic activity of SIRT1 (Milne et al., 2007), (Howitz et al., 2003), (Feige et al., 2008), (Yamazaki, 2009), (Minor et al., 2011). Treatment with RSV led to improvement in MCT and CH rat models, while treatment with SRT1720 helped improve CH-induced PH (**Table 1-5**). However, it is still debatable whether RSV (Kaeberlein et al., 2005), (Borra, Smith, & Denu, 2005) or SRT1720 (Pacholec et al., 2010), (Huber, McBurney, Distefano, & McDonagh, 2010) can directly modulate the catalytic activity of SIRT1. The beneficial effects of RSV often

require SIRT1 (Boily, He, Pearce, Jardine, & McBurney, 2009) but the mechanisms responsible for its action remain unclear (Nakata, Takahashi, & Inoue, 2012). Overall, *in vivo* modulation of HDAC function using "specific" HDAC inhibitors leads to unpredictable and off-target effects. This accentuates the need for nonpharmacological validation approaches, such as the use of genetically modified animals in order to better understand the role of HDACs in PH.

Table 1-5: Manipulation of HDAC function in PH

HDAC Inhibitor	HDAC Class	Model	Findings	Reference
Pharmacological Inhibition				
Trichostatin A (TSA)	I, II	Rat SUCH	No efficacy	(De Raaf et al., 2014)
Suberoylanilide hydroxamic acid (SAHA)	I, II, IV	Rat CH	Improvement: ↓PAP, RVH	(L. Zhao et al., 2012)
Valporic Acid (VPA)	I	Rat MCT	Improvement: ↓RVH	(Cho et al., 2010)
		Rat CH	Improvement: ↓PAP, RVH	(L. Zhao et al., 2012)
		Rat MCT + CH	Improvement: ↓RVSP, RVH	(Lan et al., 2015)
MGCD0103	I (HDAC1/2/3)	Rat CH	Improvement: ↓PAP, PVRI, RVH	(Cavasin et al., 2012)
MS-275	I	Rat CH	Improvement: ↓PAP, RVH	(Cavasin et al., 2012)
Tubastatin A	IIb (HDAC6)	Rat SUCH	Improvement: ↓RVSP, mPAP, RVH	(Boucherat et al., 2017)
Resveratrol	III (SIRT1)	Rat CH	Improvement: ↓RVSP, RVH	(D. Xu et al., 2016)
		Rat CH	Improvement: ↓RVSP, RVH	(L. Yu et al., 2017)
		Rat CH	Improvement: ↓ RVH	(B. Chen et al., 2014)
		Rat MCT	Improvement: ↓RVSP, RVH	(S. Zhou et al., 2015)
		Rat MCT	Improvement: ↓RVSP, RVH	(D.-L. Yang et al., 2010)
SRT1720	III (SIRT1)	Rat CH	Improvement: ↓RVSP, RVH	(L. Yu et al., 2017)
Genetic Inhibition				
HDAC6 knockout	IIb (HDAC6)	Mouse CH	Improvement: ↓RVSP, mPAP	(Boucherat et al., 2017)
SIRT1 knockout	III (SIRT1)	Mouse CH	Worsening: ↑ RVSP, RVH	(Zurlo et al., 2018)
SIRT3 knockout	III (SIRT3)	Mouse PH	Worsening: ↑ RVSP	(Paulin et al., 2014)
		Spontaneous Mouse CH	No effect	(Waypa et al., 2013)

HDAC: Histone deacetylase, RVSP: Right ventricle systolic pressure, RVH: Right ventricle hypertrophy, CH: chronic hypoxia, SUCH: SU5416+CH, MCT: Monocrotaline

1.3 Sirtuin 1 (SIRT1)

The sirtuins are class III histone deacetylases which require NAD^+ as a cofactor for deacetylation and share a common conserved catalytic domain of about 250 amino acids (Imai, Armstrong, Kaeberlein, & Guarente, 2000), (Smith et al., 2000), (Landry et al., 2000), (Sacconnay, Carrupt, & Nurisso, 2016). This domain is conserved across species, with the yeast sir2 (silent information regulator 2) as the founding member of this family (Brachmann et al., 1995), (Chu, Chou, Zheng, Mirkin, & Rebbaa, 2005), (Frye, 2000). There are seven mammalian sirtuins, with SIRT1 as the member that most closely resembles the yeast sir2 and is thought to be its orthologue. SIRT1 is localized in the nucleus, yet appears to be able to relocate to the cytoplasm in some cases (Jin et al., 2007). SIRT1 is expressed in all tissues at variable levels (Lemieux et al., 2005) and has a wide range of acetylated protein substrates. Direct deacetylation and co-immunoprecipitation studies have identified many acetylated proteins as substrates for SIRT1 activity, including a large number of histone and non-histone proteins (McBurney, Clark-Knowles, Caron, & Gray, 2013). In particular, SIRT1 has been proposed to play a role in maintenance of vascular integrity and homeostasis through deacetylation of several vascular stabilizing targets (Guarani & Potente, 2010).

1.3.1 SIRT1 Substrate Selectivity

SIRT1 core catalytic domain and terminus structures have been described through computational models and the crystal structure of SIRT1 (Autiero, Costantini, & Colonna, 2008), (X. Zhao et al., 2013). Human SIRT1 appears to have a compact catalytic core and an organized allosteric site located in the middle of the protein

sequence, yet have a disordered and largely unstructured N- and C-terminal portions (Autiero et al., 2008), (X. Zhao et al., 2013). While similar catalytic core to the yeast sir2, the catalysis by SIRT1 is more complex since regions of the protein on both sides of the catalytic domain significantly modulate catalytic activity (Kang et al., 2011), (Pan, Yuan, Brent, Ding, & Marmorstein, 2012). Indeed, these unstructured N- and C- terminal domains appear to play a role in interacting with the catalytic core leading to enhanced substrate affinity (Kang et al., 2011). Hence, mammalian SIRT1 appears to play additional or alternative roles to the basic yeast sir2 protein.

In order to better understand the role of human SIRT1, many groups performed direct deacetylation, co-immunoprecipitation and attempted to activate or inhibit SIRT1 activity. This led to identification of over 71 acetylated histone and non-histone proteins as substrates for SIRT1 activity and implicated SIRT1 in a plethora of cellular functions (McBurney et al., 2013). Some of these targets include cytosolic proteins such as eNOS and PDK1; however, most targets for SIRT1 activity are nuclear. Nuclear targets include transcription factors such as HIFs, forkhead box proteins class O (FOXOs) and NF-kB. SIRT1 can also deacetylate p53, acetyltransferases, such as CREB and p300, and histones H1, H3 and H4 (McBurney et al., 2013). This wide range of targets suggests that SIRT1 activity regulates a large scope of cellular processes including apoptosis (Luo et al., 2001), (Vaziri et al., 2001), (Jin et al., 2007), (Lara et al., 2009), inflammation (S. R. Yang, 2007), and chromatin structure and epigenetic regulation (Pruitt et al., 2006), (O'Hagan, Mohammad, & Baylin, 2008).

Unbiased assessment of the complete acetylome in absence of SIRT1 was first described by Chen *et al* in *Sirt1*$^{-/-}$ mouse embryonic fibroblasts (Y. Chen et al., 2012).

Their work implicated SIRT1 in deacetylation of many targets involved in regulating DNA repair, cell cycle and RNA splicing as well as revealed hyper-acetylation of acetyltransferases in the absence of SIRT1 (Y. Chen et al., 2012). Another study took a biochemical approach and exposed acetylated lysine peptides to different recombinant human SIRT proteins, to determine the deacetylation ability and specificity of each sirtuin (Rauh et al., 2013). Surprisingly, and unlike other sirtuins, SIRT1 was found to be able to bind and deacetylate a large range of acetylated lysine targets, with little specificity to surrounding amino acid sequences (Rauh et al., 2013). Additional studies have assessed the acetylome in HeLa cells, HEK293 cells and even in mouse total liver tissue in absence of SIRT1 (S. Y. Kim et al., 2015), (Schölz et al., 2015), (Armour et al., 2013). Overall, these studies provided a large number of potential SIRT1 deacetylation targets and were able to confirm some of SIRT1 independently identified targets. However, many of the observations and conclusions about SIRT1 function, activity and targets were performed *in vitro* or in cancer cell lines, which limits the translation of these results to *in vivo* and normal systems.

1.3.2 Hypoxia Inducible Factors Deacetylation by SIRT1

SIRT1 can bind and deacetylate both HIF1α and HIF2α *in vitro*; however, there are conflicting reports about the extent that deacetylation modulates HIF stability and activity. Initial studies describe that SIRT1 deacetylated active HIF2α leading to its increased activity (Dioum et al., 2009). Following, Lim *et al* showed that two regions within the SIRT1 protein catalytic domain bound HIF1α and suggested that these regions are most likely responsible for deacetylation of HIF1α (Lim et al., 2010). However, the

authors proposed that this HIF1α deacetylation by SIRT1 would lead to HIF1α inactivation and subsequent degradation even under hypoxia; reducing its activity, while SIRT1 deficiency would lead to accumulation of HIF1α (Lim et al., 2010). A recent report showed a differential effect of SIRT1 deacetylation on HIF1α and HIF2α activity in ten different cancer cell lines (Yoon, Shin, Shin, Chun, & Park, 2014). In this report, SIRT1 was shown to deacetylate and inhibit HIF1α activity in hypoxia in all cell lines studied. Alternatively, there was a cell-line dependent relationship between SIRT1 and HIF2α, where SIRT1 could deacetylate and inhibit HIF2α activity in some cell lines, but deacetylate and enhance HIF2α activity in others (Yoon et al., 2014). Recent work in human PAECs showed that knockdown of SIRT1 using siRNA leads to increased acetylation, but not activity/accumulation, of HIF1α in hypoxia (P.-I. Chen et al., 2017). However, similar to other studies about SIRT1, these studies were performed *in vitro* or in cancer cell lines, which might possess aberrant SIRT1 function or abnormal hypoxic response.

1.3.3 SIRT1 in the Vasculature

SIRT1 is highly expressed in ECs and has been implicated in protection from senesce and maintenance of normal endothelial homeostatic function (Guo, Xu, & Wang, 2016), (D'Onofrio et al., 2015). SIRT1 can deacetylate and activate eNOS, modulating endothelial NO production (Potente et al., 2007). Furthermore, SIRT1 has been implicated in control of angiogenesis in ECs through deacetylation and inactivation of FoxO1, which negatively regulates angiogenesis (Daitoku et al., 2004). Inhibition of EC-SIRT1 leads to increased expression of p53 and its downstream target plasminogen

activator inhibitor-1 (PAI-1), which can lead to vascular remodeling and senescence (Ota et al., 2007), (Wan et al., 2014). SIRT1 can also suppress the proinflammatory signaling in ECs through deacetylation of NF-kB (Breitenstein et al., 2011). Loss of SIRT1 activity leads to dysregulated vascular SMC (VSMC) function, leading to senescence and apoptosis of VSMCs in vascular injury and atherosclerosis (L. Li et al., 2011), (Gorenne et al., 2013). Moreoever, age-related loss of SIRT1 protein expression in human SMCs correlates with a loss of capacity for vascular repair, diminished stress response, and increased senescence (Thompson, Wagner, & Rzucidlo, 2014). Overall, SIRT1 plays a protective role in maintenance of vascular EC & SMC function, homeostasis and health. However, most of these studies focus on the systemic, and not pulmonary, vasculature, creating a need to address the role of SIRT1 in the pulmonary vasculature and in the response to pulmonary vascular stress.

1.3.4 Animal Models of SIRT1 Overexpression or Deficiency

Several transgenic and knockout SIRT1 mice have been created in order to address the role of SIRT1 *in vivo*. Human SIRT1 (747a.a.) and mouse SIRT1 (734a.a.) have 86% homology at both protein and DNA level, while sharing a conserved NAD^+ domain. The SIRT1 knockout mouse was first created in 2003 by McBurney *et al.* through deletion of the *Sirt1* gene exons 5 and 6 (McBurney et al., 2003). No SIRT1 protein is detectable in $Sirt1^{-/-}$ cells carrying two knockout alleles. More recently, a mouse line carrying a point mutation in the *Sirt1* gene ($Sirt1^{Y}$, $Sirt1^{tm2.1Mcby}$) that encodes a SIRT1 protein with an H355Y substitution that ablates catalytic activity was created by the same group (Seifert et al., 2012). Mice homozygous for the mutant alleles, $Sirt1^{-/-}$ and

Sirt1$^{Y/Y}$, share the phenotypes of elevated rates of perinatal lethality, small stature, high rates of respiration and male infertility. However, these 2 mouse lines differ in other respects; for example, *Sirt1*$^{-/-}$ are female sterile while *Sirt1*$^{Y/Y}$ are female fertile, *Sirt1*$^{-/-}$ have an eyelid inflammatory phenotype while *Sirt1*$^{Y/Y}$ mice generally do not, and perinatal lethality is much lower in *Sirt1*$^{Y/Y}$ mice. Other groups have also created SIRT1 knockout lines and noted similar phenotypes (H.-L. Cheng et al., 2003). Cheng *et al* developed exon 4 deleted *Sirt1*$^{-/-}$ mice and noted increased perinatal lethality and hyper-acetylation of p53 *in vivo* (H.-L. Cheng et al., 2003). Subsequent assessment of SIRT1 knockout mice hearts revealed presence of mild dilated cardiomyopathy, smaller cardiomyocyte size and abnormalities in cardiomyocyte mitochondrial morphology and function (Planavila et al., 2012). Also, SIRT1 knockouts appear to have lower angiogenic abilities in their adipose tissue (F. Xu et al., 2012). Indeed, once SIRT1 mice survive the weaning period, if unchallenged, they show only mild differences in phenotype compared to SIRT1 competent mice and do not have a survival disadvantage. The presence of only mild phenotypes at baseline does not correlate with the large number of proposed targets and functions for SIRT1; yet, stressing SIRT1 deficient mice leads to a hypersensitive response to almost any perturbation. High fat diet treatment led to worse fatty liver and glucose intolerance in SIRT1 deficient mice (Pfluger, Herranz, Velasco-Miguel, Serrano, & Tschop, 2008), (Caron et al., 2014), (J. Cheng et al., 2017). Notably, chronic cigarette smoke exposure (Yao et al., 2012), ambient particulate matter air pollution exposure (Wu, Liu, Liang, & Fu, 2012), and cecal ligation and puncture (Gao et al., 2015) all lead to worse lung inflammation and vascular leak in absence of SIRT1. Alternatively, mice overexpressing SIRT1 are resistant to cigarette smoke induced emphysema (Yao et al.,

2012). Overall, SIRT1 plays a critical role in the stress response to various perturbations; however, there has been no assessment of the pulmonary circulation response to CH exposure in SIRT1 mouse models. Of note, two weeks prior to submission of this thesis for evaluation, a manuscript was published describing the effects of conditional SIRT1 knockout on the response to CH *in vivo* (Zurlo et al., 2018). The authors note an exaggeration in RVSP, RVH and muscularization in SIRT1 knockout mice compared to hypoxic controls (Zurlo et al., 2018).

CHAPTER 2: ROLE OF SIRT1 IN THE PULMONARY VASCULAR RESPONSE TO CHRONIC HYPOXIA: DEVELOPMENT OF A NOVEL PULMONARY HYPERTENSION MODEL

2.1 Introduction

PH defines a group of diseases with the common hemodynamic feature of increased mPAP at rest ≥ 25mmHg, assessed by right heart catheterization. The increased pulmonary pressures lead to increased RV workload, which results in RV thickening and ultimately decompensation and failure. PAH, or Group 1 PH, is a complex disease of the pulmonary vasculature that presents with increased PVR due to extensive pulmonary vascular remodeling, characterized by degenerative and proliferative changes leading to loss of the distal arteriolar microvascular bed.

The CH model is used as a surrogate to study PAH in transgenic animals allowing better understanding of PAH pathology. Several studies show dysregulation in genes involved in the oxygen-sensing pathway, mainly the HIFs, in PAH. HIFs are a family of hypoxic activated transcription factors which are master regulators of the adaptation to hypoxia. In addition to hypoxic response dysregulation, abnormal lysine acetylation and dysfunction of lysine deacetylases (HDACs) has been noted in PH human patients and animal models. However, *in vivo* modulation of deacetylases using pharmacological inhibitors leads to unpredictable and off-target effects. This accentuates the need for nonpharmacological validation approaches, such as the use of genetically modified animals in order to better understand the role of HDACs in PH.

SIRT1 is a protein deacetylase that has been proposed to play a role in maintenance of vascular integrity and homeostasis in ECs and SMCs through deacetylation of several vascular stabilizing targets. Furthermore, SIRT1 has been shown to be able to modulate the activities of HIFs and the hypoxic response. To date, a clear link between SIRT1 activity and PH pathogenesis has yet to be drawn.

2.2 Objective and Hypothesis

2.2.1 Objective:

- To explore the role of SIRT1 in the pulmonary vascular hypoxic response and the pathogenesis of CH-induced PH using loss-of-function transgenic mice

2.2.2 General Hypothesis:

- SIRT1 plays a protective role in pulmonary vascular homeostasis, and knockout or inactivation of SIRT1 will lead to an increased response to vascular stress and greater pathologic pulmonary vascular remodeling in the CH-induced mouse model of PH

2.3 Materials and Methods

2.3.1 Ethics statement:

All animal protocols and treatments were approved by the University of Ottawa Animal Care Ethics Committee and adhere to the Guidelines of the Canadian Council on Animal Care.

2.3.2 SIRT1 mice:

Two strains of SIRT1 mice were used in these studies: global SIRT1 knockout mice, *Sirt1*$^{-/-}$, and global SIRT1 mutant transgenic mice, *Sirt1*$^{Y/Y}$, which lack deacetylase activity. Both *Sirt1*$^{Y/Y}$ and *Sirt1*$^{-/-}$ mice were obtained from Dr. Michael W. McBurney of the Ottawa Hospital Research Institute Cancer Therapeutics Program, and have been described previously (Seifert et al., 2012), (McBurney et al., 2003).

2.3.2.1 Global SIRT1 catalytically inactive mice (*Sirt1*$^{Y/Y}$ also known as *Sirt1*^{mcby})

Sirt1$^{Y/Y}$ mice have a point mutation in their *Sirt1* gene, corresponding to the SIRT1 deacetylase catalytic domain. The point mutation in exon 5 leads to a single amino acid substitution from histidine (H) to tyrosine (Y) in position 355. This domain is identified to be evolutionary conserved and results in a non-functional SIRT1 protein, lacking deacetylase activity (Seifert et al., 2012). ***Phenotype***: Mice homozygous for the mutant *sirt1*$^{Y/Y}$ allele share the phenotypes of small stature, elevated rates of respiration and male infertility. These mice also exhibit early postnatal lethality, but to a lower extent than *Sirt1*$^{-/-}$ mice (below). ***Breeding strategy***: In order to reduce postnatal lethality, mice were cross bred on two lines (CD1 x 129svJ) to generate outbred mutant mice.

Heterozygous mice were crossed in order to generate homozygous *Sirt1*$^{Y/Y}$ mice. ***Genotyping***: Mice were ear tagged and ear notched for genotyping. Routine genotyping was carried out on ear notch DNA isolated using the REDextract-N-Amp^{TM} kit (Sigma, XNAT). The following primers were used: 5'-TGGAAGGAAAGCAATTTTGGT-3' and 5'-CTGAGTTACCTTAGCTTGGC-3'. Cycling conditions: 94ºC for 2min, 35 cycles [94ºC for 30 sec, 58ºC for 30 sec., 72ºC for 1min.], 72ºC for 5 min, 4ºC hold. This reaction amplifies a 236bp fragment from the *sirt1+* allele and a 422bp fragment from the *sirt1Y* allele. The difference is due to the remnants of the loxP site and adjoining sequences. ***Technical Assistance***: Animal breeding was performed by Danielle Dewar-Darch. Genotyping was performed by Karen Jardine.

2.3.2.2 Global SIRT1 knockout mice (*Sirt1*$^{-/-}$)

Sirt1$^{-/-}$ mice do not have any SIRT1 protein due to the deletion of exons 5 and 6 of the *Sirt1* gene (McBurney et al., 2003)(**Supplemental Figure 1, Appendix**). ***Phenotype***: Mice homozygous for the mutant alleles, *sirt1*$^{-/-}$, share the phenotypes of small stature, elevated rates of respiration, male and female infertility and high early postnatal lethality. They also have an eyelid developmental defect. ***Breeding strategy***: In order to reduce prenatal lethality, mice were cross bred on two lines (CD1 x 129svJ) to generate outbred mutant mice. Heterozygous mice were crossed in order to generate homozygous *Sirt1*$^{-/-}$ mice. ***Genotyping***: Mice were ear tagged and ear notched for genotyping. Routine genotyping was carried out on ear notch DNA isolated using the REDextract-N-Amp^{TM} kit (Sigma, XNAT). PCR primer sequences were designed to amplify the wildtype *Sirt1* and the deleted *Sirt1*: Both Forward: 5'TTCACATTGCATGTGTGTGTG3' Wildtype

Reverse: 5'TAGCCTGCGTAGTGTTGGTG3' and knockout Reverse: 5-ATTTGGTAGGGACCCAAAGG3'. Cycling conditions: 94ºC for 2min, 35 cycles [94ºC for 30 sec, 58ºC for 30 sec., 72ºC for 1min.], 72ºC for 5 min, 4ºC hold. Primers amplify a 423-bp fragment from the normal *sirt1*+ allele whereas a 526-bp fragment from the null allele is amplified. ***Technical Assistance***: Animal breeding was performed by Danielle Dewar-Darch. Genotyping was performed by Karen Jardine.

2.3.3 The CH model:

2.3.3.1 CH setup

Hypoxia was maintained at 9% oxygen using a ventilated chamber in which nitrogen is injected under the control of an Oxycycler controller (Biospherix, Lacona, NY). A liquid nitrogen tank (120L, Linde gas) or a gas tank (T-size, Linde gas) was used as a source of nitrogen gas. A dual stage nitrogen gas regulator was connected to the gas outlet on the tank and maintained at an input pressure of 8PSIG. The gas passed through the regulator, which was connected to an oxygen sensor. The sensor measured oxygen levels inside the chamber and relayed the information to the regulator which controlled the nitrogen gas input. A small fan inside the chamber helped improve gas circulation. Two vents, one on the front right and one on the front left of the chamber, allowed gas exchange with the room and acted as a way to prevent CO_2 accumulation in the chamber. The O_2 sensor was calibrated using manufacturer's instructions using 100% nitrogen gas (used as 0% O_2 control) and room air (used as 20.9% O_2 control). The gas pressure inside the chamber was not modified making it a normobaric hypoxic treatment.

At the start of each experiment, fresh cages, food and water were provided. A maximum of six cages were placed inside the chamber, with a maximum of four mice per cage. Once the cages were placed inside the chamber, the door was sealed and the gas was turned ON. The chamber reached 9% O_2 within 30mins. The chamber was opened after seven days, and weekly thereafter, to change cages, food and water. Body weight measurements were also assessed at that point.

2.3.3.1 Animal CH exposure:

In three week hypoxia experiments, *Sirt1*$^{Y/Y}$ mice (5-7 weeks-old, male and female), *Sirt1*$^{-/-}$ mice (5-10 weeks-old, female) and wildtype *Sirt1*$^{+/+}$ littermates were exposed to either room air or to CH for 21 days. In one week experiments, *Sirt1*$^{Y/Y}$ mice (5-7 weeks-old, female), and wildtype *Sirt1*$^{+/+}$ littermates were sacrificed after 7 days of CH. In five week experiments, *Sirt1*$^{Y/Y}$ mice (5-7 weeks-old female), and wildtype *Sirt1*$^{+/+}$ littermates were kept in the hypoxic chamber for 5 weeks before assessment. In the reversal study, *Sirt1*$^{Y/Y}$ mice (5-7 weeks-old, female), and wildtype *Sirt1*$^{+/+}$ littermates were exposed to 21 days of hypoxia, relocated to room air for 14 days of normoxia, before end of study measurements. All mice were fed regular chow (Harlan) and housed in a 12hr/12hr dark light cycle.

2.3.4 Study endpoint pressure assessment and tissue collection:

2.3.4.1 Pressure measurements:

At experimental endpoint, mice were anaesthetized using an intraperitoneal injection of ketamine (100 mg/kg, Ketalean, DIN 00612316) and xylazine (10 mg/kg,

Rompun, DIN 02169592). The upper thoracic area was shaved and the animal was placed on its back on a flat platform under a dissecting microscope. A small incision was made from the animal's chin down to the right armpit and the jugular vein was exposed, subsequently, the jugular vein was tied off tightly at the cranial end, loosely tied at the caudal end, and a small, medial incision was made in the vein. Right ventricular pressure was measured by threading a 1.2 French pressure microtip catheter transducer (Transonic-Scisense, FTS-1211B-0018) and proper readings were determined by observing sequential pressure loops recorded on LabScribe2 software (iWorx-Scisense). After RV pressure measurements, the carotid artery was exposed and the catheter was inserted to measure pressure in the aortic arch. Mean right ventricle systolic pressure (RVSP) was determined by taking the average of 3-5 readings that represent a single breathing cycle in the mouse. The mean arterial pressure (MAP) was assessed using the equation: DAP+(1/3(SAP-DAP)); where SAP is systolic arterial pressure and DAP is diastolic arterial pressure. ***Technical Assistance***: Catheterization was performed by Dr. Yupu Deng, in a blinded manner.

2.3.4.2 Blood collection for plasma and hematocrit (HCT) assessment

Following hemodynamic assessment, the abdominal cavity was exposed and blood was collected from the inferior vena cava using heparinized or EDTA treated syringes. The blood was placed on ice after which it was centrifuged at 2000xg for 30mins to isolate plasma. Plasma samples were collected and stored at -80^{o}C. HCT levels were determined by using heparinized HCT tubes (Drummond Scientific, Broomall, PA). The tubes were filled with blood from the inferior vena cava and one end was sealed. The

tubes were then centrifuged in a capillary tube centrifuge for 10 mins to allow separation of plasma and red blood cells (RBCs). Levels of RBCs and total plasma were marked on a line and measured. HCT was expressed as a percent of RBC to total blood using the equation: (Distance from end of line to edge of RBC line/ Distance from end of line to edge of plasma line) x100. ***Technical Assistance***: Plasma collection and HCT tube preparation was performed in part by Dr. Ken Schlosser.

2.3.4.3 Abdominal tissue (spleen, kidney, liver) collection

Following blood collection, mice were exsanguinated by cutting the abdominal aorta. The right kidney was removed and cut transversely into two pieces. One piece was placed in a 2mL cryogenic tube (Corning/Fisher, C430488) and flash frozen in liquid nitrogen while the other piece was placed in 4% paraformaldehyde (PFA, Appendix). The spleen was removed and cleared of connective tissue, then weighed and cut into four pieces. The middle two pieces were placed in 4% PFA for fixation. Finally, the liver was dissected out and cut into a small cube ~5x5x5cm and placed in 4% PFA.

2.3.4.4 Lung tissue collection

After abdominal tissue collection, the chest cavity was opened and the four right lobes were clamped off at the level of the right bronchus. The four lobes were dissected out, and each was cut into two equal sized pieces. For protein assessment, four halves were placed in a cryogenic tube and flash frozen in liquid nitrogen, later stored at -80ºC. For RNA assessment, the other four lung halves were placed in RNAlater® stabilizing solution (Ambion, AM7021) and kept on ice. The samples were incubated at 4ºC

overnight, and then moved to -80ºC for storage. To collect the left lung tissue for histological assessment, the animal was rotated to face the collector and the trachea was exposed. The left lobe was slowly inflated with 1mL of a 1:1 mixture of saline: OCT freezing solution (VWR, CA95057-838). After adequate inflation, the lung was carefully excised and cut transversely into 5 pieces. The second and fourth pieces were placed in 4% PFA for fixation, while other pieces were organized on Surgipath Clear disposable base molds (Leica Biosystems, 3803065) and placed on dry ice. After immobilization of the tissue samples, they were covered with OCT and allowed to freeze on dry ice. The samples were wrapped with parafilm (Fisher, 13-374-10) and stored at -80ºC.

2.3.4.5 Assessment of right and left ventricle weight and heart tissue collection

The heart was removed from the chest cavity. A blinded operator removed the atria, aorta and pulmonary trunk and dissected out the right ventricle, while keeping the left ventricle plus septum intact. The weight of each piece was recorded after which the tissue was placed in a cryogenic tube, snap frozen in liquid nitrogen then stored at -80ºC. Right ventricle hypertrophy (RVH, Fulton index) was calculated using the equation: Right ventricle weight / (left ventricle plus septum) weight (RV/LV+S). ***Technical Assistance***: RV dissection was performed by Dr. Yupu Deng, in a blinded manner.

2.3.5 Tissue processing for histological assessment:

2.3.5.1 Paraffin embedding:

Tissues harvested for histopathological assessments were kept overnight in 4% PFA at 4ºC. The following morning, tissues was transferred into Tru-Flow tissue

cassettes (Fisher, 15-200-403A), and washed in a beaker with 1x phosphate buffered saline (PBS; Sigma P5493) for 8 hours at 4ºC on a shaker. Subsequently, the PBS was changed to 70% ethanol (Greenfield Ethanol Inc, PO16eaan) and stored at 4ºC for at least 24hrs before processing. The tissue was processed overnight using a tissue processor (Leica, ASP300S). The tissue was immersed for one hour in each different solution based on the following protocol: 70% EtOH (3x), 80% EtOH, 95% EtOH, 100% EtOH (3x), 100% xylene (3x, Fisher, X3S-4) and finally immersed in paraffin (62°C, 3x) (TissuePrep Embedding Media, Fisher, T565). The following morning, the tissue was taken out of the processor and embedded in paraffin blocks using an embedding station (Leica embedding station, Leica Microsystems, Wetzlar, Germany).

2.3.5.2 Tissue sectioning

Paraffin blocks were pre-chilled on ice and sliced into 5µm sections using a microtome (RM2255, Microm, HM 330, Leica Microsystems, Wetzlar, Germany). The sections were transferred to a container with 70% ethanol and then to a 43°C water bath. The sections were then carefully mounted onto glass slides (Superfrost® Excell microscope slides, Fisher, 12-550-15) and dried in a 37°C incubator overnight. ***Technical Assistance***: Part of the tissue sectioning was done with help from Anli Yang.

2.3.6 Histological Assessment:

For all histological analyses, 5µm paraffin-embedded tissue sections were deparaffinized using sequential dips in: 100% xylene (1x, 10mins, 2x 5mins), then

rehydrated in graded ethanol (2x100% 2mins, 90% 1min, 70% 1min) and immersed in double distilled water (ddH_2O, 2x5min)

2.3.6.1 Hematoxylin and eosin (H&E) staining:

Following deparaffinization and rehydration, tissue sections were stained with concentrated hematoxylin QS (VectorLabs, H-3404) for 10 mins. Subsequently, the sections were rinsed under tap water for 5 mins. Hematoxylin-stained tissue sections were placed in acid alcohol (Appendix) for 5 mins, rinsed under tap water for 5 mins, soaked in Scott's solution (Appendix) for 5 mins, rinsed under tap water for 5 mins, stained with eosin (Fisher, E-511) for 3 mins, and finally rinsed under tap water for another 5 mins. H&E stained lung sections were dehydrated by sequential dips in graded ethanol followed by immersion in 100% xylene (2 x 5 min). Tissue sections were sealed with Cytoseal XYL (Thermo scientific, 8312-4), a xylene-based mounting medium, coverslipped, and left inside the fume hood overnight to allow xylene fumes to evaporate. Slides were stored at RT and imaged using the Scanscope (Olympus)

2.3.6.2 α-smooth muscle actin (α-SMA) immunofluorescence staining:

Tissue slides were deparaffinized/rehydrated as above, then were immersed in a citric acid based antigen unmasking solution in ddH_2O (1:100, VectorLabs, H-3300) and boiled in a microwave for 12 mins for antigen retrieval. After cooling to RT for 30 mins, slides were washed twice in 1xPBS for 5 mins then once in ddH2O. The tissue was circled with a PAP pen (Super PAP Pen, Thermo Fisher Scientific, 00-8899) to create a hydrophobic region around the tissue to maintain the liquid on the tissue. The tissue was

subsequently permeabilized in 0.25% Triton-X100 for 15 mins (Sigma-Aldrich, T8787). A blocking solution consisting of 3% bovine serum albumin (Cell Signalling Technology, 9998S) and 5% normal goat serum (Cell Signaling Technology, 5425S) was applied for 90 mins at room temperature in a humidified chamber. Monoclonal mouse anti-α-smooth muscle actin (α-SMA)-Cy3 (Sigma Aldrich, C6198) antibody was incubated 2hrs at RT (1:200). The antibody was tapped off and slides washed in PBS 3x5mins. The tissue was then counterstained with DAPI diluted in 1xPBS (Sigma, D9542-5MG, 1:4000) for 15 mins. Tissue was washed with 1xPBS four times for 5 mins, then sealed using Fluorescence mounting medium (DAKO, S3023). Slides were stored in the dark at 4ºC.

2.3.6.3 Pulmonary Vascular Remodeling assessment:

Tissue slides stained with α-SMA and DAPI were imaged using the Cellomics Arrayscan (Thermo Fisher). For muscularization analysis, all vessels were analyzed in each animal lung cross section. The vessels were identified by presence of RBCs (auto-fluorescence) and were categorized as nonmuscularized (no apparent muscle), partially muscularized (with only a crescent of muscle) or fully muscularized (with a complete medial coat of muscle) (**Supplemental Figure 2, Appendix**).

2.3.7 Statistical analysis

All data are presented as mean ± standard error of the mean (SEM). Statistical analysis was performed using a one-way analysis of variance (ANOVA) with a Sidak's multiple comparisons test for multiple group comparison, using GraphPad Prism 7.02 statistical software. A statistically significant difference was accepted at $p<0.05$.

2.4 Results

2.4.1 SIRT1 knockout or inactivation worsens CH-induced PH

To investigate the involvement of SIRT1 deacetylase activity in CH-induced PH, we used the catalytically inactive SIRT1 mutant (*Sirt1*$^{Y/Y}$) transgenic mice. No differences in baseline right ventricle systolic pressure (RVSP) were observed between the SIRT1 mutant transgenic mice and their wild type littermates (*Sirt1*$^{+/+}$) in normoxia; however, *Sirt1*$^{Y/Y}$ mutants exhibited a significantly greater increase in RVSP compared to *Sirt1*$^{+/+}$ control mice after three weeks of CH (**Figure 2-1A**). A similar hemodynamic response was observed in the SIRT1 knockout mice (*Sirt1*$^{-/-}$), which displayed significantly higher RVSP compared to *Sirt1*$^{+/+}$ controls after 3 weeks of CH (**Figure 2-1B**). RVH, presented as the weight ratio of the RV to the left ventricle plus septum (LV+S), was comparable between mutants and wildtypes in normoxia; however, worse RVH was observed in *Sirt1*$^{Y/Y}$ mice compared to *Sirt1*$^{+/+}$ after three weeks of CH (**Figure 2-1C**) and similar findings were observed in the *Sirt1*$^{-/-}$ mice in response to CH (**Figure 2-1D**). Normalization of RV weight to the final body weight, instead of LV+S weight, further confirmed these findings (**Supplemental Table 1, Appendix**). Assessment of systemic arterial pressure revealed a similar drop in systolic (SAP) and mean (MAP) arterial pressure in CH animals, yet no significant differences between *Sirt1*$^{+/+}$, *Sirt1*$^{Y/Y}$, or *Sirt1*$^{-/-}$ mice in CH (**Table 2-1**). Overall, the data are consistent with a protective role for SIRT1 in CH-induced PH, where in its absence, an exaggerated CH-PH phenotype develops.

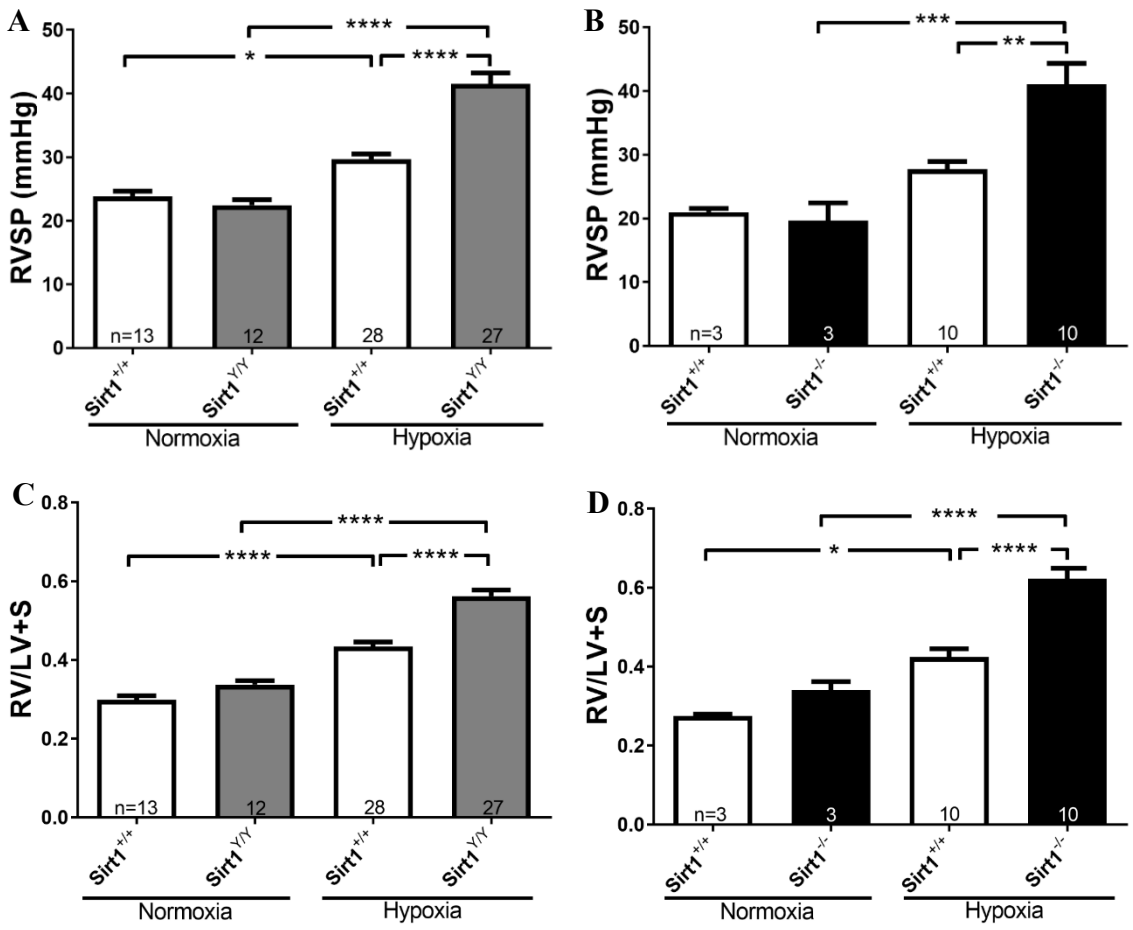

Figure 2-1: Right ventricle pressure and hypertrophy in *Sirt1*$^{+/+}$, *Sirt1*$^{Y/Y}$ and *Sirt1*$^{-/-}$ mice after three weeks of normoxia or chronic hypoxia. **A**) Right ventricle systolic pressure (RVSP) in *Sirt1*$^{Y/Y}$ and their *Sirt1*$^{+/+}$ littermates. **B**) RVSP in *Sirt1*$^{-/-}$ and their *Sirt1*$^{+/+}$ littermates. **C**) The weight ratio of the right ventricle (RV) to the left ventricle and septum (LV+S) in *Sirt1*$^{Y/Y}$ and their *Sirt1*$^{+/+}$ littermates (RV/LV+S). **D**) The RV/(LV+S) weight ratio in *Sirt1*$^{-/-}$ and their *Sirt1*$^{+/+}$ littermates. n number indicated on bars. *p<0.05, **p<0.01, ***p<0.001, ****p<0.0001.

Table 2-1: **Systemic pressure in *Sirt1*$^{+/+}$, *Sirt1*$^{Y/Y}$ and *Sirt1*$^{-/-}$ mice after three weeks of normoxia or chronic hypoxia**

Treatment	Strain	N number	SAP (mmHg)	MAP (mmHg)
Normoxia	*Sirt1*$^{+/+}$	7	110.3±7.4	87.4±5.5
	Sirt1$^{Y/Y}$	8	120.8±14.3	92.7±11.2
Chronic Hypoxia (3 weeks)	*Sirt1*$^{+/+}$	22	80.9±1.6*	57.4±1.9*
	Sirt1$^{Y/Y}$	16	81.2±2.5*	60.7±2.8*
	Sirt1$^{-/-}$	9	83.9±4.0	63.9±5.0

SAP: Systolic Arterial Pressure; **MAP**: Mean Arterial Pressure, *p<0.05 vs. normoxia

2.4.2 SIRT1 knockout or inactivation exaggerates CH-induced pulmonary vascular remodeling

Examination of lung histology did not reveal any pulmonary vascular or non-vascular abnormalities in SIRT1 mice under normoxic conditions. Following three weeks of CH, we were able to observe muscularization of arterioles in H&E sections (**Figure 2-2A-B**), which was confirmed using α-smooth muscle actin (α-SMA) staining to highlight the muscularized vessels (**Figure 2-2C**). Quantification of pulmonary vascular remodeling using α-SMA staining (**Supplemental Figure 2, Appendix**) revealed a significant decrease in the percent of nonmuscular small (<50μm) and mid-sized (50-100μm) arterioles in CH-*Sirt1*$^{+/+}$ and CH-*Sirt1*$^{Y/Y}$ mice (**Figure 2-2D-E**, *p<0.05 vs normoxia) but not in larger arterioles (>100 μm, **Figure 2-2F**). This was accompanied by a statistically significant increase in the percentage of partially muscular small arterioles (<50μm) in hypoxia (**Figure 2-2D**, *p<0.05 vs normoxia). Interestingly, hypoxic *Sirt1*$^{Y/Y}$ and hypoxic *Sirt1*$^{-/-}$ mice had significantly less non-muscular <50μm arterioles accompanied by increased <50μm partially muscular arterioles, compared to *Sirt1*$^{+/+}$ in hypoxia (**Figure 2-2D**, +p<0.05 vs CH-*Sirt1*$^{+/+}$). Further assessment of pulmonary vascular remodeling and vascular bed integrity using FMA revealed microvascular pruning in CH-*Sirt1*$^{Y/Y}$ mouse lungs compared to CH-*Sirt1*$^{+/+}$ (**Supplemental Figure 3, Appendix**). This was accompanied by abnormalities in vascular structure and a lack of perfusion to the smaller capillaries in the lungs of the mutant transgenic mice, suggesting dysregulated angiogenesis and possible "drop-out" of distal arterioles (**Supplemental Figure 3, Appendix**). These findings implicate SIRT1 in the regulation of pulmonary vascular remodeling in response to CH, where the lack of SIRT1 activity leads to higher

vascular muscularization and pruning of the small arterioles in the lungs, contributing to a more severe PH phenotype.

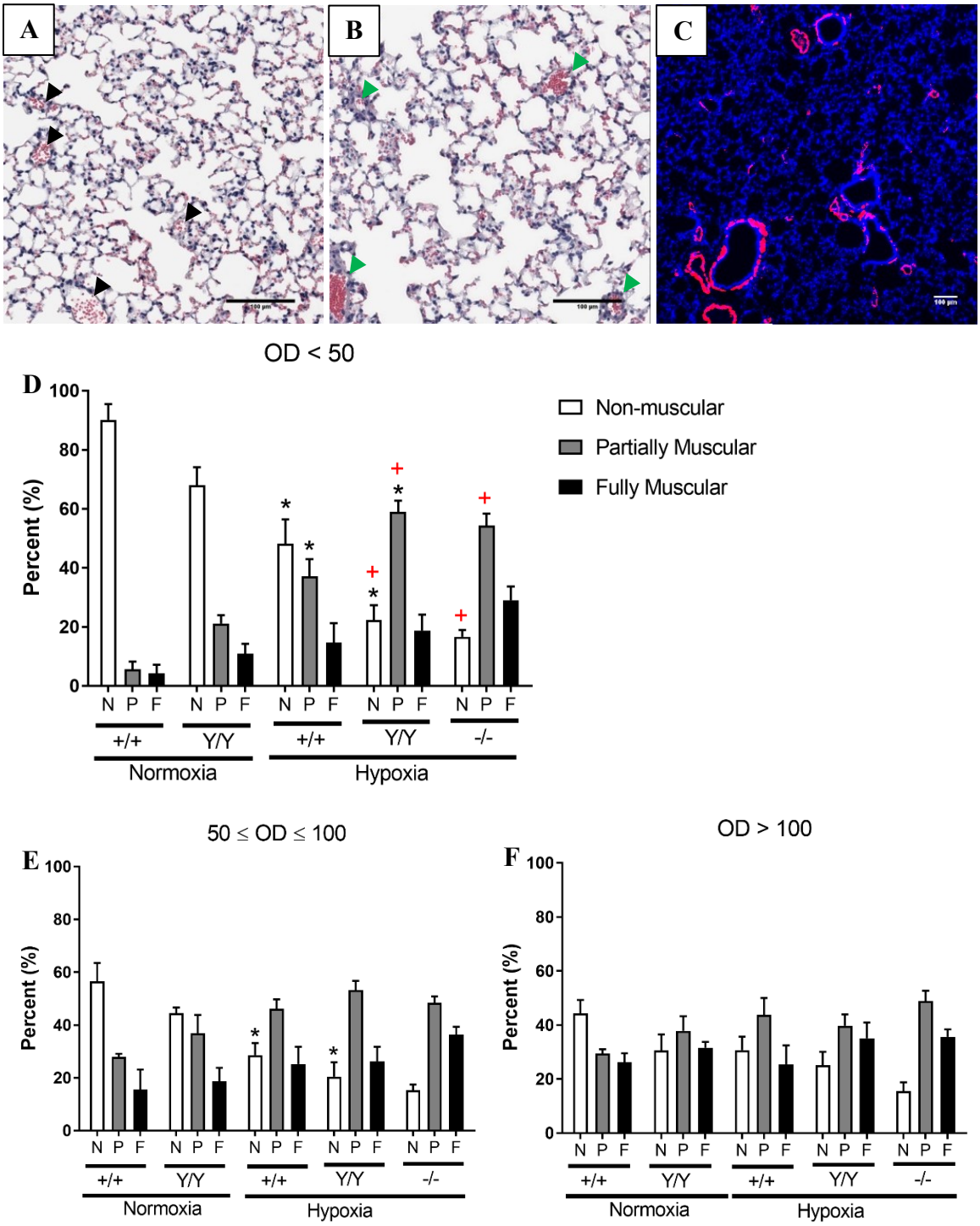

Figure 2-2: Histological and muscularization assessment of *Sirt1*$^{+/+}$, *Sirt1*$^{Y/Y}$ and *Sirt1*$^{-/-}$ mice lungs after three weeks of normoxia or chronic hypoxia. A) Representative photomicrograph of lung tissue showing normal lung vessels (black arrows) **B**) Representative photomicrograph of lung tissue showing muscularized vessels after hypoxia (green arrows). **C**) Representative photomicrograph of lung tissue showing muscularized vessels stained using α-smooth muscle actin (Red) after hypoxia, counterstained with DAPI (Blue). Scale is 100μm. **D-F**) Quantification of muscularized vessels with outer diameter (OD) smaller than 50μm (**D**), OD between 50-100μm (**E**) and OD larger than 100μm (**F**) using α-SMA staining. *$p<0.05$ vs. normoxic controls. +$p<0.05$ versus CH-*Sirt1*$^{+/+}$ mice. n=3-8 mice per group.

2.4.3 SIRT1 knockout or inactivation exacerbates hypoxia-induced erythrocytosis

Increased RBC production, or erythrocytosis, is part of the adaptive response to prolonged exposure to hypoxia (Koh & Powis, 2012). *Sirt1*$^{+/+}$ mice show an increase in hematocrit (HCT), the percent volume of RBCs in total blood, after three weeks of exposure to CH (from 40% to 59%, p<0.0001) (**Figure 2-3A**). Remarkably, both *Sirt1*$^{Y/Y}$ and *Sirt1*$^{-/-}$ mice, which exhibited similar baseline HCT levels as *Sirt1*$^{+/+}$ at normoxia, developed significantly higher HCT levels in hypoxia, both reaching a mean of 71% (**Figure 2-3**). In addition, hypoxic *Sirt1*$^{Y/Y}$ and *Sirt1*$^{-/-}$ mice developed splenomegaly, evident by the doubled spleen/BW weight ratio, which was not observed in the hypoxic *Sirt1*$^{+/+}$ animals (**Supplemental Table 2, Appendix**). It appears that in absence of SIRT1 activity there is exacerbated hypoxic erythrocytosis leading to higher HCT levels.

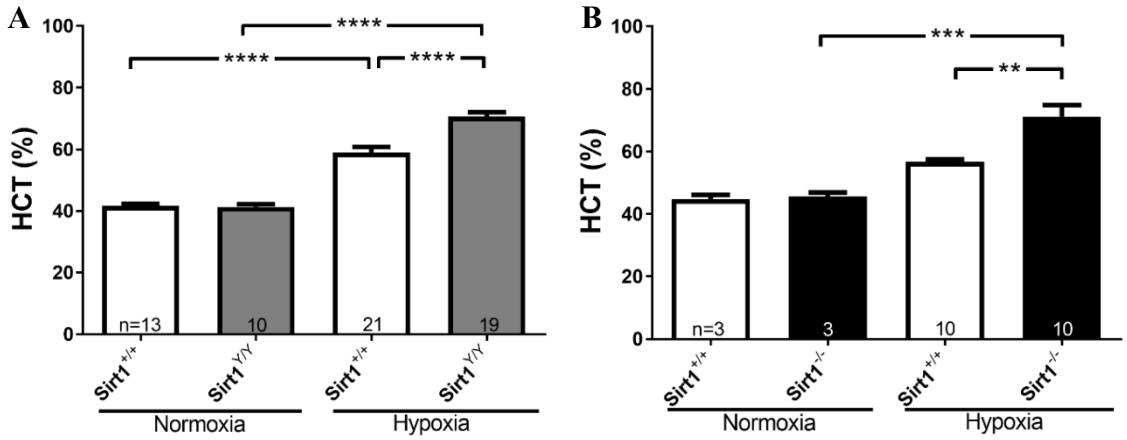

Figure 2-3: Hematocrit levels in *Sirt1*$^{+/+}$, *Sirt1*$^{Y/Y}$ and *Sirt1*$^{-/-}$ mice after three weeks of normoxia or chronic hypoxia. **A**) HCT (hematocrit) levels in *Sirt1*$^{+/+}$ or *Sirt1*$^{Y/Y}$ mice. **B**) HCT levels in *Sirt1*$^{+/+}$ or *Sirt1*$^{-/-}$ mice. n number indicated on bars. *p<0.05, **p<0.01, ***p<0.001, ****p<0.0001.

2.4.4 The exaggerated hypoxic response in absence of SIRT1 activity is reversible upon re-exposure to normoxia

To determine the reversibility of the exaggerated response to hypoxia, we returned *Sirt1*$^{+/+}$ and *Sirt1*$^{Y/Y}$ mice to normoxia after an initial three-week exposure to hypoxia (or maintained them in hypoxia) for an additional two weeks. The exposure to normoxic conditions for two weeks led to normalization of RVSP near baseline levels in both *Sirt1*$^{+/+}$ and *Sirt1*$^{Y/Y}$ animals (**Figure 2-4A**), while the RVSP increased further in hypoxic animals at 5 weeks (**Figure 2-4A**). Interestingly, the increased RVSP in *Sirt1*$^{Y/Y}$ compared to wild-type mice at three weeks (**Figure 2-1A**) was lost at five weeks, due to a partial "catch up" by the *Sirt1*$^{+/+}$ animals (**Figure 2-4A**). RVH also normalized in *Sirt1*$^{+/+}$ and *Sirt1*$^{Y/Y}$ mice that were returned to normoxia, with a trend towards higher RVH in *Sirt1*$^{Y/Y}$ mice (**Figure 2-4B**). Mice exposed to CH for 5 weeks continued to show elevated RVH, which was exacerbated in *Sirt1*$^{Y/Y}$ mice (**Figure 2-4B**). HCT levels also normalized in all mice returned to normoxia, while elevated HCT levels in hypoxic animals were maintained and further increased in *Sirt1*$^{Y/Y}$ mice compared to *Sirt1*$^{+/+}$ controls (**Figure 2-4C**). Finally, lung remodeling returned to normal following 2 weeks of normoxia (**Figure 2-4D-E**), while animals exposed to further hypoxia continued to exhibit arterial muscularization (**Figure 2-4F-G**). This reversibility upon re-location to normoxia, even with the exaggerated CH-PH in SIRT1 mice, suggests that while SIRT1 plays a role in modulation of the hypoxic response, its inactivation does not lead to irreversible pathological consequences.

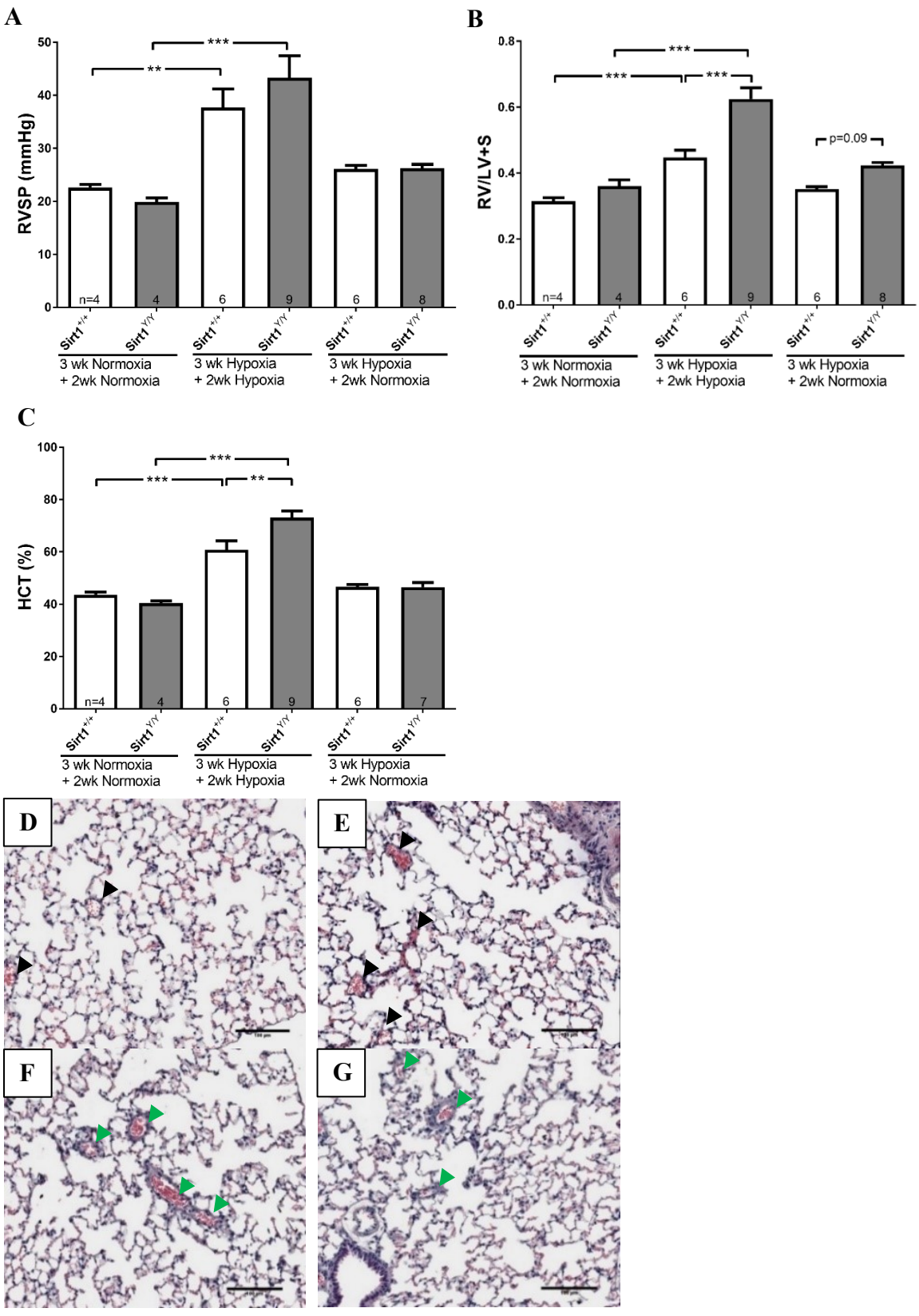
A
RVSP (mmHg)
50
40
30
20
10
0
**
***
n=4
4
6
9
6
8
Sirt1+/+
Sirt1V/V
3 wk Normoxia
+ 2wk Normoxia
3 wk Hypoxia
+ 2wk Hypoxia
3 wk Hypoxia
+ 2wk Normoxia
B
RV/LV+S
0.8
0.6
0.4
0.2
0.0
***
***
***
p=0.09
n=4
4
6
9
6
8
Sirt1+/+
Sirt1V/V
3 wk Normoxia
+ 2wk Normoxia
3 wk Hypoxia
+ 2wk Hypoxia
3 wk Hypoxia
+ 2wk Normoxia
C
HCT (%)
100
80
60
40
20
0
***
***
**
n=4
4
6
9
6
7
Sirt1+/+
Sirt1V/V
3 wk Normoxia
+ 2wk Normoxia
3 wk Hypoxia
+ 2wk Hypoxia
3 wk Hypoxia
+ 2wk Normoxia
D
E
F
G

Figure 2-4: Hemodynamic, hematocrit and histological assessment of *Sirt1*$^{+/+}$ and *Sirt1*$^{Y/Y}$ mice after five weeks of hypoxia or relocation to normoxia for two weeks, following three initial weeks of hypoxia. **A**) Right ventricle systolic pressure (RVSP) in *Sirt1*$^{+/+}$ and *Sirt1*$^{Y/Y}$ mice. **B**) The right ventricle (RV) to the left ventricle and septum (LV+S) in *Sirt1*$^{+/+}$ and *Sirt1*$^{Y/Y}$ mice. **C**) Hematocrit (HCT) levels in *Sirt1*$^{+/+}$ and *Sirt1*$^{Y/Y}$ mice. **D-E**) Representative photomicrographs of *Sirt1*$^{+/+}$ (**D**) and *Sirt1*$^{Y/Y}$ (**E**) lung tissue showing return of muscular vessels to normal (black arrows). **F-G**) Representative photomicrographs of *Sirt1*$^{+/+}$ (**F**) and *Sirt1*$^{Y/Y}$ (**G**) lung tissue showing muscularized vessels at 5 weeks of hypoxia (green arrows). Scale is 100µm. wk=week. n number indicated on bars. *p<0.05, **p<0.01, ***p<0.001.

2.4.5 The exaggerated hypoxic response in absence of SIRT1 activity appears as early as one week of hypoxic exposure

To determine the timeline of development of the exaggerated hypoxic response, we placed *Sirt1*$^{+/+}$ and *Sirt1*$^{Y/Y}$ mice in hypoxia for one day or one week. After only one day of hypoxic exposure, animals did not exhibit any increases in RVSP, RVH or HCT (**Supplemental Figure 4, Appendix**), suggesting that development of PH pathology requires a longer CH exposure. However, a one-week CH exposure resulted in a significant increase in RVSP in *Sirt1*$^{+/+}$ mice, which was higher in *Sirt1*$^{Y/Y}$ mice (**Figure 2-5A**). Similarly, the RVH was exacerbated in hypoxic *Sirt1*$^{Y/Y}$ mice versus *Sirt1*$^{+/+}$ controls (**Figure 2-5B**). Interestingly, there was no significant difference between *Sirt1*$^{+/+}$ and *Sirt1*$^{Y/Y}$ mice in HCT, which increased in response to one week of CH to the same extent (**Figure 2-5C**). This suggests that the loss of SIRT1 activity plays a role in the early pulmonary response to CH, but its effect on systemic HCT takes longer than one week.

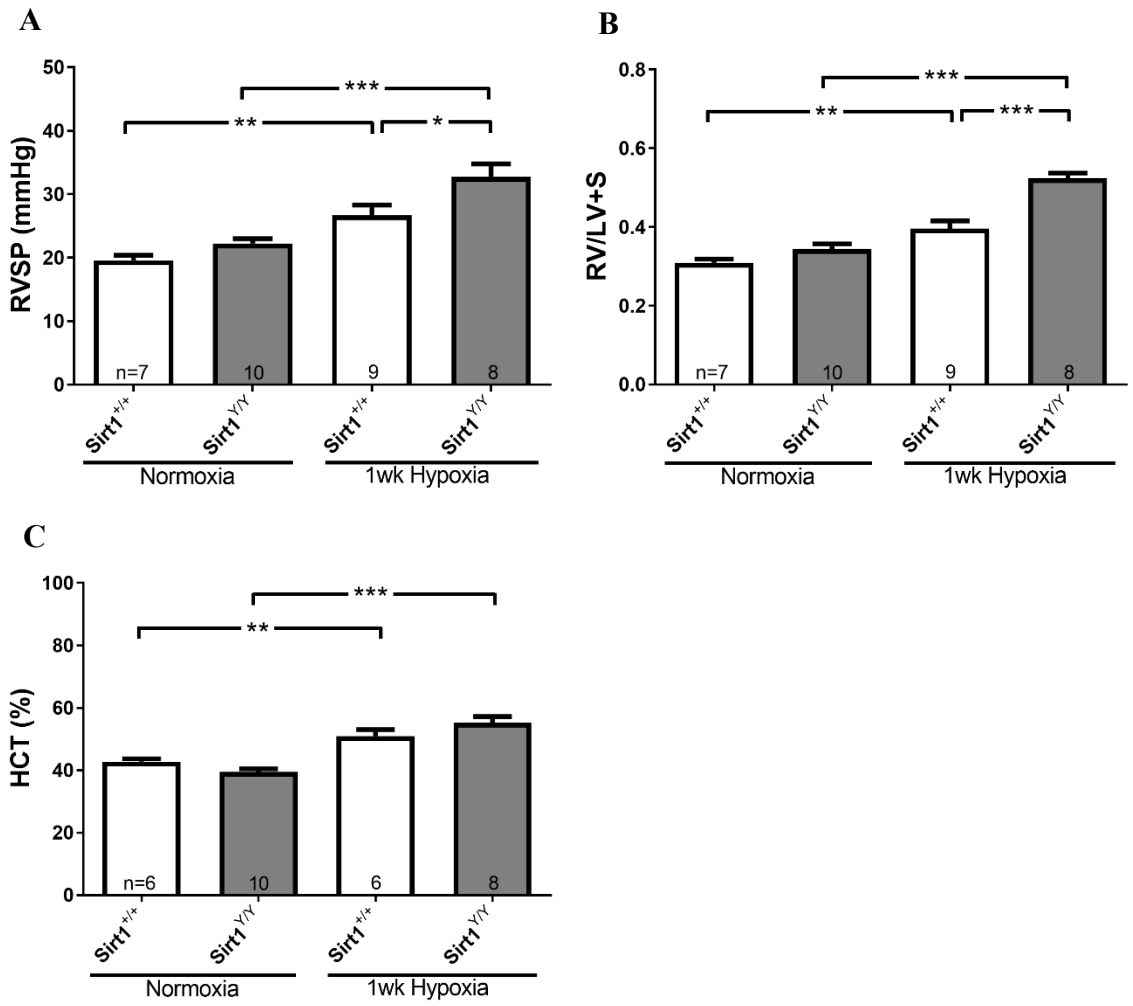

Figure 2-5: **Hemodynamic and hematocrit assessment of *Sirt1*$^{+/+}$ and *Sirt1*$^{Y/Y}$ mice after one week of normoxia or hypoxia**. **A**) Right ventricle systolic pressure (RVSP). **B**) The weight ratio of the right ventricle (RV) to the left ventricle and septum (LV+S). **C**) Hematocrit levels (HCT). n number indicated on bars. *p<0.05, **p<0.01, ***p<0.001.

2.5 Discussion

In this chapter, we establish an important role for SIRT1 in the response to CH and the development of PH. Absence of SIRT1, or its activity, led to exaggerated increases in RVSP, RVH and lung arterial remodeling in response to CH, compared to SIRT1 competent mice. SIRT1 knockout or inactivation was also associated with elevated HCT levels and splenomegaly. When hypoxic animals were returned to normoxia, the exaggerated PH phenotype normalizes, whereas continued exposure to hypoxia led to a more severe phenotype. With loss of SIRT1 activity, we also noted a relatively early exaggeration in RV pressure and hypertrophy, but not HCT, after one week of hypoxia exposure. This provides strong evidence directly implicating SIRT1 in modulation of the CH response *in vivo* and in the pathogenesis of PH.

SIRT1 is not involved in maintaining lung vascular structure and function in absence of hypoxic stress

In normoxic conditions, mice lacking SIRT1 (*Sirt1*$^{-/-}$) or SIRT1 activity (*Sirt1*$^{Y/Y}$) had similar RVSP and RVH, as well as similar systemic pressure and HCT, to *Sirt1*$^{+/+}$ mice (**Figure 2-1/2-3**). Furthermore, there were no differences in pulmonary vascular structure in these mice (**Figure 2-2**). The only difference appeared to be in body weight, since SIRT1 mice were smaller than *Sirt1*$^{+/+}$ mice (**Supplemental Table 1, Appendix**). This suggests that the absence of SIRT1 activity does not affect the pulmonary vasculature, the cardiovascular system or erythropoiesis in the absence of a hypoxic challenge. This is in line with previous descriptions of SIRT1 null mice, which generally fail to exhibit a strong phenotype without a challenge, but respond strongly to stress

(Caron et al., 2014), (Yao et al., 2014). While previous work has suggested the presence of dilated cardiomyopathy in SIRT1 knockout mice at baseline (Planavila et al., 2012), we did not observe any gross abnormalities in RVSP, systemic pressure or in heart size in the absence of SIRT1. With that in mind, we did not investigate the possibility of an age-dependent phenotype in the absence of SIRT1, which would not manifest in the young 8-13 week old mice used in this study. Overall, this is consistent with a role of SIRT1 as a mediator of stress-induced signaling, since in absence of stress, pulmonary vascular structure and function appear normal.

SIRT1 plays an important role in the pulmonary, but not the systemic, vascular hemodynamic response to hypoxia

In CH, absence of SIRT1 (*Sirt1*$^{-/-}$) or SIRT1 activity (*Sirt1*$^{Y/Y}$) increased the severity of the PH phenotype, with elevated RVSP observed as early as day 7 of hypoxic exposure (**Figure 2-5**), suggesting that SIRT1 activity is important for the regulation of the response to CH. Mice are not an ideal species for studying PH (J. Gomez-Arroyo et al., 2012), and the increase in RVSP in wildtype mice exposed to CH in our study was very modest; not reaching statistical significance in some experiments. While this could be due to low n number, our use of an outbred strain (CD1 x SVJ129), as opposed to inbred mice, may have contributed to this modest hypoxia response, since it is well established that different mouse strains show different degrees of responsiveness to CH (Tada et al., 2008). In our case, the use of outbreeding was necessary in order to reduce the perinatal lethality observed in absence of SIRT1 or activity (McBurney et al., 2003), (Seifert et al., 2012). Therefore, our mixed strain has a different response to hypoxia than

that of the inbred strains commonly used for these studies, resulting in less uniform and more variable RVSP values. This inherent variability in the background strain, could also explain the lack of significant difference between *Sirt1*$^{+/+}$ and CH-*Sirt1*$^{+/+}$ mice in RVSP (**Figure 2-1B**) and HCT (**Figure 2-3B)**. Unfortunately, the high perinatal lethality in *Sirt1*$^{-/-}$ mice, compared to *Sirt1*$^{Y/Y}$, made it challenging to obtain enough of these mice. This limited our ability to use knockout mice for subsequent *in vivo* experiments and mechanistic studies, reducing our statistical power.

Thickening of the RV, RVH, is a consequence of the increased PAP leading to increased afterload on the RV, and is a good surrogate for the hemodynamic severity of PH. In animal models of PH, RVH is quantified as the ratio of the RV weight to the LV plus S weight. RVH is a robust parameter that is not affected by transient pressure differences or acute changes in PVR that may occur during the measurement of RVSP, allowing for an integrated measurement of hemodynamic changes in the pulmonary circulation over time. Absence of SIRT1 (*Sirt1*$^{-/-}$) or SIRT1 activity (*Sirt1*$^{Y/Y}$) led to worse RVH in hypoxia, appearing as early as one week of hypoxia in *Sirt1*$^{Y/Y}$ mice (**Figure 2-5B**). Additionally, even in experiments where increases in RVSP did not reach significance, RVH was clearly increased in hypoxia. Technical variability and user bias in RVH measurements were reduced in our studies by using the same blinded operator.

The systemic circulation response to hypoxia differs from the HPV response observed in the lungs. Unlike the lungs, chronic exposure to severe hypoxia (<10% O_2) leads to strong vasodilation and reduced systemic vascular resistance. This is due to high release of local peripheral vasodilators and subsequent SMC vasodilation, resulting in decreased systemic arterial pressure (Ivy & Scott, 2015), (Sander, 2016). Our assessment

of systemic mean arterial pressure in the aortic arch revealed a significant decrease in MAP after three weeks of CH, which was similar in all transgenic lines, regardless of SIRT1 presence or absence (**Table 2-1**). This similar decrease in MAP confirms that SIRT1 exerts minimal effects on the vasodilation response within the systemic circulation under CH, suggesting a limited role of SIRT1 in modulation of the systemic vascular response to CH.

SIRT1 plays an important role in pulmonary vascular remodeling and pruning in CH

Pulmonary vascular remodeling in response to CH exposure is an important contributor to increased pulmonary vascular resistance and subsequent PH development in this model (Kurt R Stenmark et al., 2009). CH-induced pulmonary structural changes include the appearance of SMCs in small non-muscular arterioles (<100μm diameter, "muscularization") and hyperplasia of muscular arterioles due to increased accumulation of SMCs (Kurt R Stenmark et al., 2009), (Kurt R. Stenmark et al., 2006), (J. Gomez-Arroyo et al., 2012). In addition, degenerative changes leading to loss of the distal arteriolar microvascular bed (vascular pruning) have been reported in the CH model (Chandra et al., 2011), (Abdalla et al., 2015).

In line with increased RVSP and RVH, we observed significantly higher partial muscularization of <50μm arterioles in hypoxic *Sirt1*$^{+/+}$ mice, which was further increased in hypoxic *Sirt1*$^{Y/Y}$ and *Sirt1*$^{-/-}$ mouse lungs (**Figure 2-2D**). Increased muscularization of small arterioles strongly corresponds to increased RVSP and RVH, suggesting that <50μm arteriole muscularization plays a large role in driving the

hemodynamic changes in this model. Remarkably, total percent muscularization levels of <50μm arterioles (partial + full muscularization) were higher in *Sirt1*$^{-/-}$ compared to *Sirt1*$^{Y/Y}$ mice (78% CH-*Sirt1*$^{Y/Y}$ vs 83% CH-*Sirt1*$^{-/-}$). This was not driven by partial muscularization (59% CH-*Sirt1*$^{Y/Y}$ vs 54% CH-*Sirt1*$^{-/-}$), but higher levels of full muscularization in *Sirt1*$^{-/-}$ mice (19% CH-*Sirt1*$^{Y/Y}$ vs 29% CH-*Sirt1*$^{-/-}$). This corresponds with the increased hypoxic RVH observed in the *Sirt1*$^{-/-}$ mice compared to *Sirt1*$^{Y/Y}$ mice (RVH 0.56 CH-*Sirt1*$^{Y/Y}$ vs 0.62 CH-*Sirt1*$^{-/-}$) suggesting a more severe PH. This is consistent with previous publications of a more severe baseline phenotypes in *Sirt1*$^{-/-}$ compared to *Sirt1*$^{Y/Y}$ mice (Seifert et al., 2012). These findings implicate SIRT1 in protection from excessive pulmonary vascular remodeling and muscularization of small arterioles in response to hypoxia.

Despite the severe hemodynamic response to hypoxia, we did not observe any differences in partial or fully muscular arterioles at 50-100μm or >100μm between *Sirt1*$^{+/+}$, *Sirt1*$^{Y/Y}$ or *Sirt1*$^{-/-}$ lungs. Indeed, larger arterioles are normally muscularized at normoxia and only thicken in response to hypoxia (Mirrakhimov & Strohl, 2016), (Kurt R. Stenmark et al., 2006). Our method of quantification of absence, partial or full muscularization in 2-dimensional thin lung cross sections is used to addresses presence or absence of muscularization only. Therefore, this method does not account for potential vascular thickening in larger arterioles or pruning and loss of smaller arterioles, the latter requiring a 3-dimensional approach to evaluate. Therefore, in order to further characterize changes in 3-dimensional architecture of the lung vasculature, we used FMA to visualize the number and structure of microvessels in *Sirt1*$^{+/+}$ and *Sirt1*$^{Y/Y}$ lungs after exposure to CH. Vascular remodeling in response to CH was accompanied by loss of

perfusion of distal arterioles, resulting from pruning of the microvasculature, which was greater in *Sirt1*$^{Y/Y}$ mice compared to *Sirt1*$^{+/+}$ mice (**Supplemental Figure 3, Appendix**). Using FMA only allows visualization of the vascular lumen, making it challenging to determine whether the mechanism of vascular loss was due to a degenerative change or occlusive remodeling due to growth dysregulated cells (Chaudhary et al., 2017). However, since no proliferative intimal lesions were seen in the CH model, even in SIRT1 deficient mice, the vascular pruning likely resulted from precapillary arteriolar loss due to EC apoptosis induced by hypoxia, which has been observed previously *in vitro* (C. Li et al., 2003) and with SUCH treatment *in vivo* (Ciuclan et al., 2011), (Vitali et al., 2014). Certainly, degenerative changes leading to loss of the distal arteriolar microvascular bed have been noted previously in mouse CH models using similar 3-dimentional approaches to FMA (Chandra et al., 2011), (Abdalla et al., 2015).

The abnormal vascular structure may also suggest a blunted pulmonary microcirculation angiogenic response to CH exposure in *Sirt1*$^{Y/Y}$ mice compared to *Sirt1*$^{+/+}$ mice. This is supported by previous work where siRNA knockdown of SIRT1 in ECs *in vitro* reduced their ability to form sprouts and networks (Potente et al., 2007). Furthermore, EC-specific SIRT1 knockout *in vivo* led to impairment of neovascularization in a model of hind-limb ischemia, evident by lower capillary density in the ischemic limb, suggesting an impaired angiogenic response in absence of endothelial SIRT1 (Potente et al., 2007). This implicates SIRT1, and potentially endothelial SIRT1, in maintenance of appropriate pulmonary angiogenic response.

SIRT1 is a key regulator of the response to CH-induced erythrocytosis

Erythropoiesis is a naturally occurring process through which new RBCs differentiate from hematopoietic stem cells in the bone marrow or spleen (Liang & Ghaffari, 2016). Hematopoietic stem cells carry a specialized receptor, the erythropoietin (EPO) receptor, to which binding of EPO leads to differentiation into RBCs (Liang & Ghaffari, 2016). EPO is a secreted hormone produced by the liver during fetal development, while it is produced by interstitial fibroblasts in the peritubular capillary bed of the renal cortex of the kidneys in adults (Liang & Ghaffari, 2016), (Uversky & Redwan, 2016). At the cellular level, EPO production is mediated by oxygen tension and iron levels, which is fine-tuned through the hypoxia inducible factors (mainly HIF2α) and the iron regulatory proteins (mainly IRP1) (Liang & Ghaffari, 2016).

Three weeks of CH led to erythrocytosis in $Sirt1^{+/+}$ animals, increasing RBC volume from 40% to 59% (**Figure 2-3**). In absence of SIRT1 ($Sirt1^{-/-}$) or its activity ($Sirt1^{Y/Y}$), these levels were further increased to 71%, with some animals reaching the mid-80%. We also observed splenomegaly in the hypoxic $Sirt1^{Y/Y}$ and $Sirt1^{-/-}$ mice, but not in the hypoxic $Sirt1^{+/+}$ mice (**Supplemental Table 2, Appendix**). This increase is similar to previously reported splenomegaly in EPO overexpressing transgenic mice, which was associated with increased extramedullar RBC production (Vogel et al., 2003). This suggests that in SIRT1 knockout or mutant transgenic mice, the increase in RBC production may originate from the spleen.

We originally believed that the exaggerated HCT response might be contributing to the increased pulmonary pressures in the SIRT1 mice due to rheological effects on blood viscosity; however, several lines of evidence confirmed that was not the case. First,

the exaggerated RVSP and RVH were observed in SIRT1 mutants by one week of hypoxia, while HCT levels were not significantly different between hypoxic *Sirt1*$^{+/+}$ and *Sirt1*$^{Y/Y}$ mice, and were still close to the normal ranges (around 50%, **Figure 2-5**). Second, the systemic pressure, MAP, was similar between *Sirt1*$^{+/+}$, *Sirt1*$^{Y/Y}$ and *Sirt1*$^{-/-}$ mice in CH, suggesting that the high HCT levels did not affect systemic blood viscosity. Third, previous studies of EPO overexpressing mice, which develop HCT of ~80%, have shown no increase in RVSP or RVH in normoxia or exaggeration in CH (Weissmann et al., 2005). This supports the notion that high HCT is not a significant contributor to the PH phenotype in this model.

Taken together, the elevated HCT levels observed in our study implicate SIRT1 activity in the control of normal hypoxic driven erythrocytosis from bone marrow and spleen. However, the exaggerated HCT response does not account for the increased pulmonary pressure observed in SIRT1 deficient mice, which is largely due to narrowing of arterioles, arterial remodeling, as well as pruning of the microcirculation leading to loss of cross-sectional vascular area.

Recovery from CH is not affected by absence of SIRT1

It is well-established that the CH model in wildtype mice is reversible upon relocation to normoxia and does not lead to formation of complex intimal remodeling or plexiform lesions (Vitali et al., 2014). Indeed, progressive and non-reversible PH development after CH exposure have only been observed in one transgenic mouse model, the constitutive over-expression of IL-6 under a lung-specific promoter (Steiner et al., 2009). Relocation to normoxia in wildtype mice leads to normalization of pulmonary

hemodynamics and HCT levels (Ciuclan et al., 2011), (Weisel et al., 2014). In addition, there is normalization of the pulmonary vascular remodeling, which involves reduction in SMC hyperplasia, return of the medial layer to normal thickness, and 'de-muscularization' of the distal arterioles (Weisel et al., 2014). At the molecular level, recovery from CH involves reactivation of PHDs/FIH, which rapidly and efficiently hydroxylate HIFα subunits, leading to HIFα degradation and termination of hypoxic signaling (Marxsen et al., 2004), (Ginouvès, Ilc, Macías, Pouysségur, & Berra, 2008).

In our model, SIRT1 appears to exert a protective effect by modulating the severity of CH-induced PH (**Figure 2-1/2-2/2-3**). Accordingly, we hypothesized that the combination of CH and SIRT1 deficiency might lead to progressive PH, even after relocation to normoxia. However, the elevated levels of RVSP, RVH and HCT, which developed after 3 weeks of hypoxia, subsequently normalized to near baseline levels in both $Sirt1^{+/+}$ and $Sirt1^{Y/Y}$ after re-exposure to normoxia for two weeks (**Figure 2-4**). This was accompanied by normalization in the level of muscularization within the lungs (**Figure 2-4**). These findings clearly show that the hypoxic response "termination pathway", which is mainly mediated by the PHD hydroxylation activity, is not affected by SIRT1 deficiency or inactivation. Additionally, the return of systemic HCT levels to normal suggests that SIRT1 does not interfere with systemic hypoxic response termination during recovery. Of note, a trend towards higher RVH in $Sirt1^{Y/Y}$ mice compared to $Sirt1^{+/+}$ mice persisted at 2 weeks of normoxia (**Figure 2-4**). The slower rate of RV recovery, compared to pulmonary and systemic changes, suggests a possible role of SIRT1 in RV protection from hypertrophy. Alternatively, it is possible that the slower recovery is merely due to the more severe initial hypertrophy at 3 weeks in the $Sirt1^{Y/Y}$

mice. Similar delay in RVH recovery has been previously shown in the SUCH mice relocated to normoxia for 10 days (Ciuclan et al., 2011), as well as EC-BMPR2 KO mice relocated to normoxia (Diebold et al., 2015). Of interest, previous work with SIRT1 knockout mice noted presence of RVH in *Sirt1*$^{-/-}$ pups that was not maintained into adulthood (McBurney et al., 2003). Since normal mammalian heart and lung vascular development occurs in a hypoxic environment (Dunwoodie, 2009), this neonatal hypertrophy is most likely due to a stronger hypoxic response in utero, which is not maintained after birth, similar to our normoxic recovery mice.

While absence of SIRT1 had minimal effects on recovery in normoxia, continuation of hypoxic exposure, up to 5 weeks, led to progressive increases in pulmonary hemodynamics, RV remodeling and HCT. This was observed in both wildtype and mutant transgenic animals such that the difference in RVSP between *Sirt1*$^{+/+}$ and *Sirt1*$^{Y/Y}$ mice was lost. The mechanisms underlying this "catch up" of PH severity in *Sirt1*$^{+/+}$ mice are not clear; however, it is possible that SIRT1 deficiency accelerated the structural and functional lung vascular changes in response to CH. Thus, over time, the accumulated increase in vascular remodeling in *Sirt1*$^{+/+}$ mice leads to a progressive increase in PVR and RV pressure. However, since differences in RVH were still maintained, the notion of SIRT1 playing additional roles in protection of RVH in response to increased afterload gains additional support. Overall, SIRT1 plays a key role in dampening the pulmonary and systemic response to hypoxia, but does not appear to be important in the regulation of vascular structure and function under normoxic conditions in which the hypoxic system is inactivated.

Conclusion

SIRT1 knockout or inactivation exacerbates RV pressure, hypertrophy, pulmonary vascular remodeling and HCT in response to CH, consistent with a protective role for SIRT1 in preventing the development of severe CH-induced erythropoiesis and PH. This suggests that SIRT1 activity may be particularly important under conditions characterized by abnormal hypoxic activation and the SIRT1 pathway may be a potential therapeutic target for PAH therapies. Gaining better understanding of the mechanism of SIRT1 action in hypoxia, and potential of SIRT1 activation, would allow us to explore the potential therapeutic implications of SIRT1 activity.

CHAPTER 3: ROLE OF SIRT1 IN THE PULMONARY VASCULAR RESPONSE TO CHRONIC HYPOXIA: EVALUATION OF THE HYPOXIC RESPONSE IN ABSENCE OF SIRT1 ACTIVTY

3.1 Introduction:

In this chapter, we set out to expand on the concepts introduced in **Chapter 1 and 2** with respect to the relevance of SIRT1 to modulating the hypoxic response. This includes SIRT1 modulation of HIF1α and the metabolic hypoxic response as well as SIRT1 modulation of HIF2α and the pulmonary endothelial hypoxic response.

3.1.1 HIF1α Induces the Metabolic Hypoxic Response

In normal cellular metabolism, the pyruvate dehydrogenase complex (PDC) catalyzes the conversion of pyruvate to acetyl-CoA, which allows the progression of oxidative phosphorylation and the tricarboxylic acid (TCA) cycle (Sugden & Holness, 2003). Pyruvate dehydrogenase kinases (PDKs) and pyruvate dehydrogenase phosphatases (PDPs) can phosphorylate or de-phosphorylate the PDC, thus leading to PDC inactivation or activation, respectively (Sugden & Holness, 2003). The Warburg effect refers to cells in which aerobic glycolysis replaces normal oxidative phosphorylation, leading to decreased oxygen consumption and increased lactate production (Rehman & Archer, 2010), (Burns & Manda, 2017). This includes increased expression of glucose transporters, hexokinases, PDKs and lactate dehydrogenases (LDHs) as well as an increase in levels of transcription factors that maintain this effect, including MYC, HIF1α, NF-kB and OCT1 (Burns & Manda, 2017). Each factor plays an important role in maintaining aerobic glycolysis and preventing oxidative phosphorylation. For example, while PDKs inactivate PDC, thereby preventing acetyl-CoA production from pyruvate for the TCA cycle, LDH converts the pyruvate to lactate to generate energy glycolytically (Burns & Manda, 2017).

Hypoxia can create a Warburg-like effect, where stabilization of HIF1α leads to an early switch of metabolism to glycolysis (Burns & Manda, 2017), (Dengler et al., 2008). Although anaerobic glycolysis is less efficient than oxidative phosphorylation, it allows 100 times faster energy production from glucose, allowing cell survival in hypoxia (Valvona, Fillmore, Nunn, & Pilkington, 2016). The metabolic switch involves HIF1α mediated transcriptional initiation of several hypoxic response targets carrying an HRE sequence. For example, LDHA, which participates in glycolytic metabolism through conversion of pyruvate to lactate as well as nicotinamide adenosine dinucleotide (NAD)H to NAD^+, has HREs in its gene promoter for binding and enhancement of transcription by HIF1α (Semenza et al., 1996), (Valvona et al., 2016). In addition, HIF1α leads to increased levels of PDK1, which has a high ability to phosphorylate several residues to deactivate the PDC, shifting metabolism towards glycolysis (Sugden & Holness, 2003), (J. Kim, Tchernyshyov, Semenza, & Dang, 2006). HIF1α can also lead to transcription of targets that play an important role in the hypoxic response, though they are not directly involved in metabolism. BCL-2 and adenovirus E1B 19-kDa-interacting protein 3 (BNIP3) is a mitochondrial membrane localized protein that has the ability to interact with the anti-apoptotic proteins BCL-2/BCL-xL (Chinnadurai, Vijayalingam, & Gibson, 2008). Hypoxic expression of BNIP3, which has been implicated in several cell death pathways, is mediated through the activity of HIF1α (Bruick, 2000). Another HIF1α target, N-Myc Downstream Regulated 1 (NDRG1), does not play a role in metabolism yet is important for the hypoxic response (Ellen, Ke, Zhang, & Costa, 2007).

As discussed in **Chapter 1** (**Section 1.2.5**), normoxic activation of HIF1α leads to a Warburg-like shift in SMCs metabolism, resulting in a hyper-proliferative phenotype in

PAH, which is in part mediated by elevated levels of downstream HIF1α targets (Rehman & Archer, 2010). Indeed, PAH patients have higher serum LDH levels, which correspond to worse outcomes (E.-C. Hu et al., 2015). Furthermore, both PDK1 and PDK2 have been shown to be elevated in PAH patient lung tissue (Evangelos D. Michelakis et al., 2017). Data from transgenic animal models support a potential role for HIF1α in CH-induced PH, especially in SMCs. In fact, heterozygous global and targeted SMC HIF1α knockout mice are protected from development of CH-PH (A. Y. Yu et al., 1999), (Ball et al., 2014), yet EC deletion of HIF1α does not affect the degree of development of CH-PH (Cowburn et al., 2016). Some HIF1α downstream targets, such as PDK1, are elevated in the CH model of PH (Evangelos D Michelakis et al., 2002), (Geng et al., 2016), while higher BNIP3 levels appear to mediate autophagy in MCT-induced PH (Deng et al., 2017). Therefore, increased HIF1α activity, particularly in SMCs, may contribute to pulmonary vascular remodeling in human PAH and PH animal models. Still, it remains to be determined whether HIF1α activity is affected by absence of SIRT1 or SIRT1 inactivation and whether inhibiting the HIF1α-mediated metabolic shift in CH can prevent the exaggerated pathology in our model.

3.1.1.1 Evidence that SIRT1 Modulates Hypoxic Metabolism and HIF1α activity

SIRT1 activity and NAD^+ have both been linked to modulation of metabolic responses (Kennedy et al., 2016), (Knight & Milner, 2012). NAD^+, a dinucleotide consisting of a single adenine and a single nicotinamide base, functions as an electron acceptor or coenzyme for metabolic reactions (Kennedy et al., 2016), (Knight & Milner, 2012). As a co-factor for SIRT1 deacetylation activity, NAD^+ abundance can regulate

SIRT1 activity, allowing modulation of downstream targets and subsequent modulation of the metabolic status (Kennedy et al., 2016), (Knight & Milner, 2012). SIRT1 can regulate mitochondrial biogenesis through deacetylation of key transcription factors such as PGC1α and STAT3 and regulate glycolysis through regulation of PGC1α and p53 (Knight & Milner, 2012). Mice lacking SIRT1, or its activity, have been shown to have a worse metabolic syndrome in response to high fat diet, including worse fatty liver phenotype and glucose intolerance (Pfluger et al., 2008), (Caron et al., 2014), (J. Cheng et al., 2017). Most importantly, as detailed in **Table 3-1**, SIRT1 can modulate the function of HIF1α, the master regulator of the metabolic hypoxic response. While acetylation of HIF1α by the acetyltransferase PCAF (p300/CBP-associated factor) enhances HIF1α activity (Lim et al., 2010), SIRT1 can bind and deacetylate HIF1α leading to reduced activity (**Table 3-1**). Alternatively, SIRT1 can modulate the effects indirectly through transcriptional regulation of HIF1α levels. However, our knowledge of the mechanism of SIRT1 function in hypoxia and its effect on HIF1α activity is limited to *in vitro* work, mainly in cancer cell lines, known for their abnormal hypoxic and metabolic profiles, which warrants subsequent assessment of the SIRT1-HIF1α relationship *in vivo*. Of note, recently published work describing CH-treated SIRT1 knockout mice shows increased protein expression of HIF1α and downstream target levels in the lungs in absence of SIRT1 (Zurlo et al., 2018).

Table 3-1: Modulation of HIF1α activity by SIRT1

Cell type	SIRT1 role	SIRT1 effect	Reference
Cancer Line	No interaction	No interaction	(Dioum et al., 2009)
Cancer Line (3)	Direct Deacetylation	↓ Activity	(Lim et al., 2010)
Cancer Line	No interaction	No interaction	(R. Chen et al., 2012)
Cancer Line	Direct Deacetylation	↑ Activity	(Laemmle et al., 2012)
Myeloid-derived suppressor cells	Indirect	↓ Levels	(Medina et al., 2011)
Cancer Line (10)	Direct Deacetylation	↓ Activity	(Yoon et al., 2014)
Cancer Line	No interaction	No interaction	(R. Chen et al., 2015)
Cancer Line (2)	Direct Deacetylation	↓ Activity	(Joo et al., 2015)
Neuronal (SH-SY5Y)	Direct Deacetylation (Inferred)	↓ Activity ↓Transcription	(Dong et al., 2016)
PAECs	Direct Deacetylation (Inferred)	↓ Activity	(P.-I. Chen et al., 2017)

3.1.1. 2 Dichloroacetate Inhibits Hypoxic Metabolism and HIF1α activity

Working under the premise of activation of HIF1α and aerobic glycolysis under normoxic conditions in PAH, several groups validated the efficacy of dichloroacetate (DCA) (**Table 3-2**). DCA functions by binding and inhibiting the catalytic activity of PDK1-4, with the highest affinity to PDK2 > PDK1 = PDK4 > PDK3 (Kato, Li, Chuang, & Chuang, 2007), (E. D. Michelakis, Webster, & Mackey, 2008), (Stacpoole, 2017). PDK inhibition by DCA prevents phosphorylation of the PDC, thus allowing the production of acetyl-CoA and subsequent oxidative phosphorylation (Sugden & Holness, 2003). Due to its small size, DCA can achieve high cellular bioavailability, allowing it to reverse glycolysis and reduce lactate production (E. D. Michelakis et al., 2008). Several studies using DCA showed efficacy in treatment of lactic acidosis; however, DCA led to severe side effects in these patients (James et al., 2017). Subsequently, several phase I clinical trials using lower doses of DCA in patients with recurrent malignant brain tumors show better tolerability (James et al., 2017).

In PH, the effects of DCA are attributed to the reversal of the metabolic shift from glycolytic to oxidative phosphorylation in PASMCs in these models (Evangelos D Michelakis et al., 2002). Recently, DCA was tested in a phase I clinical trial for PAH leading to some promising effects (NCT01083524) (Evangelos D. Michelakis et al., 2017). DCA improved hemodynamic parameters, PVR and reactivated the PDC in patient samples, yet only in a sub-population of PAH patients (Evangelos D. Michelakis et al., 2017). The lack of effect was attributed to point mutations in genes involved in maintenance of metabolic mitochondrial balance, including the *SIRT3* and *UCP2* genes (Evangelos D. Michelakis et al., 2017). Surprisingly, even with the large diversity of animal models used to test DCA, its efficacy has never been assessed in the SUCH rat model, or in a mouse CH model, and definitely not in a model of increased HIF1α activation.

Table 3-2: Use of Dichloroacetate in PH models

Model	DCA dose or [concentration]	DCA effect on PH Parameters	Additional DCA effects	Reference
CH, d1/d10 prevention	70mg/kg/day [0.75g/L]	Improved mPAP, PVR, RVH, muscularization		(Evangelos D Michelakis et al., 2002)
MCT, prevention	80mg/kg/day [0.75g/L]	Improved mPAP, RVH, muscularization	Improved survival, ↓ lung cell proliferation, ↑ lung apoptosis	(McMurtry et al., 2004)
MCT, reversal	80mg/kg/day [0.75g/L]	Improved mPAP,	Improved survival	(McMurtry et al., 2004)
Transgenic mice (SMC, 5HTT OE)	80mg/kg/day	Improved RVSP, RVH, muscularization	↓ lung cell proliferation, ↑ lung apoptosis	(Guignabert et al., 2009)
MCT, d10 reversal	70mg/kg/day [0.75g/L]	Improved RVSP, RVH, muscularization	↑ RV oxygen consumption	(Lin Piao et al., 2010)
Fawn-hooded Rat	[0.75g/L]	Improved PAAT* No improvement in RVSP		(L Piao et al., 2013)
MCT+PN; d8 prevention	80mg/kg/day	Improved RVH, muscularization	↓HIF1α lung protein	(B. Li, Yan, Shen, Liu, & Ma, 2014)
MCT+PN; d29 reversal	80mg/kg/day	No improvement		
CH (d7), prevention	[1g/L]	Improved mPAP, PVR, RVH, muscularization	↓ lung cell proliferation	(Huertas et al., 2015)
Clinical Trial	3-6.25mg/kg, twice/day	Improved mPAP in subset of patients	Improved PVR in subset of patients	(Evangelos D. Michelakis et al., 2017)

* Assessed by echocardiogram. PAAT: Pulmonary Artery Acceleration Time, RVSP: Right ventricle systolic pressure, RVH: Right ventricle hypertrophy, CH: chronic hypoxia, MCT: Monocrotaline; SMC: Smooth muscle cell, 5-HTT OE: Serotonin transporter overexpression; PVR: Pulmonary vascular resistance

3.1.2 Possible Role for HIF2α in the Pulmonary Endothelial and Systemic Response to Chronic Hypoxic

Even with 48% sequence similarity to HIF1α, in hypoxia, HIF2α activates a different set of target genes from those activated by HIF1α. Specific target genes activated by HIFs are highly dependent on cell type, hypoxic level and duration of hypoxia (Keith et al., 2012), (Prabhakar & Semenza, 2012), (Koh & Powis, 2012). For example, PHDs have different affinity for HIF1α and HIF2α, and are less efficient at hydroxylating HIF2α; therefore, HIF2α is activated at higher oxygen levels (less severe hypoxia) than HIF1α (Keith et al., 2012), (Prabhakar & Semenza, 2012), (Koh & Powis, 2012). Furthermore, translation of HIF2α, but not HIF1α, is linked to iron metabolism due to presence of an iron-responsive element (IRE) in the 5' untranslated region of the *HIF2A* mRNA (Liang & Ghaffari, 2016). Finally, the temporal sequence of activation for HIF1α and HIF2α is different, with the former mediating rapid responses to hypoxia while the latter is more important for chronic adaptation (Koh & Powis, 2012). Thus, while HIF1α mediates rapid modulation of mitochondrial metabolism and early angiogenic responses in hypoxia, HIF2α regulates adaptation to long-term hypoxic exposure by controlling erythropoiesis and pulmonary vascular remodeling, acting predominantly in ECs (Koh & Powis, 2012).

As discussed in **Chapter 1** (**Section 1.2.2.1**), mutations in the *HIF2A* and *PHD2* genes in humans, limiting HIF2α activation, have been implicated in adaptation to high altitude, usually associated with maintenance of normal levels of blood hemoglobin, reduction in the HPV response and normal PAP and PVR at high altitude (Sylvester et al., 2012). Pathologically, normoxic HIF2α activation has been observed in PAH

patients' pulmonary arteries (Labrousse-Arias et al., 2016). Indeed, overexpression of an active form of HIF2α in transgenic mice results in severe PH, associated with increased erythrocytosis (Tan et al., 2013); while heterozygous global knockout of HIF2α protects against the development of severe CH-PH (Brusselmans et al., 2003). HIF2α modulates the CH response through several targets responsible for oxygen delivery and vascular remodeling. EPO, the first identified hypoxic-induced target and main driver of erythropoiesis, is a HIF2α target (Rankin et al., 2007). Activation of HIF2α in the kidneys in response to CH, leading to production of EPO, allows erythrocytosis and enhanced peripheral oxygen delivery. In the pulmonary vasculature, HIF2α activation leads to pathological remodeling and vascular changes in response to CH. HIF2α can modulate the hypoxic transcription of the vasoconstrictor and mitogen ET-1 in the lungs (Hickey et al., 2010), (Tan et al., 2013), and specifically, the endothelium (Dai et al., 2016). HIF2α also regulates pulmonary and endothelial CH-mediated transcription of plasminogen activator inhibitor 1 (PAI-1), a glycoprotein member of the serine-protease inhibitors superfamily (Cesari, Pahor, & Incalzi, 2010), (Schuliga, Westall, Xia, & Stewart, 2013), (Pinsky et al., 1998), (Dai et al., 2016). PAI-1 inhibits plasminogen activators, thus preventing fibrinolysis and creating a pro-thrombotic environment (Cesari et al., 2010), and can lead to pulmonary SMC proliferation (Dimova, Samoylenko, & Kietzmann, 2004). In addition, HIF2α regulates production of pulmonary and endothelial chemokines and growth factors in CH such as stromal-cell derived growth factor 1 (SDF1 or CXCL12), a homeostatic chemokine, which is involved in regulation of cell migration (Teixidó, Martínez-Moreno, Díaz-Martínez, & Sevilla-Movilla, 2017), (Hitchon et al., 2002), (Dai et al., 2016). Through binding to its receptors, CXCL12 can mediate

hematopoiesis, cardiogenesis, neurogenesis and SMC proliferation (Teixidó et al., 2017), (Dai et al., 2016).

Additional lines of evidence specifically implicate HIF2α, as opposed to HIF1α, in regulating the pulmonary CH response in the endothelium. In fact, EC-specific knockout of HIF2α, but not HIF1α, protects against development of severe CH-PH (Cowburn et al., 2016). Furthermore, EC-specific PHD2 knockout models developed by four independent groups implicated endothelial HIF2α activation, but not HIF1α, in the development of PH (Dai et al., 2016), (Kapitsinou et al., 2016), (Wang et al., 2016), (Tang et al., 2017). Activation of all HIFs selectively in ECs through endothelial targeted PHD2 knockout resulted in severe PH, progressing to right heart failure, and formation of complex lesions similar to the plexiform lesions seen in human PAH (Dai et al., 2016), (Kapitsinou et al., 2016), (Wang et al., 2016), (Tang et al., 2017). Further crossings with endothelial specific HIF1α and HIF2α knockout mice attenuated PH development in this model, but only when PHD2 deficiency is combined with endothelial HIF2α deletion, and not HIF1α, confirming that endothelial HIF2α is mainly responsible for onset of severe PH in this model (Dai et al., 2016), (Kapitsinou et al., 2016). Finally, lung ECs isolated from PAH patients have normoxic activation of HIF2α, which provides further support for a role of increased endothelial HIF2α activation in PAH (Tang et al., 2017). Overall, increased HIF2α activity, especially in the endothelium, correlates with worse pathological consequences in pulmonary vascular remodeling in CH, and possibly human PAH. Yet, the extent of the effect of SIRT1 absence or inactivity on HIF2α activity and endothelial response in CH is yet to be determined. It also remains to be addressed whether compensating for SIRT1 activity can affect the CH response.

By combining our knowledge about the roles of HIF1α and HIF2α in the hypoxic response, strong evidence suggests that HIF1α may be more important in SMCs, specifically in regulating the early metabolic response to hypoxia. While, HIF2α appears to act largely in ECs and plays the predominant role in mediating the long-term effect of CH, including elevated pressure and complex remodeling.

3.1.2.1 Evidence that SIRT1 Modulates HIF2α activity

Similar to HIF1α, HIF2α activity can be modulated through acetylation and deacetylation. HIF2α can be acetylated by CBP (CREB-binding protein) leading to enhanced HIF2α activity (R. Chen et al., 2012), while acetylation by p300 leads to reduced HIF2α activity (R. Chen et al., 2015). Currently, most studies suggest that SIRT1 activity leads to enhanced HIF2α activation, apart from one report showing a cell-type dependent response, where SIRT1 can limit HIF2α activation in most cell lines assessed (**Table 3-3**). However, similar to SIRT1-HIF1α studies, our knowledge of the mechanism of SIRT1 function on HIF2α activity is limited to *in vitro* work and based on cancer cell lines exposed to acute hypoxia, highlighting the need for studies addressing the effects of SIRT1 on HIF2α activity *in vivo* and CH.

Table 3-3: Modulation of HIF2α activity by SIRT1

Cell type	SIRT1 role	SIRT1 effect	Reference
Cancer Line	Direct Deacetylation	↑ Activity	(Dioum et al., 2009)
Cancer Line (3)	Direct Deacetylation	↑ Activity	(Lim et al., 2010)
Cancer Line	Direct Deacetylation	↑ Activity	(R. Chen et al., 2012)
Cancer Line (7)	Direct Deacetylation	↓ Activity	(Yoon et al., 2014)
Cancer Line (3)	Direct Deacetylation	↑ Activity	(Yoon et al., 2014)
Cancer Line	Direct Deacetylation	↑ Activity	(R. Chen et al., 2015)

3.1.2.2 SIRT1 Maintains Vascular EC Homeostasis

Strong *in vivo* evidence supports the idea that endothelial SIRT1 is crucial for maintenance of systemic vascular integrity and homeostasis. EC specific knockout of SIRT1 leads to impairment of neovascularization in a model of hind-limb ischemia, evident by lower capillary density in the ischemic limb, suggesting an impaired angiogenic response in the absence of endothelial SIRT1 (Potente et al., 2007). Follow up studies using these mice revealed the presence of left ventricle (LV) diastolic dysfunction and reduced capillary density with old age (Maizel et al., 2014). In addition, the authors noted worsening in EC-SIRT1 KO mice compared to controls in response to transverse aortic constriction (Maizel et al., 2014). Assessment of kidneys in EC-SIRT1 KO mice revealed increased interstitial fibrosis at baseline, and worse outcome in acute and chronic nephrotoxic injury models (Vasko et al., 2014). Conversely, endothelial overexpression of SIRT1 protected mice from high fat diet-induced endothelial dysfunction, while limiting atherosclerosis in SIRT1-OE-apoE$^{-/-}$ double transgenic mice (Q. J. Zhang et al., 2008). Some of these findings were confirmed by other groups, linking EC-SIRT1 overexpression with improved vasodilation of aortic rings (Wan et al., 2014). In a streptozotocin-induced diabetic mouse model, endothelial SIRT1 overexpression led to decreased expression of senescence associated markers as well as a reduction of oxidative stress (H. Z. Chen et al., 2012). Combined, these results clearly implicate endothelial SIRT1 as having a pivotal role in the maintenance of vascular EC homeostasis *in vivo*; however, no studies have yet to assess the role of EC-SIRT1 in the pulmonary response to CH.

3.1.2.3 Resveratrol, a Putative SIRT1 Activator, Limits the Pulmonary Chronic Hypoxic Response

Resveratrol (RSV, 3,5,4′-trihydroxy-trans-stilbene) is a naturally occurring polyphenol that can be found in several plant species, especially in red grape skin (Dang, 2014). Interest in RSV originated from its potential to explain the "French Paradox", where people with French descent have a lower incidence of coronary heart disease, yet consume a diet high in saturated fats (Renaud & de Lorgeril, 1992). The relationship between RSV and SIRT1 started getting attention when RSV was identified as a SIRT1 activator in a chemical activity based assay using a fluorescently labeled acetylated p53 peptide (Howitz et al., 2003). RSV was shown to increase SIRT1 activity in this assay by 13-fold through increased substrate binding affinity (Howitz et al., 2003). Further evidence for the SIRT1-RSV link has been established when RSV successfully extended the lifespan of several model organisms including yeast, worms, flies and fish (Wood et al., 2004), (Dang, 2014). However, the SIRT1-RSV relationship came under scrutiny when it was determined that fluorophore presence is needed for the enhanced substrate binding and stimulation of SIRT1 deacetylation in the activity assay (Borra et al., 2005), (Pacholec et al., 2010), (Kaeberlein et al., 2005). Therefore, some believe that RSV can only "mimic" SIRT1 overexpression (da Cunha, Demasi, & Kowaltowski, 2011). Previous *in vitro* studies implicate RSV in inhibition of hypoxia-induced VEGF release by ECs as well as limiting PASMCs hypoxia-induced proliferation (Balaiya, Murthy, & Chalam, 2013), (Guan et al., 2017). Others have shown that RSV can also decrease accumulation of HIF1α *in vitro* in hypoxia (Lee et al., 2015) or competitively bind and inhibit PDEs, which leads to vasodilation (Park et al., 2012).

Aside from the controversies regarding RSV's ability to activate SIRT1, and even without a clear mechanism, RSV has been shown to have beneficial health effects in mice (Baur, 2010b), protect from development of metabolic syndrome in mice fed high fat diet (Baur et al., 2006) and play a role in protection from cardiovascular disease (Baur, 2010a). In fact, several clinical trials using RSV have observed beneficial effects in coronary artery disease, atherosclerosis, hypertension and diabetes (Berman, Motechin, Wiesenfeld, & Holz, 2017). However, a definitive molecular link between SIRT1 and RSV is yet to be identified until better molecular assays for SIRT1 activity are developed, and definitive proof of the relationship is established *in vivo*.

As summarized in **Table 3-4**, RSV has been effective in preventing PH in the MCT (Csiszar et al., 2009), (D.-L. Yang et al., 2010), (S. Zhou et al., 2015) and the CH rat models (D. Xu et al., 2016), (L. Yu et al., 2017), (B. Chen et al., 2014), as well as partially reversing MCT-induced PH (Paffett, Lucas, & Campen, 2012). Interestingly, while all these studies propose some mechanistic insight into the therapeutic role of RSV in these models, none confirmed any direct link to SIRT1, the exception being Zhou *et al*, who showed that RSV promoted recovery from the MCT-induced decrease in SIRT1 protein levels in the lungs (S. Zhou et al., 2015). However, Yu *et al* did not note any improvement in the decreased lung SIRT1 protein levels in CH using RSV (L. Yu et al., 2017). As of yet, none of these studies have addressed the role of RSV in CH in mice or in the absence of SIRT1 activity, which would create a clearer link between RSV and SIRT1 activation *in vivo*.

Table 3-4: Use of Resveratrol in rat PH models

Model	RSV dose	RSV effect on PH Parameters	Additional RSV effects	Reference
MCT, prevention	25mg/kg/day	Improved RVSP, RVH, muscularization	↓ lung cell proliferation, ↓IL-6, IL-1, TNFα lung mRNA, ↑ BMPR2 lung mRNA	(Csiszar et al., 2009)
MCT, prevention	20mg/kg/day; 60mg/kg/day	Improved RVSP, PAAT*, RV thickness*	↓ lung apoptosis	(D.-L. Yang et al., 2010)
MCT, reversal	3mg/kg/day	Improved RVSP, RVH, muscularization		(Paffett et al., 2012)
CH, prevention	100mg/kg/day	Improved RVH	Nenonate rat model	(B. Chen et al., 2014)
MCT, prevention	2.5mg/kg/day; 20mg/kg/day	Improved mPAP, RVSP, RVH, muscularization	↑ SIRT1 lung protein	(S. Zhou et al., 2015)
CH, prevention	40mg/kg/day	Improved RVSP, RVH, muscularization	↓HIF1α lung protein	(D. Xu et al., 2016)
CH, prevention	25mg/kg/day	Improved RVSP, RVH, muscularization	↓ lung cell proliferation, no change in SIRT1 protein	(L. Yu et al., 2017)

* Assessed by ECHO. PAAT: Pulmonary Artery Acceleration Time, RVSP: Right ventricle systolic pressure, RVH: Right ventricle hypertrophy, CH: chronic hypoxia, MCT: Monocrotaline

3.1.3 Does HIF3α Modulate the Hypoxic Response?

The human *HIF3A* gene is predicted to generate up to 10 different splice variants (Duan, 2016),(Ravenna et al., 2016). The full length human HIF3α contains similar domains to HIF1α and HIF2α (bHLH, PAS and ODD domains), yet, a lucine zipper domain (LZIP), which is involved in protein-protein interactions, replaces the C-TAD domain (**Figure 1-1**) (Duan, 2016), (Ravenna et al., 2016). Compared to human *HIF3A*, the mouse *Hif3a* gene gives rise to fewer, though similar, splice variants (Duan, 2016),(Ravenna et al., 2016). Alongside the full length HIF3α, the mouse gene can produce a short splice variant lacking the ODD/N-TAD/LZIP domains called IPAS

(Inhibitory PAS) as well as a long splice variant containing an alternative first exon called NEPAS (Neonatal embryonic PAS) (Duan, 2016), (Ravenna et al., 2016). Several studies have implicated IPAS protein in playing a negative regulatory role in hypoxic transcription by binding to HIF1α and inhibiting its activity (Y Makino et al., 2001), (Yuichi Makino, Kanopka, Wilson, Tanaka, & Poellinger, 2002). Alternatively, the full length HIF3α and NEPAS protein variants can bind and inhibit both HIF1α and HIF2α activity directly or competitively by binding and sequestering HIF1β subunits (Yamashita et al., 2008). Interestingly, genetic deletion of the *Hif3a/NEPAS* gene in mice results in viable progeny with enlargement of both RV and LV, yet no increase in RV pressure or pulmonary vascular remodeling (Yamashita et al., 2008). In addition, ECs isolated from HIF3α/NEPAS knockout mice exhibit severe impairment in angiogenic activity, as evident by decreased migration and network formation *in vitro* (Kobayashi et al., 2015), (Yamashita et al., 2008). Of note, in normoxia, the absence of HIF3α/NEPAS in ECs leads to higher HIF2α transcription, which results in increased HIF2α protein levels only when the cells are placed in hypoxia (Kobayashi et al., 2015). No studies have yet to address the relationship between HIF3α and SIRT1 function.

3.2 Objectives and Hypotheses

3.2.1 Objectives:

- Define the consequences of absent SIRT1 activity on the relative function of the two main HIFs (HIF1α and HIF2α), as assessed by expression of their target genes
- Determine whether preventing HIF1α mediated increase in glycolytic metabolism using DCA can modify the exaggerated CH-induced PH in the absence of SIRT1 activity
- Determine the contribution of endothelial SIRT1 in the regulation of the pulmonary vascular response to CH
- Determine the efficacy of the putative SIRT1 agonist/mimic RSV on the response to CH in the presence and absence of SIRT1 activity

3.2.2 Specific Hypotheses:

- SIRT1 regulates the pulmonary vascular response to CH primarily by modulating the hypoxia-induced increase in activity of HIF2α; given its important role in the long-term adaptation to low oxygen
- DCA will prevent the development of exaggerated CH-induced PH in SIRT1 mutant mice by restoring the balance of mitochondrial metabolism towards glucose oxidation
- The endothelium plays a dominant role in maintenance of pulmonary vascular homeostasis, and endothelial-targeted knockout of SIRT1 will replicate the exaggerated pulmonary response to hypoxia, but not the increased HCT

- RSV will prevent the development of exaggerated CH-induced PH in absence of SIRT1 activity, by acting as a SIRT1 mimic and thereby compensating for the loss of SIRT1 activity

3.3 Materials and Methods

3.3.1 Lung/Plasma protein assessment

3.3.1.1 Protein extraction

For each mouse, ~10 mg of tissue was removed from -80ºC and placed in 250µL of cold 1x RIPA buffer (Radioimmunoprecipitation assay buffer, Millipore, 20-188) in ddH_2O containing one tablet of protease inhibitor (cOmplete™ ULTRA Tablets, Mini, EASYpack Protease Inhibitor Cocktail, Roche, 5892970001) and one stainless steel bead (Qiagen, 69989) in a 2mL tube. The tissue was homogenized and lysed using the TissueLyser II (Qiagen, 4mins at 20Hz) and then placed back at -80ºC overnight. Samples were then centrifuged at 4°C for 20 min at 12 000 rpm. Following the spin, the supernatant was collected, quantified for total protein and stored at -80°C.

3.3.1.2 Protein quantification

Protein extracts were quantified using a bicinchoninic acid (BCA, B9643, Sigma) assay. For each sample, 100µL BCA reagent mix (Appendix) prepared immediately before use was combined with 4µL of protein extract. Triplicates of each sample as well as a bovine serum albumin (BSA, Cell signaling technologies, 9998s) standard were loaded onto a 96-well plate (Corning, 3598) and incubated for 25mins at 37°C. Absorbance was read at 562nm using a POLARstar Omega microplate reader (BMG Labtech). Samples were diluted in fresh RIPA buffer to a concentration of 1.5ug/µL and assayed again to determine the exact protein content before further immunoblotting or enzyme-linked immunosorbent assay (ELISA) assessment.

3.3.1.3 Gel electrophoresis

Protein samples were prepared in a final 1x Laemmli buffer (Bio-Rad, 1610747) with 10% beta-mercaptoethanol (Sigma-Aldrich, M6250) and boiled for 5mins at 95°C before being loaded on 4-20% Tris-SDS polyacrylamide gels (4–20% Mini-PROTEAN® TGX™ Precast Gel, Bio-Rad, 4561094). A total of 30µg of total protein was loaded and gels were initially run at 85V for 20 min, then at 160V for 90 min or until the bottom ladder marker (PageRuler™ Prestained NIR Protein ladder, Thermo Fisher, 26635) reached the bottom of the gel. All gels were migrated in Mini-PROTEAN® Tetra Cell chambers (BioRad, 165-8004) with 1x Tris/Glycine/SDS running buffer (10x, Bio-Rad, 1610732).

3.3.1.4 Membrane Transfer

A dry transfer was performed using the iBlot ® Dry-transfer System (Life Technologies) onto nitrocellulose membranes (IB301001, Life Technologies). The membranes were pre-soaked in transfer buffer before transfer (Novex NuPAGE transfer buffer, Thermo Fisher, NP0006)

3.3.1.5 Antibody detection

For transgene expression studies, membranes were blocked in 5% BSA in 0.1% TBS-T (10x Tris Buffered Saline with Tween® 20, cell signaling technologies, 9997S) for 1hr at room temperature. Primary antibodies were incubated overnight at 4°C in 5% BSA in 0.1% TBS-T. The following day, membranes were washed in 0.1% TBS-T (3x5 min) and incubated with the corresponding IRDye infrared secondary antibodies (IRDye

800CW goat anti-rabbit (Mandel Scientific, LI-COR, 926-32211) at 1:10000 for 2hr at room temperature and imaged using the Li-COR Odyssey Infrared Imaging System (Li-Cor Biosciences). Antibodies used were LDHA (Cell signaling technologies, 2012S), BNIP3(Cell signaling technologies, 3769S) Secondary antibodies used were IRDye800 anti-rabbit. Total protein was determined using an IRDye for total protein as per manufacturer instructions and was used for normalization (REVERT™ Total Protein Stain Kit, Mandel Scientific, LI-COR, 926-11010).

3.3.1.6 Blot Quantification

Western blots were quantified by spot densitometry using the Li-COR Odyssey software (Image studio, v5.2). The pixel intensity value for each band was measured on non-saturated blots. The values for proteins were normalized to those of total protein for each sample.

3.3.7 Enzyme-Linked ImmunoSorbent Assays (ELISAs):

3.3.7.1 Erythropoietin ELISA

Erythropoietin protein levels were measured in 50µL of plasma using an EPO sandwich ELISA (Abcam, ab119593) as per manufacturer's instructions.

3.3.7.2 Mouse PAI-1 ELISA

PAI-1 protein levels were measured in 50µL (50µg) of lung tissue isolate using a PAI-1 sandwich ELISA (R&D systems, DY3828-05) as per manufacturer's instructions.

3.3.7.3 Endothelin-1 ELISA

Endothelin-1 protein levels were measured in 75µL (75µg) of tissue using an ET-1 sandwich ELISA (R&D systems, DET100) as per manufacturer's instructions.

3.3.2 Lung RNA assessment

3.3.2.1 Total RNA isolation

The miRNeasy Mini Kit (Qiagen, 217004) was used for total RNA isolation from tissue and the manufacturer's protocols were followed. Briefly, tissue was allowed to thaw on ice, removed from RNAlater® and placed in 2mL tube with 700µL of QIAzol Lysis Reagent and a 5mm stainless steel bead (Qiagen, 69989). The tissue was disrupted and homogenized using the TissueLyser II (Qiagen, 4mins, 20Hz). Chloroform (Sigma, C2432) was added to each tube and the samples were centrifuged to allow separation into three phases. The top aqueous phase, containing the RNA, was mixed with 1.5x volume of 100% anhydrous ethanol and transferred to the RNeasy mini spin column. After several washes, the RNA was eluted from the column using 100µL of RNase-free water.

3.3.2.2 Total RNA quantification:

RNA quality and quantity were determined by measuring absorbance using the NanoDrop™ 2000/2000c spectrophotometer (Thermo Fisher Scientific). Briefly, 2µL of sample was loaded and absorbance was measured. RNA concentration was determined from absorbance readings at 260nm, while purity was assessed with the 260/280nm and 260/230nm ratios. Respective ratios of 1.9-2.1 and 2-2.2 were indicative of high sample purity free from protein or other organic reagents contamination, respectively.

3.3.2.3 Reverse transcription of mRNA into cDNA:

Reverse transcription of the mRNA into cDNA was performed with 1500ng total RNA using a reverse transcription kit (QuantiTect Rev.Transcription Kit, Qiagen, 205311) following the manufacturers protocol. Briefly, a reaction of 1500ng of RNA, 4µL of genomic DNA wipeout buffer and top up to 28µL with ddH_2O was combined in a small PCR tube (PCR tube 0.2ml thin wall, clear, flat cap, Axygen, 12-722-262). The sample was incubated for 3mins at 42ºC using T100 Thermal Cycler (Bio-Rad). A master mix was created to contain reverse transcriptase (RT, 2µL per sample), RT buffer (8µL per sample) and primer mix (2µL per sample). 12µL of this mastermix was added to each tube, and the tubes were returned to the T100 Thermal Cycler (Bio-Rad). Cycling conditions: 42ºC for 20mins, 95ºC for 3min, 4ºC hold. The cDNA samples were further diluted in RNAse-free H_2O to create a 1/20 dilution.

3.3.2.4 Real-Time quantitative Polymerase Chain Reaction (RT-qPCR)

Quantitative real time PCR assays were conducted using a CFX384 Real-Time System (Bio-Rad). All primers were obtained from Qiagen and were pre-validated (Quantitect primers, Qiagen). Triplicates were carried out for each sample. The following 10µl reaction mixture was used: 4µl of cDNA, 5µl SYBR Green (QuantiTect SYBR Green PCR Kit, Qiagen, 204143) and 1µl of primers. The cycling conditions were used for all experiments: SYBR activation: 95ºC for 15mins, 40 cycles [95°C for 10s, 55°C for 30s, 72°C for 30secs], melt curve at 55°C with 0.5°C increments/ cycle up to 95°C. All samples were normalized using β-actin as a housekeeping control. Relative quantification

was performed using the ΔΔCT method.

3.3.3 Animal experiments

3.3.3.1 Animal Experiments Ethics statement:

All animal protocols and treatments were approved by the University of Ottawa Animal Care Ethics Committee and adhered to the Guidelines of the Canadian Council on Animal Care.

3.3.3.2 Resveratrol treatment:

Sirt1$^{Y/Y}$ mice (5-7 weeks-old, male and female) and wildtype *Sirt1*$^{+/+}$ littermates were exposed to either room air or to chronic hypoxia for 21 days with or without trans-Resveratrol (Biotivia) in diet (0.5g/kg) for an inspired dose of 35mg/kg/day.

3.3.3.3 Dichloroacetate treatment

Sirt1$^{Y/Y}$ mice (5-7 weeks-old, male and female) and wildtype *Sirt1*$^{+/+}$ littermates were exposed to either room air or to chronic hypoxia for 21 days with or without DCA (Sodium Dichloroacetate, Sigma-Aldrich, 347795) in drinking water (0.75g/L) for an inspired dose of 70mg/kg/day as reported previously (Evangelos D Michelakis et al., 2002).

3.3.3.4 Endothelial Cell (EC) Sirtuin 1 knockout mice (*EC-Cre-Sirt1*$^{f/f}$)

VE-Cadherin mice were obtained from Jackson laboratories (B6.FVB-Tg(Cdh5-cre)7Mlia/J, Stock No:006137) and carried the Cre Recombinase under the

expression of the endothelial cell specific promoter VE-Cadherin. SIRT1 floxed mice were obtained from Jackson laboratories (B6;129-*Sirt1*^{tm1Ygu}/J, Stock No: 008041) and carried a *loxP*-flanked neomycin cassette just upstream of exon 4 and a third *loxP* site downstream of exon 4. *EC-Cre-Sirt1*$^{f/f}$ mice lack SIRT1 protein in ECs due to recombination of loxP sites leading to deletion of exon 4 and a floxed SIRT1 gene (H. Li et al., 2007). ***Phenotype***: Viable, fertile. No phenotype was observed in this line. ***Breeding strategy***: Mice were on a C57BL6 background. Heterozygous mice (*EC-Cre-Sirt1*$^{f/+}$) were crossed in order to generate homozygous *EC-Cre-Sirt1*$^{f/f}$ mice. ***Genotyping***: Mice were ear tagged and ear notched for genotyping. Genomic DNA was used for genotyping using the REDextract-N-Amp^{TM} kit (Sigma, XNAT). PCR primer sequences were designed to amplify the wt *Sirt1*, and the floxed *Sirt1*: *Sirt1* Forward: 5' GGT TGA CTT AGG TCT TGT CTG 3' *Sirt1* Reverse: 5' CGT CCC TTG TAA TGT TTC CC 3'. Cre primers used were Forward primer: 5' GCG GTC TGG CAG TAA AAA CTA TC 3' and Reverse Primer: 5' GTG AAA CAG CAT TGC TGT CAC TT 3' xx. Cycling conditions: 95ºC for 3min, 35 cycles [95ºC for 30 sec, 50ºC for 1 min, 72ºC for 1min.], 72ºC for 5 min, 4ºC hold. SIRT1 primers amplify a 550-bp fragment from the normal *sirt1*+ allele whereas a 750-bp fragment from the floxed allele is amplified. Cre primers amplify a 100-bp fragment from *Cre*+ mice. ***Hypoxic treatment:*** In 3 week hypoxia experiments, *EC-Cre-Sirt1*$^{f/f}$ mice (5-6 week-old females) and het *EC-Cre-Sirt1*$^{f/+}$ littermates were exposed to either room air or to chronic hypoxia for 21 days. All mice were fed regular chow (Harlan) and housed in a 12hr/12hr dark light cycle.

3.3.4 Study endpoint pressure assessment and tissue collection:

3.3.4.1 Pressure measurements:

At experimental end point, mice were anaesthetized using an intraperitoneal injection of ketamine (100 mg/kg, Ketalean, DIN 00612316) and xylazine (10 mg/kg, Rompun, DIN 02169592). The upped thoracic area was shaved and the animal was placed on its back on a flat platform under a dissecting microscope. A small incision was made from the animal's chin down to the right armpit and the jugular vein was exposed, subsequently, the jugular vein was tied off tightly at the cranial end, loosely tied at the caudal end, and a small, medial incision was made in the vein. Right ventricular pressure was measured by threading a 1.2 French pressure microtip catheter transducer (Transonic-Scisense, FTS-1211B-0018) and proper readings were determined by observing sequential pressure loops recorded on LabScribe2 software (iWorx-Scisense). After RV pressure measurements, the catheter was inserted into the carotid artery to measure pressure in the aortic arch. Mean right ventricle systolic pressure (RVSP) was determined by taking the average of 3-5 readings that represent a single breathing cycle in the mouse. ***Technical Assistance***: Catheterization was performed by Dr. Yupu Deng, in a blinded manner.

3.3.4.2 Blood collection for plasma and hematocrit assessment

Following hemodynamic assessment, the abdominal cavity was exposed. Hematocrit (HCT) levels were determined by using heparinized hematocrit tubes (Drummond Scientific, Broomall, PA, 10007500HC/5). The tubes were filled with blood from the inferior vena cava and one end was sealed. The tubes were then spun in a

capillary tube centrifuge for 10 minutes to allow separation of plasma and red blood cells (RBCs). Levels of RBCs and total plasma were marked on a line and measured. Hematocrit was expressed as a percent of RBC to total blood using the equation: (Distance from end of line to edge of RBC line/ Distance from end of line to edge of plasma line) x100. ***Technical Assistance***: HCT tube preparation was performed in part Dr. Ken Schlosser.

3.3.4.3 Assessment of right ventricle and left ventricle weight and heart tissue collection

The heart was removed from the chest cavity. A blinded operator removed the atria, aorta and pulmonary trunk and dissected out the right ventricle, while keeping the left ventricle plus septum. The weight of each piece was recorded after which the tissue was placed in a cryogenic tube, snap frozen in liquid nitrogen then stored at -80ºC. Right ventricle hypertrophy (RVH, fulton index) was calculated using the equation: Right ventricle weight / (left ventricle plus septum) weight (RV/LV+S). ***Technical Assistance***: RV dissection was performed by Dr. Yupu Deng, in a blinded manner.

3.3.5 Statistical analysis

All data are presented as mean ± standard error of the mean (SEM). Statistical analysis was performed using a one-way analysis of variance (ANOVA) with a Sidak's multiple comparisons test for multiple group comparison, using GraphPad Prism 7.02 statistical software. A statistically significant difference was accepted at $p<0.05$.

3.4 Results

3.4.1 HIF1α mRNA and activity are increased in SIRT1 deficient hypoxic lungs

We initially sought to determine HIF1α and HIF2α expression and acetylation levels in lungs after hypoxia; however, we were unsuccessful in detecting the alpha subunits due to their rapid degradation in normoxia. HIF1α has a half-life of ~5 mins in normoxia (Berra, Roux, Richard, & Pouysségur, 2001), while HIF2α has a half-life of ~11 mins in normoxia (Lorenzo et al., 2013). Instead, we determined the mRNA levels and activity of specific HIF members in the lungs. Under normoxic conditions, there were no differences between HIF1α mRNA levels in lung tissue from *Sirt1*$^{Y/Y}$ and wild-type mice. However, genetic catalytic inactivation of SIRT1 led to a strong trend towards increased levels of HIF1α mRNA in *Sirt1*$^{Y/Y}$ hypoxic lungs ($p=0.06$), while SIRT1 knockout led to a significant increase in lung HIF1α in hypoxia compared to CH-*Sirt1*$^{+/+}$ animals ($p<0.001$; **Figure 3-1A**). In order to determine HIF1α activity, we measured mRNA levels of specific targets of HIF1α. While there was no difference in LDHA mRNA levels in lungs from *Sirt1*$^{+/+}$ and *Sirt1*$^{Y/Y}$ mice under normoxic conditions, both wild-type and SIRT1 mutant transgenic mice showed a similar significant increase in response to hypoxia (**Figure 3-1B**). Only in hypoxic *Sirt1*$^{-/-}$ lungs were the LDHA mRNA levels significantly increased compared to the CH-*Sirt1*$^{+/+}$ mice (**Figure 3-1B**), mirroring the increase in HIF1α expression in these KO mice. Assessment of another two HIF1α targets, BNIP3 and NDRG1, revealed a similar pattern of expression; BNIP3 and NDRG1 mRNA levels were significantly higher in hypoxic *Sirt1*$^{+/+}$ and *Sirt1*$^{Y/Y}$ lungs compared to normoxic controls and levels were further elevated in *Sirt1*$^{-/-}$ lungs (**Figure 3-1C-D**). Overall, SIRT1 limits CH-induced increases in lung mRNA levels of HIF1α

and its downstream targets, an effect modestly regulated through SIRT1 deacetylation activity.

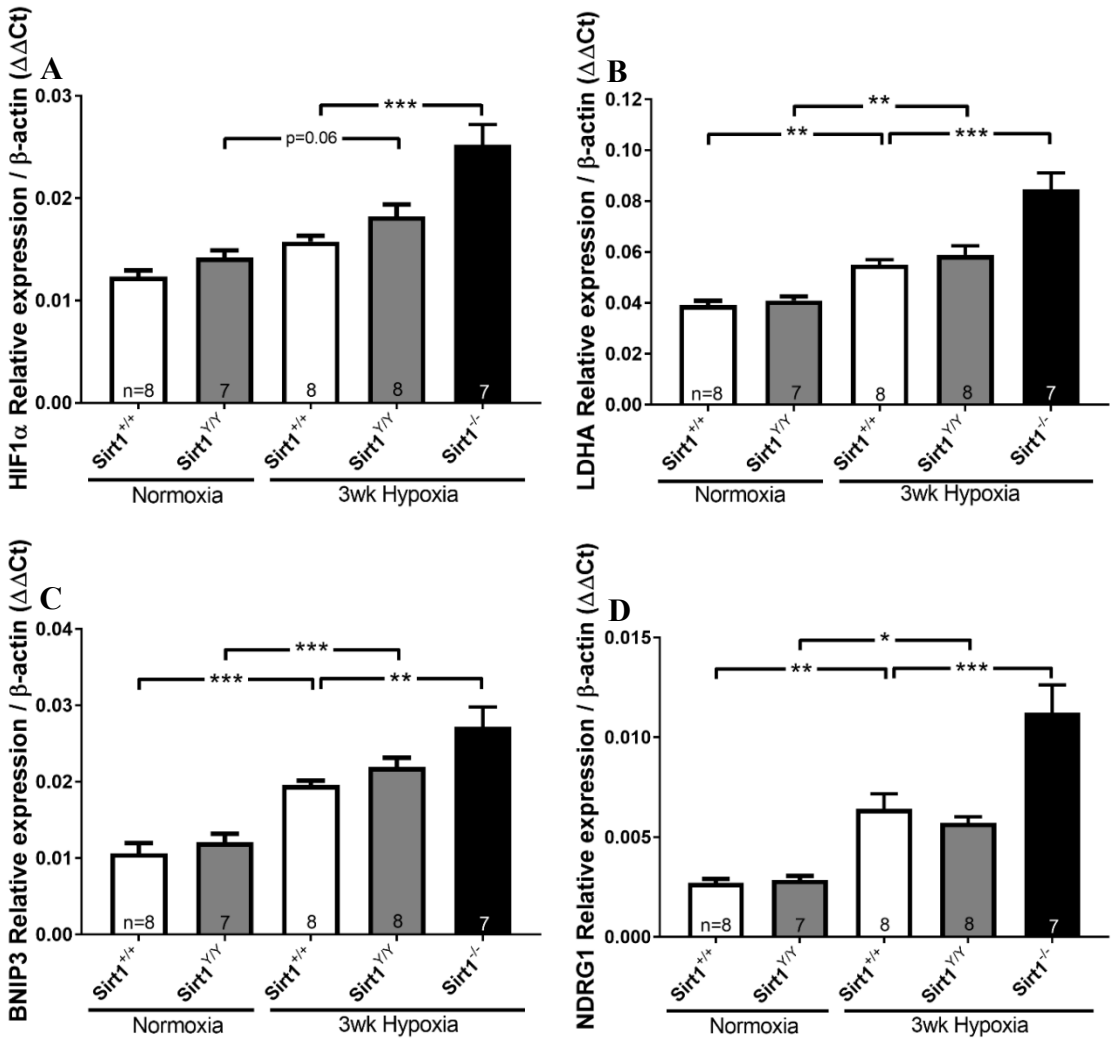

Figure 3-1: **mRNA levels of HIF1α and selective HIF1α targets in lung tissue from *Sirt1*$^{+/+}$, *Sirt1*$^{Y/Y}$ and *Sirt1*$^{-/-}$ in normoxia or chronic hypoxia for 3 weeks**. **A**) Hypoxia inducible factor (HIF)-1α mRNA. **B**) Lactate dehydrogenase A (LDHA) mRNA levels. **C**) BCL-2 and adenovirus E1B 19-kDa-interacting protein 3 (BNIP3) mRNA levels. **D**) N-Myc Downstream Regulated 1 (NDRG1) mRNA levels. n number indicated on bars. *p<0.05, **p<0.01, ***p<0.001.

3.4.2 Increased protein expression of HIF1α targets correlates with their enhanced mRNA levels in hypoxic lungs

We selected two HIF1α targets, LDHA and BNIP3, to further assess protein levels in the lungs by western blotting. Unlike NDRG1, those targets have been extensively validated as HIF1α specific and their function in hypoxia is better understood. Similar to the mRNA findings, LDHA protein levels in *Sirt1*$^{+/+}$ and *Sirt1*$^{Y/Y}$ mice were significantly elevated after three weeks of hypoxia compared to normoxic controls (**Figure 3-2A**), but not significantly increased in the mutant transgenic mice. In contrast, hypoxia induced a robust and significant increase in LDHA levels in *Sirt1*$^{-/-}$ mice (**Figure 3-2A**). Furthermore, all mouse lines showed a strong increase in lung BNIP3 protein levels in response to hypoxia, which tended to be greater in the SIRT1 mice compared to wild-type mice, but this only reached significance in lungs of *Sirt1*$^{Y/Y}$ animals (**Figure 3-2B**). Overall, the changes in protein levels of HIF1α targets mimics the changes in mRNA levels in hypoxia, and are similarly enhanced by SIRT1 deficiency.

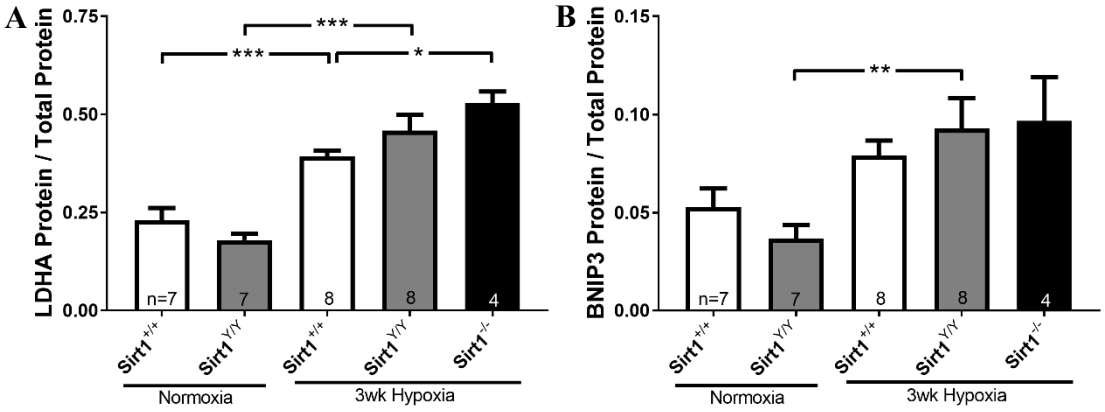

Figure 3-2: **Protein expression of selective HIF1α targets in lung tissue from *Sirt1*$^{+/+}$, *Sirt1*$^{Y/Y}$ and *Sirt1*$^{-/-}$ in normoxia or chronic hypoxia for 3 weeks assessed by western blot**. **A**) Lactate dehydrogenase A (LDHA) protein levels. **B**) BCL-2 and adenovirus E1B 19-kDa-interacting protein 3 (BNIP3) protein levels. n number indicated on bars. *p<0.05, **p<0.01, ***p<0.001. Representative blots in **Supplemental Figure 5**.

3.4.3 Knockout or inactivation of SIRT1 does not affect HIF2α mRNA levels, but can enhance HIF2α activity in hypoxia

Unlike HIF1α, lung HIF2α mRNA levels were not affected by inactivation of SIRT1 or SIRT1 knockout, either under normoxic conditions or on exposure to CH (**Figure 3-3A**). Next, we measured mRNA levels of HIF2α specific targets in order to determine HIF2α activity in hypoxic lungs. Under hypoxic conditions, there was no increase in ET-1 mRNA in *Sirt1*$^{+/+}$ or *Sirt1*$^{Y/Y}$ lungs compared to normoxic controls, whereas, ET-1 mRNA levels were significantly elevated in *Sirt1*$^{-/-}$ lungs compared to CH-*Sirt1*$^{+/+}$ lungs (**Figure 3-3B**). Of note, mRNA levels of ET-1 at one week of CH were significantly increased, but to a similar extent in the lungs of *Sirt1*$^{+/+}$ and *Sirt1*$^{Y/Y}$ mice (**Supplemental Figure 6, Appendix**). mRNA levels of PAI-1, another HIF2α target, were not increased by exposure to hypoxia in *Sirt1*$^{+/+}$ lungs (**Figure 3-3C**). In contrast, there was a significant increase in PAI-1 mRNA in lungs from CH-*Sirt1*$^{Y/Y}$ mice compared to normoxic *Sirt1*$^{Y/Y}$ and CH-*Sirt1*$^{+/+}$ lungs (**Figure 3-3C**), with a particularly exaggerated response in hypoxic *Sirt1*$^{-/-}$ compared to hypoxic *Sirt1*$^{+/+}$ mice (**Figure 3-3C**). A similar pattern of increased PAI-1 mRNA levels was observed at one week of hypoxia (**Supplemental Figure 6, Appendix**). Finally, the HIF2α target CXCL12 mRNA levels were elevated in hypoxia but to a similar extent regardless of SIRT1 status (**Figure 3-3D**). Overall, SIRT1 does not influence HIF2α mRNA levels; it appears to modulate HIF2α activity observed by the upregulation of mRNA levels of known HIF2α targets, especially in complete SIRT1 knockout.

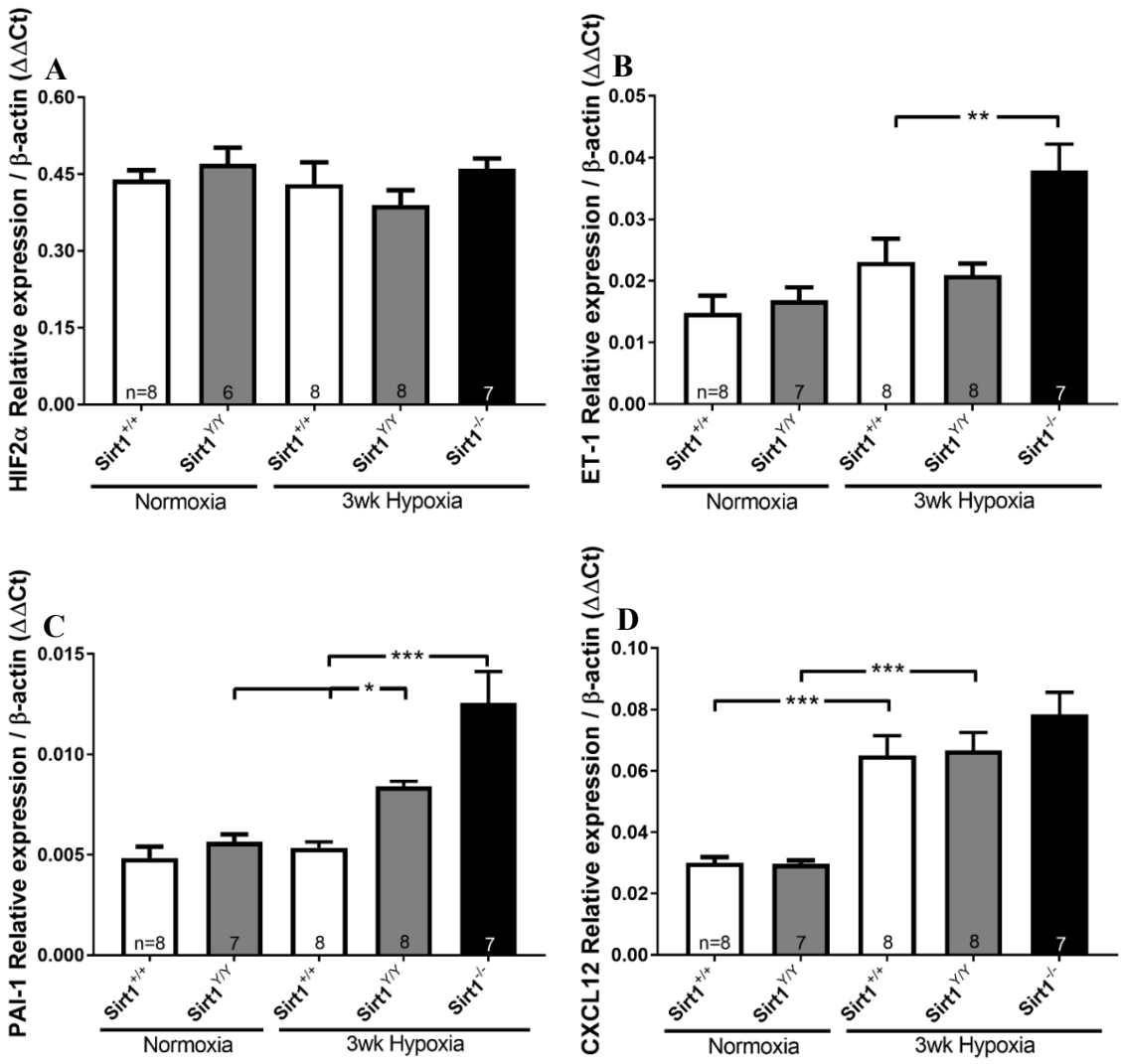

Figure 3-3: **mRNA levels of HIF2α and selective HIF2α targets in lung tissue from *Sirt1*$^{+/+}$, *Sirt1*$^{Y/Y}$ and *Sirt1*$^{-/-}$ in normoxia or chronic hypoxia for 3 weeks**. **A**) Hypoxia inducible factor (HIF)-2α mRNA levels. **B**) Endothelin-1 (ET-1) mRNA levels. **C**) Plasminogen activator inhibitor 1 (PAI-1) mRNA levels. **D**) Stromal-cell derived factor 1 (SDF-1, CXCL12) mRNA levels. n number indicated on bars. *p<0.05, **p<0.01, ***p<0.001.

3.4.4 Protein expression of HIF2α targets is increased in hypoxia, especially in lack of SIRT1 activity

The HIF2α targets ET-1 and PAI-1 were selected to assess protein levels in the lungs. Lung ET-1 protein levels were significantly elevated in response to hypoxia;

however, the magnitude of increase was similar regardless of the SIRT1 status (**Figure 3-4A**). In contrast, PAI-1 protein levels were significantly increased by hypoxia in both *Sirt1*$^{Y/Y}$ and *Sirt1*$^{-/-}$ mice compared to wildtype mice, with the knockout mice again showing the greatest response (**Figure 3-4B**). Since PAI-1 can also be secreted, we assessed its levels in plasma. A similar trend of increased PAI-1 in plasma was observed, with *Sirt1*$^{Y/Y}$ showing an exaggerated increase in CH (**Supplemental Figure 7, Appendix**). Overall, HIF2α targets protein expression is elevated in hypoxia and, similar to their mRNA levels, are further increased by SIRT1 deficiency, especially in complete SIRT1 knockout.

Since EPO is a known HIF2α target and plays a central role in erythropoiesis (Jelkmann, 2013), plasma EPO levels were assessed. At three weeks of CH, EPO levels were similar in *Sirt1*$^{+/+}$ and *Sirt1*$^{Y/Y}$ mice, and were almost at normoxic levels in both strains (**Figure 3-4C**). However, early assessment revealed that EPO levels were significantly elevated in *Sirt1*$^{Y/Y}$ mice after one day of hypoxia compared to normoxic *Sirt1*$^{Y/Y}$ controls and hypoxic *Sirt1*$^{+/+}$ mice (**Figure 3-4C**). The increase in EPO levels in the mutant transgenic SIRT1 mice appears to be greater not only in magnitude but also duration, with continued elevation up to one week, though at lower levels, which did not reach significance (**Figure 3-4C**). This higher EPO production implicates increased and/or sustained kidney HIF2α activation by hypoxia when SIRT1 is inactive.

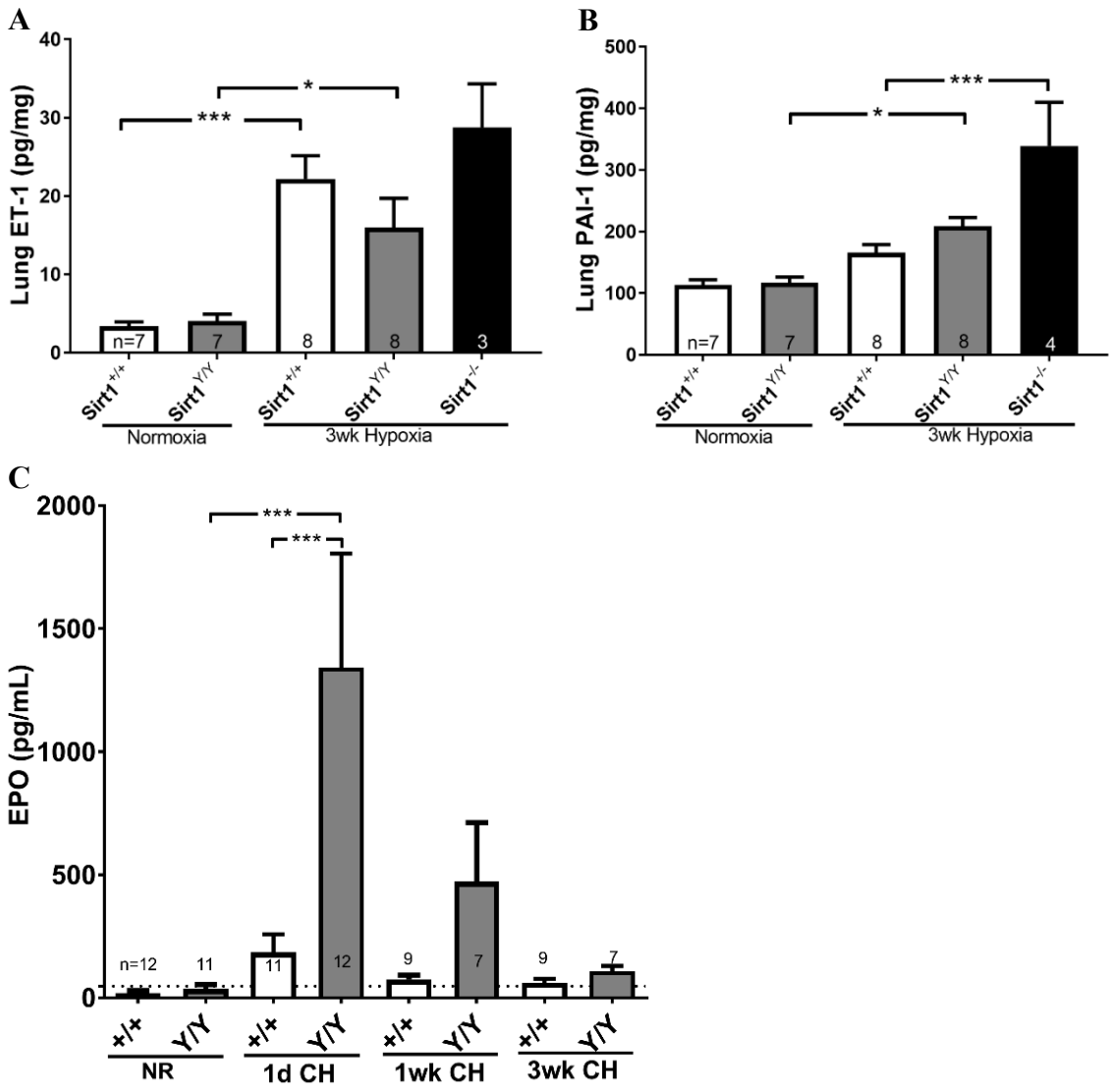

Figure 3-4: Protein expression of selective HIF2α targets in lung tissue or plasma from *Sirt1*$^{+/+}$, *Sirt1*$^{Y/Y}$ and *Sirt1*$^{-/-}$ in normoxia or chronic hypoxia for 3 weeks measured by ELISA. A) Endothelin 1 (ET-1) lung protein levels. **B**) Plasminogen activator inhibitor (PAI-1) lung protein levels. **C**) Erythropoietin (EPO) plasma levels in *Sirt1*$^{+/+}$ (+/+) and *Sirt1*$^{Y/Y}$ (Y/Y) mice in normoxia (NR) or chronic hypoxia for 1day (1d CH), 1 week (1wk CH) or 3 weeks (3wk CH). The dotted line represents the detection limit of the ELISA. n number indicated on bars. *p<0.05, **p<0.01, ***p<0.001.

3.4.5 HIF3α, but not HIF1β, lung mRNA levels are modulated by SIRT1

Inactivation of SIRT1 or hypoxic exposure did not lead to any changes in HIF1β lung mRNA levels (**Figure 3-5A**). However, assessment of HIF3α revealed a strong trend towards higher levels in mutant mice, both *Sirt1*$^{Y/Y}$ and *Sirt1*$^{-/-}$, but no difference between normoxia and hypoxia (**Figure 3-5B**). To determine the specific expression pattern of each HIF3α splice variant, we performed additional experiments using splice variant specific and previously tested primers (Weir et al., 2011) in *Sirt1*$^{Y/Y}$ mice. Using primers that amplified the full length HIF3α, but not the NEPAS or IPAS variants, we determined that absence of SIRT1 activity led to significantly increased full length HIF3α in normoxia, and a trend towards increase in hypoxia (p=0.1, **Figure 3-5C**). Using primers to amplify both full length HIF3α and NEPAS, but not IPAS, we noted a strong trend towards increased HIF3α mRNA expression in absence of SIRT1 activity both in normoxia and hypoxia (p=0.09 and p=0.05 respectively, **Figure 3-5D**). Finally, using primers to amplify IPAS only, we noted a weaker trend towards increased IPAS mRNA in absence of SIRT1 activity (p=0.1, both) and that IPAS expression was around 10 times lower than the other splice variants in the lungs of these animals (**Figure 3-5E**). Overall, SIRT1 deficiency was associated with a trend towards hypoxic-independent increases in HIF3α mRNA, which implicates SIRT1 activity in repression of HIF3α transcription.

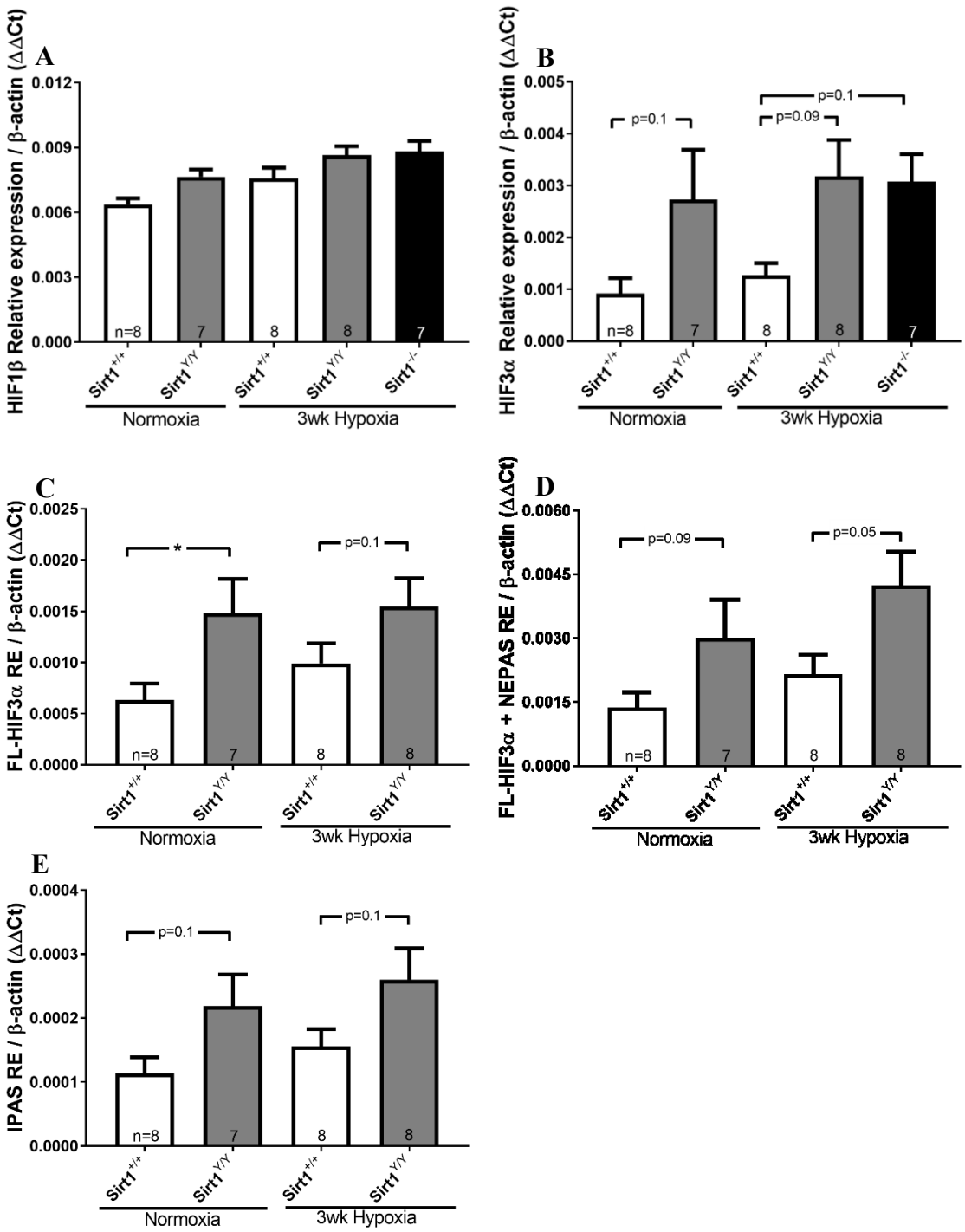

Figure 3-5: Levels of HIF1β and HIF3α mRNA in lung tissue from *Sirt1*$^{+/+}$, *Sirt1*$^{Y/Y}$ and *Sirt1*$^{-/-}$ in normoxia or chronic hypoxia for 3 weeks. **A**) HIF1β mRNA levels. **B**) HIF3α mRNA levels (all variants). **C**) Full length (FL) HIF3α mRNA levels. **D**) Full length HIF3α and NEPAS (Neonatal Embryonic PAS splice variant) mRNA levels. **E**) IPAS (Inhibitory PAS splice variant) mRNA levels. RE: Relative expression. n number indicated on bars. *p<0.05 or indicated.

3.4.6 DCA fails to resolve CH-induced PH, regardless of SIRT1 activity

A pathological shift towards glycolytic metabolism in the lungs have been reported to contribute to PH animal models and human PAH, mediated by increased HIF1α and PDK levels and activity, and can be reversed using the PDK inhibitor DCA (**Table 3-2**). In our model, HIF1α activity was elevated in hypoxia and exaggerated in the absence of SIRT1 (**Figure 3-1/3-2**). Furthermore, in hypoxia, PDK1 mRNA levels were elevated in SIRT1 mutant transgenic and knockout mice, but not *Sirt1*$^{+/+}$ mice (**Figure 3-6A**), suggesting that PDK inhibition using DCA might provide an effective option for prevention of metabolic shift, and thus development of PH in this model. Surprisingly, DCA treatment during CH did not result in any improvement in the hypoxic RVSP/RVH phenotype in *Sirt1*$^{+/+}$ or *Sirt1*$^{Y/Y}$ mice (**Figure 3-6B-C**). Instead, DCA led to significantly higher RVSP in DCA-CH-*Sirt1*$^{+/+}$ mice compared to non-DCA treated CH-*Sirt1*$^{+/+}$ mice, and had no effect on RVSP in CH-*Sirt1*$^{Y/Y}$ mice (**Figure 3-6B**). In addition, DCA did not have any protective effect on RVH or HCT compared to CH-*Sirt1*$^{+/+}$ or CH-*Sirt1*$^{Y/Y}$ mice (**Figure 3-6C-D**). Indeed, higher baseline levels of RVSP, RVH and HCT in DCA treated hypoxic wildtype mice resulted in absence of differences when compared to DCA treated hypoxic *Sirt1*$^{Y/Y}$ mice, while differences between CH-*Sirt1*$^{+/+}$ and CH-*Sirt1*$^{Y/Y}$ were maintained (+$p<0.05$, **Figure 3-6B-D**). To confirm efficacy of our DCA and delivery method, we assessed DCA treatment in the rat CH model following previously published protocols (**Table 3-2**). In rats, DCA partially prevented development of CH-induced increases in RVSP and RVH (**Supplemental Figure 8, Appendix**) confirming the functionality and method of DCA delivery used by our group. These findings suggest that PDK inhibition is not efficient at preventing wildtype mouse CH-induced PH, possibly

due to limited role for HIF1α mediated metabolic imbalance in this model. Additionally, PDK inhibition cannot compensate for absence of SIRT1 activity in CH-induced PH, suggesting that SIRT1 activity plays a limited role in CH-induced metabolic changes.

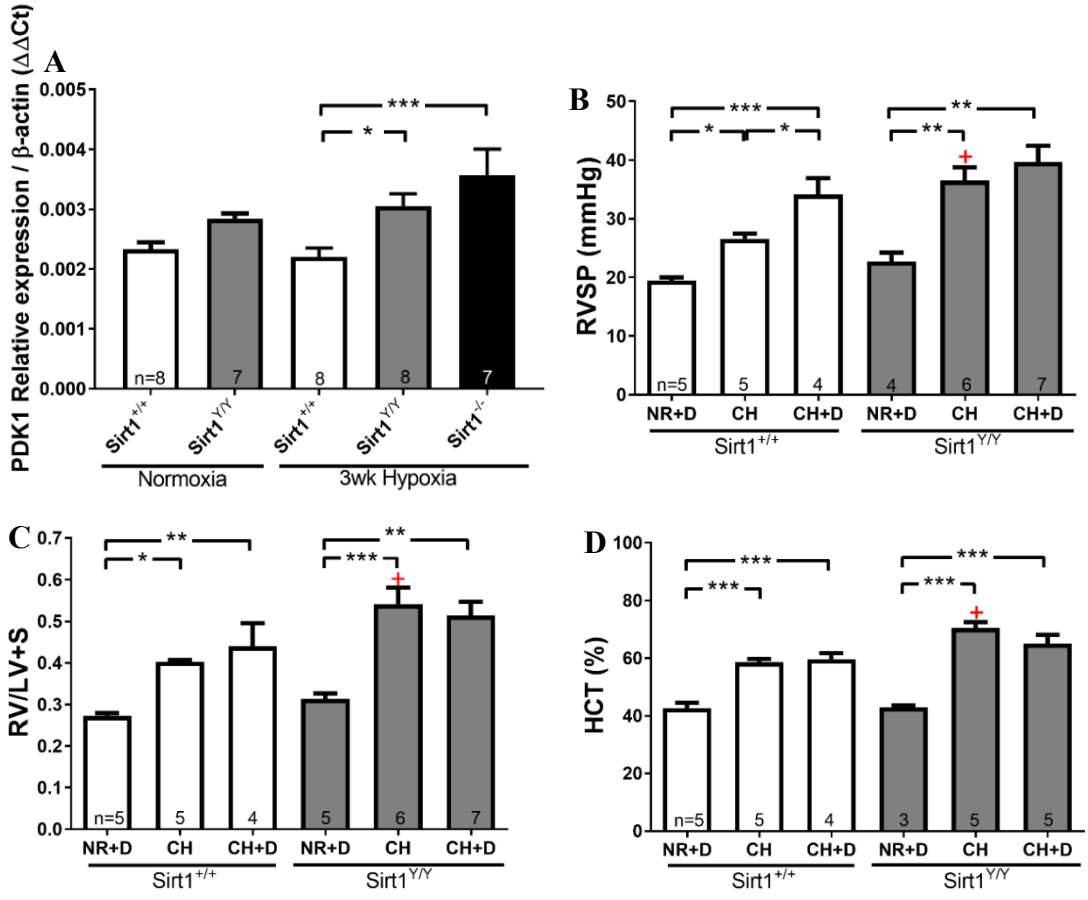

Figure 3-6: PDK1 mRNA levels and hemodynamic assessment in *Sirt1*$^{+/+}$ or *Sirt1*$^{Y/Y}$ at 3 weeks of normoxia or chronic hypoxia, with or without Dichloroacetate (D) in drinking water. **A**) Pyruvate dehydrogenase kinase (PDK1) mRNA levels. **B**) Right ventricle systolic pressure (RVSP). **C**) The weight ratio of the right ventricle (RV) to the left ventricle and septum (LV+S). **D**) Hematocrit (HCT) levels. NR= Normoxia, CH=Chronic hypoxia for three weeks, D=Dichloroacetate (70mg/kg/day) n number indicated on bars. *p<0.05, **p<0.01, ***p<0.001. +p<0.05 vs *Sirt1*$^{+/+}$.

3.4.7 RSV can partially prevent exaggeration of CH-induced PH in SIRT1 mutant transgenic mice, but is ineffective in SIRT1 competent mice

RSV has been previously shown to be effective in preventing rat CH-induced PH (**Table 3-4**), yet, a clear mechanism of RSV action or ability to mediate SIRT1 activity is still lacking. Therefore, we sought to determine whether RSV would prevent development of CH-induced PH, in the presence or absence of SIRT1 activity. Treatment with RSV for three weeks in CH prevented development of exaggerated RVSP in *Sirt1*$^{Y/Y}$ mice, but did not lead to any statistically significant effect on CH-induced RVSP in *Sirt1*$^{+/+}$ mice ($p= 0.3$) (**Figure 3-7A**). RSV did not reduce the CH-induced RVH in *Sirt1*$^{+/+}$ or *Sirt1*$^{Y/Y}$ animals (**Figure 3-7B**), yet, RSV led to lower CH-induced HCT in *Sirt1*$^{Y/Y}$ mice (72% CH-*Sirt1*$^{Y/Y}$ vs. 65% RSV-CH-*Sirt1*$^{Y/Y}$; $p<0.05$; **Figure 3-7C**). Interestingly, while RSV reduced the exaggerated RVSP/HCT in *Sirt1*$^{Y/Y}$ mice, RVH and HCT levels were still higher than RSV treated *Sirt1*$^{+/+}$ mice ($+p<0.05$, **Figure 3-7**). Overall, RSV ameliorates the exaggerated effects of SIRT1 deficiency on CH-induced RVSP and HCT, but not RVH, yet fails to elicit a response in SIRT1 competent mice. This protective effect of RSV, which was observed in absence of SIRT1 activity, supports the idea that RSV action is not mediated through SIRT1 activity, but RSV can act to partially compensate or mimic SIRT1 function in CH. In addition, the inability of RSV to reduce RVH/HCT in SIRT1 mice to wildtype levels suggests that RSV can only partially mimic or compensate for lack of SIRT1 activity.

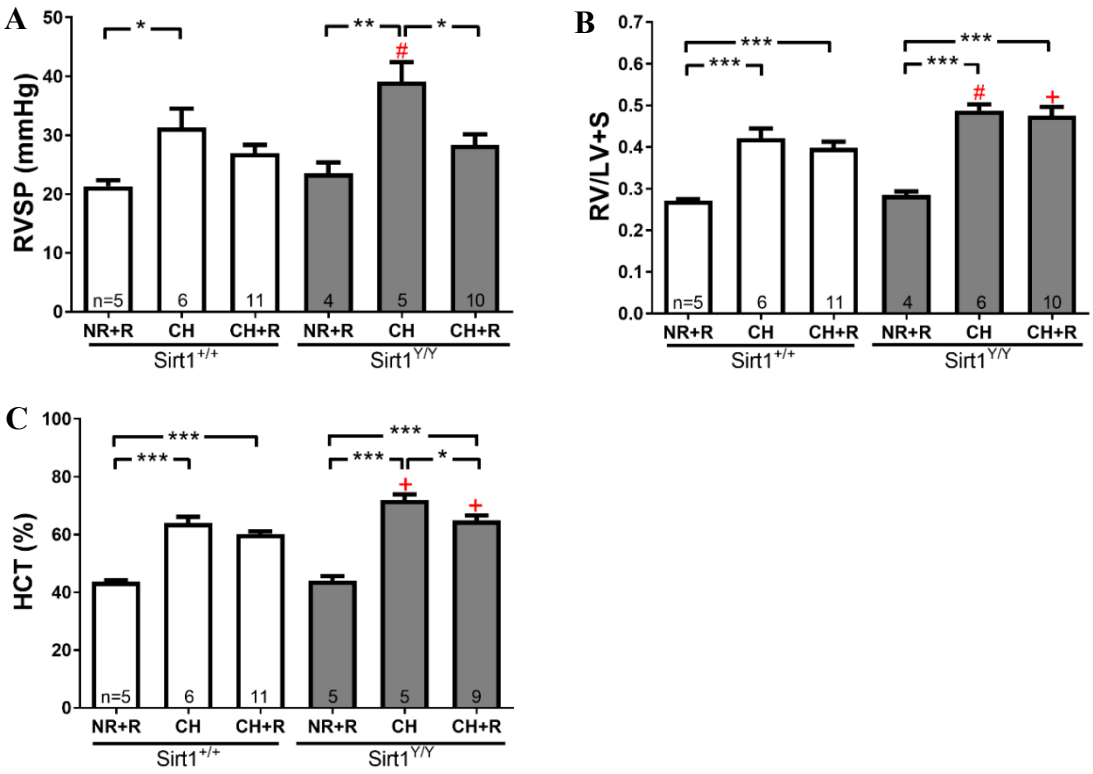

Figure 3-7: Hemodynamic assessment in *Sirt1*$^{+/+}$ or *Sirt1*$^{Y/Y}$ at 3 weeks of normoxia or chronic hypoxia, with or without Resveratrol (R) treatment in diet. **A**) Right ventricle systolic pressure. **B**) The weight ratio of the right ventricle (RV) to the left ventricle and septum (LV+S). **C**) Hematocrit levels. NR= Normoxia, CH=Chronic hypoxia for three weeks, R=Resveratrol (35mg/kg/day). n number indicated on bars. *p<0.05, **p<0.01, ***p<0.001. #p=0.05, +p<0.05 vs *Sirt1*$^{+/+}$.

3.4.8 Lack of endothelial SIRT1 leads to exaggerated CH-induced PH

To investigate the involvement of endothelial SIRT1 in CH-induced PH, we used targeted endothelial cell SIRT1 knockout (*EC-Cre-Sirt1*$^{f/f}$) mice. No differences in baseline normoxic RVSP were observed between the SIRT1 mice and their wild type heterozygous littermates (*EC-Cre-Sirt1*$^{f/+}$); however, *EC-Cre-Sirt1*$^{f/f}$ mutants exhibited a significant increase in RVSP compared to *EC-Cre-Sirt1*$^{f/+}$ control mice after three weeks of CH (30mmHg *EC-Cre-Sirt1*$^{f/+}$ vs. 35mmHg *EC-Cre-Sirt1*$^{f/f}$, $p<0.05$; **Figure 3-8A**). RVH was comparable in normoxic mice; however, exaggerated RVH was observed in *EC-Cre-Sirt1*$^{f/f}$ mice compared to *EC-Cre-Sirt1*$^{f/+}$ after three weeks of CH (0.39 *EC-Cre-Sirt1*$^{f/+}$ vs. 0.43 *EC-Cre-Sirt1*$^{f/f}$, $p<0.05$, **Figure 3-8B**). A similar trend was observed when RV weight was normalized to body weight (**Figure 3-8C).** Finally, while both *EC-Cre-Sirt1*$^{f/+}$ and *EC-Cre-Sirt1*$^{f/f}$ mice showed a significant increase in HCT after three weeks of CH, unlike *Sirt1*$^{Y/Y}$ or *Sirt1*$^{-/-}$ mice, *EC-Cre-Sirt1*$^{f/f}$ mice did not develop exaggerated HCT levels in hypoxia compared to *EC-Cre-Sirt1*$^{f/+}$ (56% *EC-Cre-Sirt1*$^{f/+}$ vs. 58% *EC-Cre-Sirt1*$^{f/f}$, **Figure 3-8D**). Overall, the data are consistent with a protective role for endothelial SIRT1 in CH-induced increases in RVSP and RVH.

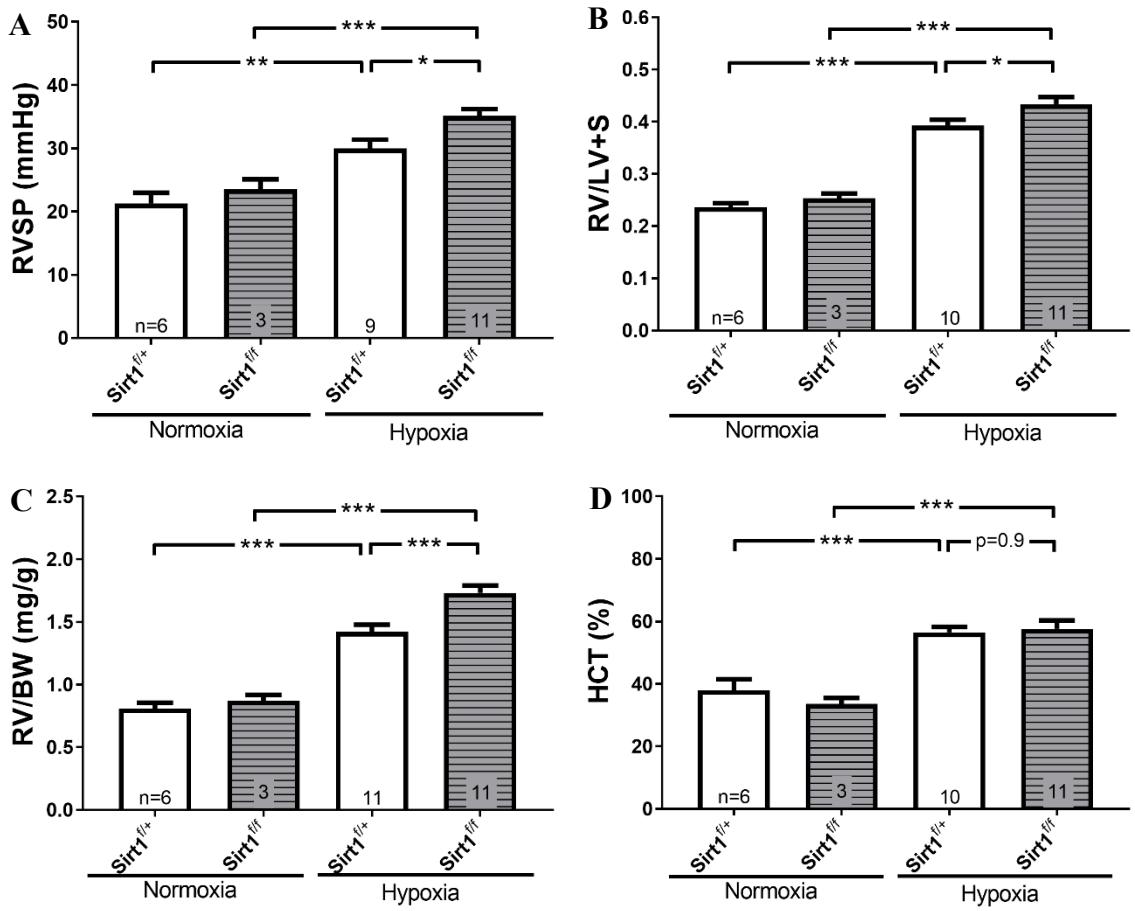

Figure 3-8: Right ventricle hemodynamics and hematocrit in *EC-Cre-Sirt1$^{f/+}$* and *EC-Cre-Sirt1$^{f/f}$* mice after three weeks of normoxia or chronic hypoxia. **A**) Right ventricle systolic pressure (RVSP) in *Sirt1$^{f/f}$* and their *Sirt1$^{f/+}$* littermates. **B**) The weight ratio of the right ventricle (RV) to the left ventricle and septum (LV+S) in *Sirt1$^{f/f}$* and their *Sirt1$^{f/+}$* littermates. **C**) The weight ratio of the right ventricle (RV) to body weight (BW) in *Sirt1$^{f/f}$* and their *Sirt1$^{f/+}$* littermates **D**) Hematocrit (HCT) levels in *Sirt1$^{f/+}$* and their *Sirt1$^{f/+}$* littermates. n number indicated on bars. *p<0.05, **p<0.01, ***p<0.001.

3.5 Discussion

SIRT1 limits CH-induced increases in HIF1α mRNA and downstream targets

Activation of the hypoxic pathway is dependent on the levels and activity of the HIFα subunits. While stabilization of HIFα subunits in hypoxia mostly occurs at the protein level, leading to increased HIFα protein accumulation without mRNA changes; increased mRNA levels in response to hypoxia can also lead to higher protein accumulation. Alternatively, the activity of stabilized HIFα subunits can be regulated by post translational modifications, such as, protein acetylation status. In our model, we were unable to measure HIF1α protein levels, yet HIF1α mRNA levels trended towards an increase in hypoxia in the absence of SIRT1 activity, and were significantly increased in complete SIRT1 knockout (**Figure 3-1A**). Protein and mRNA levels of downstream targets of HIF1α, including LDHA, BNIP3 and NDRG1 were elevated in hypoxia to a similar extent in *Sirt1*$^{+/+}$ and *Sirt1*$^{Y/Y}$ lungs; however, this was exaggerated in SIRT1 knockout mice (**Figure 3-1/3-2**). This provides support for an increase in HIF1α activity in complete absence of SIRT1, but not in absence of SIRT1 activity, which strongly corresponds with the increased HIF1α mRNA levels.

SIRT1 modulates the HIF1α pathway in CH, but not necessarily through deacetylation: Similar to our findings, previous work has shown that SIRT1 knockdown using siRNA can lead to increased HIF1α mRNA levels (Dong et al., 2016). The authors attributed this effect to increased acetylation of histones at the *HIF1A* gene promoter site in the absence of SIRT1 activity (Dong et al., 2016). In addition, a recent report determined that SIRT1 conditional knockout mice, which develop exaggerated CH-induced PH, have higher levels of HIF1α protein and the glucose transporter GLUT1, a

downstream target of HIF1α, after 3 weeks of CH (Zurlo et al., 2018). Alternatively, another recent report showed that SIRT1 knockdown, using SIRT1 siRNA, enhanced acetylation of HIF1α in PAECs, yet did not provide compelling evidence that it would lead to higher HIF1α protein levels or increased activity in hypoxia (P.-I. Chen et al., 2017). This could be explained by the fact that hypoxic assessment was performed only after a short period of exposure in this study (24-48hrs of hypoxia), whereas our study was focused on prolonged hypoxic exposure. Indeed, most of the previous studies conducted *in vitro* rely on short-term hypoxic exposure and provide contradicting evidence regarding whether SIRT1 can directly deacetylate HIF1α (**Table 3-1**). Based on previous evidence and our findings, we believe that lack of SIRT1 leads to increased HIF1α pathway activation through increased transcription and subsequent accumulation of HIF1α, even though this was indirectly assessed. Moreover, since the increase in HIF1α pathway activation was observed in SIRT1 knockouts, and to a lesser extent SIRT1 transgenic mutants, we propose that the role of SIRT1 in HIF1α-mediated CH response might be deacetylation-independent.

SIRT1 exerts effects independent of deacetylation in CH: Previous studies have implicated SIRT1 in deacetylation-independent activities, such as NF-kB inhibition (Ghosh, Spencer, Ng, McBurney, & Robbins, 2007), enhancement of apoptosis (Ghosh et al., 2007), neuroprotection (Pfister, Ma, Morrison, & D'Mello, 2008) and stimulation of sumoylation (Campagna et al., 2011). Remarkably, another deacetylation-independent function of SIRT1 is the ability to recruit and/or activate other histone modifiers, such as methyl transferases, leading to transcriptional repression (Y. Zhang et al., 2009), (Vaquero et al., 2007). In one report, the authors show that the N-terminus of SIRT1,

lacking the catalytic domain, can stimulate activity of SUV39H1, a histone lysine methyl transferase, thus modulating transcription (Vaquero et al., 2007). Another report shows that SIRT1 can recruit and support activity of Dot1, a methyl transferase, leading to methylation and suppression of transcription, independently of SIRT1 deacetylation functions (Y. Zhang et al., 2009). Thus, it seems plausible that complete SIRT1 knockout, but not inactivation, leads to lower recruitment/activation of other methyltransferases, leading to less repressed histone state, which could be mediated independent of deacetylation. Additionally, knockout of SIRT1 in mouse embryonic fibroblasts leads to higher acetylation levels of several proteins in the chromatin remodeling complex, including BAF57 (Smarce1) (Y. Chen et al., 2012), which has been linked to modulation of HIF1α transcription in hypoxia (Kenneth & Rocha, 2008). In our model, the significant increase in HIF1α mRNA and downstream target levels in SIRT1 knockouts corresponds to worse pulmonary vascular muscularization and RVH compared to SIRT1 inactivated mice (**Chapter 2**). Therefore, it is possible that part of the protective effects of SIRT1 in CH-induced PH are mediated through repression of HIF1α transcription leading to limited HIF1α protein and activity, which appears to be mediated through additional functions of SIRT1. This repression of HIF1α by SIRT1 highlights the role for SIRT1 in the HIF1α-mediated metabolic shift, a major contributor to increased SMC proliferation in CH.

DCA fails to prevent hypoxia-induced PH in wildtype and SIRT1 inactive mice

The role of metabolic shift in the response to CH has not been previously studied in mouse models and, given the many important differences that exist between species,

one cannot assume that they will behave in a manner analogous to rats. Certainly, we could not prevent PH development using DCA in our mouse CH model (**Figure 3-6**), yet, DCA was able to partially prevent higher RVSP and RVH in our rat CH model (**Supplemental Figure 8, Appendix**). The DCA doses used in our study are similar to those effectively used previously in transgenic mice overexpressing the serotonin transporter in SMCs (Guignabert et al., 2009), making it less likely that inadequate dosing was responsible for the lack of DCA effect we observed. We believe that the inherent differences between mice and rats in the way they develop PH pathology in the CH model explains the difference in response to DCA.

DCA fails to prevent hypoxia-induced PH due to differences in the CH response in mice and rats: Mice respond differently to many PH stimuli compared to rats, including the response to CH, at both physiological and molecular levels. Mice require at least three weeks of hypoxia to show a significant increase in mPAP, while rats develop PH after only one week (Hoshikawa et al., 2003). Moreover, the degree of elevation in mPAP and pulmonary vascular muscularization is substantially lower in mice than rats in CH (Hoshikawa et al., 2003). Interestingly, mice have a higher oxygen consumption rate than rats at high altitude (Jochmans-Lemoine et al., 2015) and under hypoxia (Jochmans-Lemoine, Shahare, Soliz, & Joseph, 2016). Molecularly, this is accompanied by higher levels of HIF1α protein in hypoxic mice than rats, yet lower levels of the downstream targets, PDK1 and GLUT1 (Jochmans-Lemoine et al., 2016). In fact, microarray data show large differences in target genes activated in hypoxic mice versus hypoxic rats (Hoshikawa et al., 2003). These differences are most likely attributed to the environment these animals live in; mice appear to live comfortably at altitudes as high as 4000m,

while rats are not found at elevations higher than 3000m (Jochmans-Lemoine et al., 2016). Overall, it appears as if the metabolic dysfunction, noted in human PAH and rat CH-PH, plays a smaller role in mouse CH-PH and contributes to DCA being ineffective in mice.

DCA fails to prevent hypoxia-induced PH due to the limited role for HIF1α, compared to HIF2α, in CH mice: Since DCA mainly exerts its activities on the metabolic shift mediated by HIF1α, it is possible that the exaggerated phenotype observed in our model was mediated mainly by HIF2α, and to a lesser extent through HIF1α. Indeed, as shall be discussed in subsequent sections, our data suggests that HIF2α is highly active in both *Sirt1*$^{Y/Y}$ and *Sirt1*$^{-/-}$ lungs, while HIF1α is more active in *Sirt1*$^{-/-}$ lungs. Furthermore, another group confirmed that DCA was ineffective in preventing development of PH in the endothelial PHD2 KO model, which results in stabilization of HIF2α (Personal communication with Zhiyu Dai, American Heart Association Scientific Session, 2016). Therefore, we suggest that the mouse CH model is driven by HIF2α activation rather than HIF1α, making modulation of HIF1α-driven metabolic changes ineffective. The use of DCA in *Sirt1*$^{-/-}$ mice might provide some further confirmation to our findings, yet we were limited by the number of knockout mice we could obtain due to their high lethality. Interestingly, even though a large part of the role of SIRT1 in metabolic modulation has been proposed to be through regulating HIF1α, it seems clear that any effect of SIRT1 on the HIF1α mediated metabolic shift is fairly limited in this model.

SIRT1, and specifically endothelial SIRT1, modulates the HIF2α pathway in response to CH

Activation of the HIF2α pathway is dependent on the levels (mRNA, protein) and activity (e.g. acetylation) of the HIF2α subunits. In our model, HIF2α mRNA levels were unchanged in SIRT1 inactivated and knockout mice compared to wildtype mice, in both normoxic and hypoxic conditions (**Figure 3-3A**). However, increases in mRNA or protein expression of the HIF2α targets, ET-1, EPO and PAI-1, were higher in hypoxia in SIRT1 KO and YY mice (**Figure 3-3/3-4**). Increased ET-1 and PAI-1 levels can directly contribute to the increased pulmonary muscularization and subsequent exaggerated hemodynamics. ET-1 is well known to be overexpressed in PAH (Giaid et al., 1993) and endothelin receptor antagonists are a mainstay for modern PAH specific therapy (Channick et al., 2001). PAI-1, which was strongly elevated in the lungs of SIRT1 mutant mice, is linked to SMC proliferation (Schuliga et al., 2013), (Dimova et al., 2004). In addition, circulating EPO levels were significantly elevated in *Sirt1*$^{Y/Y}$ mice (**Figure 3-4C**), the consequences of which are observed as higher HCT levels as well as splenomegaly in SIRT1 mutants and knockouts (**Chapter 2**). However, it is important to note that increased HCT levels per se, do not account for the worse pulmonary vascular response to CH in the SIRT1 deficient mice, as discussed in Chapter 2. Since we were unable to determine HIF2α protein levels, we do not know whether SIRT1 absence affects HIF2α protein levels or HIF2α protein activity in CH.

SIRT1 modulates HIF2α activity in CH, likely mediated by deacetylation: While no previous work described the effect of SIRT1 on HIF2α protein levels, we cannot rule out the possibility that SIRT1 can limit the CH response through modification of HIF2α

protein levels/accumulation in hypoxia. Yet, previous work strongly supports the idea that SIRT1 can alter the activity of HIF2α through binding and deacetylation (**Table 3-3**). However, our studies support that SIRT1-mediated effects limit HIF2α activity, while most studies associate HIF2α deacetylation with enhanced activity. We believe the contradiction of previous work with our findings is due to a combination of three reasons. First, as evident by its restricted expression, HIF2α plays a specialized function depending on the cell type. For example, EPO can only be produced by kidney interstitial fibroblasts in adults, while ET-1 and PAI-1 are mainly produced by the endothelium, mediated by HIF2α activity. A previous report suggests a potential "cell-specific" relationship between SIRT1 and HIF2α, where deacetylation led to HIF2α activation in some cell lines, but inhibition of HIF2α activity in others (Yoon et al., 2014). Therefore, it is possible that in kidney fibroblasts and pulmonary ECs, SIRT1 deacetylates and limits HIF2α activation, while in other cell types, it plays an opposite function. Second, all previous studies have been conducted *in vitro* using SIRT1 knockdown by siRNA, while our study was conducted *in vivo* in genetically manipulated animals expressing mutant SIRT1 or completely lacking SIRT1. Thus, the effect in a whole organism does not always reflect studies *in vitro* or studies using transient RNA silencing. Third, our study was conducted in prolonged hypoxic conditions, while all previous work focused on short-term hypoxic exposure. This could distort the findings, especially since HIF2α is mainly responsible for long-term adaptations to hypoxia. Taken together, in our *in vivo* model of CH, it is clear that SIRT1 has a limiting effect on HIF2α activity. However, since we relied on selected targets to estimate HIF2α activity, we cannot rule out the possibility that SIRT1 could have a direct effect on these targets, independent of HIF2α.

In fact, previous work has showed that SIRT1 can reduce PAI-1 expression thorough deacetylation of histones in the promoter region of PAI-1 in atherosclerosis (Wan et al., 2014), while SIRT1 siRNA in ECs can lead to increased production of ET-1 (Mortuza, Feng, & Chakrabarti, 2015). However, in our mice, we did not observe any increases in PAI-1 or ET-1 levels under normoxia (**Figure 3-3/3-4**), suggesting that lack of SIRT1 activity alone is not sufficient to induce their expression *in vivo*. Yet, in hypoxia, the increased PAI-1 or ET-1 expression in SIRT1 animals could be attributed to increased HIF2α pathway activation or the hyperacetylation of promoter sites in absence of SIRT1 activity, allowing easier access for the transcriptional machinery. Overall, SIRT1 can limit the HIF2α pathway activation in CH *in vivo* by several potential mechanisms, thus inhibiting development of PH pathophysiology. This is especially the case for HIF2α targets in the kidneys and lungs, and specifically, the lung endothelium.

Endothelial SIRT1 knockout is sufficient to reproduce the exaggerated phenotype observed in global SIRT1 knockout mice: ECs play a significant role in modulation of the pulmonary hypoxic response and pathogenies of PAH. While ECs express both HIF isoforms, the dominant isoform is HIF2α, which is also known as EPAS1 (for "endothelial PAS domain-containing protein 1"). We found that global SIRT1 knockout led to higher activity of HIF2α in the lungs in CH, therefore, it seems plausible that the exaggerated phenotype observed in lack of SIRT1 in ECs is mediated by increased activation of HIF2α, which subsequently leads to increased muscularization and vascular pruning leading to worse PH pathology. In fact, continuous activation of HIF2α, but not HIF1α, in ECs is sufficient to cause severe PH in mice (Dai et al., 2016). Due to the restriction of SIRT1 knockout to cells of endothelial lineage, we did not

observe any increase in HCT levels in CH; yet the mice exhibited exaggerated PH. This is in line with our previous assertion that the increased EPO/HCT plays a limited role in the PH pathology in this model. Clearly, endothelial SIRT1 plays a significant role in protection from CH-induced PH, most likely mediated through the activity of HIF2α.

Resveratrol partially compensates for loss of SIRT1 activity, limiting the response to CH only in absence of active SIRT1

The natural polyphenol RSV has shown beneficial effects in coronary artery disease, atherosclerosis, hypertension and diabetes (Berman et al., 2017). However, there is debate whether these beneficial effects of RSV are mediated through its ability to activate SIRT1 or by a SIRT1-independent mechanism.

RSV fails to prevent hypoxia-induced PH in SIRT1-wild type mice: RSV has previously been used to prevent development of CH-induced PH (**Table 3-4**). Previous studies using RSV focused on rat models of PH, which differ greatly in their CH response from mice as discussed earlier. Furthermore, these studies failed to provide evidence of SIRT1 activation after RSV treatment *in vivo*. In our normal SIRT1 mice, RSV failed to prevent CH-induced PH, but ameliorated CH-induced RVSP and HCT in $Sirt1^{Y/Y}$ mice (**Figure 3-7**). Inadequate dosing does not appear to be the cause of the absent effect of RSV in SIRT1 competent mice since we observed a significant reduction in RVSP and HCT in RSV treated $Sirt1^{Y/Y}$ mice exposed to CH. This suggests that RSV at this dose is effective in eliciting a response in this model, but only in absence of SIRT1 activity. Thus, these data support the idea that RSV *does not* activate SIRT1 directly, but can partially mimic its activity in a manner that compensates for the absence of SIRT1.

RSV can compensate for absence of SIRT1 activity through several potential mechanisms in CH: RSV treatment *in vitro* led to decreased HIF1α protein and activity in hypoxia, which was accompanied by decreased levels of VEGF (Lee et al., 2015). While RSV effects on HIF2α have not been assessed, it is possible that it plays a similar role in inhibiting HIF2α activation, especially since RSV also blunted the increase in HCT in response to CH in our mice (**Figure 3-7C**), which is well recognized to be under the control of HIF2α. Interestingly, RSV has been shown to be able to competitively bind and inhibit PDEs, which are cAMP/cGMP hydrolases that can limit vasodilation (Park et al., 2012). PDE5 inhibitors are approved for the treatment of PAH, and act by inhibiting the degradation cGMP and potentiating the effects of NO-induced vasodilation (Wharton et al., 2005), (E D Michelakis et al., 2003). While RSV was not shown to bind PDE5 specifically, it could bind and inhibit PDE1, PDE3 and PDE4, which can hydrolase either cAMP, or both cAMP and cGMP (Park et al., 2012). Therefore, RSV may be playing a role in enhancement of vasodilation, which can lead to reduced RVSP, while RVH needs a longer time to recover/adapt to the lower PVR. Further support for RSV's role in vasodilation is its ability to increase the expression of eNOS mRNA and protein and inhibit ET-1 expression and secretion in ECs (Schmitt, Heiss, & Dirsch, 2010). Alternatively, RSV might inhibit PASMCs proliferation in response to hypoxia (Guan et al., 2017), which could limit muscularization of vessels and thereby contribute to the reduced RVSP. Overall, RSV might be an attractive therapeutic option for HAPH or PAH presented with increased HIF pathway activation.

SIRT1 modulates lung HIF3α transcriptional regulation *in vivo*

Several studies have reported that full length HIF3α, NEPAS and IPAS play a negative regulatory role in the hypoxic response through inhibition of HIF1α and HIF2α activity (Duan, 2016),(Ravenna et al., 2016). In our model, higher HIF3α mRNA was observed in SIRT1 mutant animals, both in normoxic and hypoxic conditions, as well as in SIRT1 knockouts in hypoxia (**Figure 3-5**). This suggests that SIRT1 maintains a transcriptionally repressed state for HIF3α, most likely through histone deacetylation at the *HIF3A* gene promoter site.

In normoxia, increased full length HIF3α/NEPAS mRNA probably leads to limited physiological effects due to the presence of the ODD domain and subsequent rapid and efficient hydroxylation and degradation by PHDs. However, since the IPAS subunit does not have an ODD domain, it is not degraded in normoxia. Yet, the PHD system, which is more efficient than IPAS in inhibiting hypoxic activation of HIFα subunits, would be active, ensuring rapid degradation of HIFα subunits. Therefore, it is unlikely that IPAS would play a significant role in normoxic conditions. In hypoxia, there is inactivation of PHD/FIH and stabilization of the HIFα subunits, including HIF3α/NEPAS. High levels of stable HIF3α/NEPAS protein should serve to limit the activation of the hypoxic response (Duan, 2016),(Ravenna et al., 2016). Since we could not measure HIF3α/NEPAS protein levels due to rapid degradation, we do not know if the increase in HIF3α/NEPAS mRNA levels leads to higher accumulation of protein in CH. However, working under the assumption that the protein accumulation is proportional to mRNA levels, HIF3α/NEPAS should limit hypoxic activation. Yet, in our model, we observe exaggeration of hypoxic response mediated by increased HIF1α and HIF2α activity in absence of SIRT1 activity, suggesting that increased HIF3α/NEPAS

expression in our model could be participating in enhancing, not limiting, the hypoxic response.

Due to presence of the bHLH domain in full length HIF3α/NEPAS, which plays a role in DNA binding, some previous studies focused on the potential of transcriptional activity of HIF3α in hypoxia (P. Zhang et al., 2014). In fact, the authors identified several potential hypoxic HIF3α transcriptional targets through HRE binding of promoter regions in zebrafish, some of which were co-transcribed by HIF3α and HIF1α, while others were unique to HIF3α (P. Zhang et al., 2014). Recent work in human cancer cells determined that HIF3α can bind the DNA and initiate transcription of *RhoC* and *ROCK1* genes in hypoxia leading to increased migration and invasion, providing further evidence that HIF3α has transcriptional activation abilities in hypoxia (X. Zhou, Guo, Chen, Xie, & Jiang, 2018). This provides some support to the idea that the exaggerated HIF3α/NEPAS levels in absence of SIRT1 or inactivity might contribute to worsening, rather than limiting, the CH-response.

Overall Conclusions:

Our study provides strong *in vivo* evidence that SIRT1 can limit HIF1α pathway activation in CH, which appears to be mediated modestly though deacetylation. Interestingly, HIF1α-mediated metabolic shift appears to play a limited role in the development of PH pathology in this mouse model. Our studies also provide the first *in vivo* evidence that SIRT1 limits the HIF2α pathway in lungs and kidneys in CH, which appears to be mediated mainly by endothelial SIRT1. Our data also provide compelling *in vivo* evidence of the efficacy of RSV in prevention of CH-induced PH in absence of

active SIRT1 in a manner that partially compensates for SIRT1 activity. Finally, we provide the first evidence that SIRT1 activity can limit HIF3α transcription in the lungs, a relationship that should be further explored. Overall, SIRT1 plays an important role in preventing overactivation of the pulmonary and systemic hypoxic response through regulation of the HIF pathway activation in CH, which limits pathological vascular remodeling and PH in this model.

Limitations and challenges

Antibody specificity: We faced several challenges when studying HIFs. Lack of specific antibodies, especially in light of the rapid degradation of HIFα subunits in normoxia, was a major issue. We optimized over 4 antibodies for HIF1α, none of which gave a specific band until a newly developed monoclonal antibody by Cell Signaling Technologies. We also tried 4 antibodies for HIF2α before determining a working antibody from Novus Biologicals. HIF3α was very challenging due to presence of large number of splice variants. We tried 4 antibodies, all of which gave a large number of non-specific bands present in normoxic and hypoxic cells and tissues, including a monoclonal antibody. We then used an ELISA for HIF3α, which produced a similar signal from normoxic and hypoxic samples, suggesting either complete degradation or non-specific binding.

Normoxic degradation of HIFα subunits: The short half-life of alpha subunits in normoxic conditions due to rapid and efficient degradation greatly limited our ability to detect their expression in lung tissue. Indeed, HIF1α has a half-life of ~5mins in normoxia (Berra et al., 2001), while HIF2α has a half-life of ~11mins in normoxia

(Lorenzo et al., 2013). Furthermore, not only is PHD expression hypoxia driven (Marxsen et al., 2004), relocation from hypoxia to normoxia leads to increased PHD activity and decreased oxygen affinity, leading to very efficient hypoxic termination as soon as PO_2 levels increase (Marxsen et al., 2004), (Ginouvès et al., 2008). Thus, since we were unable to assess protein levels of the alpha subunits in tissue, we assessed their activities indirectly by measuring expression levels of their downstream targets, which gave us a clear indication of their activity *in vivo*. Yet, as a consequence of not being able to detect the HIFα subunits in lungs, we could not perform any assessments to determine their level of acetylation. In order to overcome the challenges of HIFα degradation, we turned to *in vitro* work and obtained a sealed hypoxic chamber to maintain hypoxic conditions when collecting proteins. Since there are cell type dependent contradictions in the literature about SIRT1 relationship with HIF1α/HIF2α (**Table 3-1/3-3**), we tried to choose a cell type most representative of the lung vasculature in hypoxia *in vivo*, namely pulmonary microvascular ECs. However, we were faced with other challenges when trying to isolate these cells from our transgenic lines.

In vitro hypoxic assessment in ECs: As we attempted isolation of lung ECs, we realized that most available kits are optimized for isolation for $CD31^+$ ECs, which are not a good representative for microvascular ECs. CD34 would have been a better marker for isolation due to its abundant expression in the mouse lung microvasculature, yet the system of microbeads that allowed for efficient CD31 EC selection (Miltenyi) did not have any CD34 beads. We attempted CD34 FACS sorting for these cells, yet obtained low yields with commercial antibodies and did not have cell growth. Thus, we settled for CD31 bead selection to isolate ECs. CD31 isolated ECs established passage 0 colonies

when isolated for *Sirt1*$^{+/+}$ and *Sirt1*$^{Y/Y}$ lungs, yet did not grow when isolated from *Sirt1*$^{-/-}$ mice, an interesting observation that emphasizes the importance for SIRT1 in EC biology. Due to variability in colony size and numbers of *Sirt1*$^{Y/Y}$ ECs at P0, we passaged the cells once to allow for equal numbers per well. At this point, *Sirt1*$^{Y/Y}$ cells attached but did not proliferate further, which we believe is due to senescence. *Sirt1*$^{+/+}$ ECs were able to attach and proliferate, but did not go beyond P2. To overcome this problem, we utilized commercially available mouse CD31 lung ECs and treated them with SIRT1 siRNA. However, wildtype ECs from commercial suppliers arrived at p3 and became senescent at p7 and could only be expanded in a 1:2 ratio. In addition, treatment with SIRT1 siRNA led to early senescence in these cells, which led to complete absence of hypoxic response, as assessed by qRT-PCR of robust HIF targets such as VEGF. At this point, we decided to use a high proliferating EC type that we knew would grow and culture well as well as utilized a commercial molecular inhibitor of SIRT1, Ex-527, which was a proposed to be a SIRT1 activity inhibitor (Gertz et al., 2013). Human umbilical vein endothelial cells (HUVECs) were cultured in hypoxia and confirmed to have HIF1α/HIF2α expression using the carefully optimized antibodies. However, the response of HUVECs to hypoxia is not entirely similar to pulmonary ECs, which mostly vasoconstrict in response to hypoxia. As well, we had no method to test Ex-527 efficacy in inhibition of SIRT1 activity (as detailed below). Additionally, some studies suggest that Ex-527 efficiently inhibits SIRT6 as well as SIRT1 (Kokkonen et al., 2014), and SIRT6 has been linked to modulation of the hypoxic response (Zhong et al., 2010), which is our parameter of interest. Therefore, we were unable to draw any meaningful conclusions from studies using HUVECs or Ex-527. Luckily, we were able to study the

role of endothelial SIRT1 *in vivo* and determined that it is crucial for protection from CH-induced PH.

Assessment of SIRT1 activity: Another issue we faced during these studies was assessment of SIRT1 activity. We know that SIRT1 activity is not directly proportional to the amount SIRT1 protein, but depends critically on NAD^+ levels, which usually fluctuate. Thus, we attempted to assess the levels of SIRT1 activity *in vivo*. We had the advantage of having tissue from SIRT1 wildtype, SIRT1 inactive (Y/Y) and SIRT1 knockout (-/-) mice, resulting in excellent negative controls. The only commercially available SIRT1 activity kit was none other than the original acetylated-p53-fluorescent kit, described in the introduction (**Section 3.1.2.3**). While the positive control recombinant SIRT1 provided with the kit worked perfectly to produce a signal indicating deacetylation of p53, we were unable to obtain any signal from our crude tissue samples. To determine that it is not a detection issue due to low levels of SIRT1, we increased protein concentration. However, we still were unable to detect any signal with a total protein concentration to 250µg of protein per well. At this point we purified SIRT1 using immunoprecipitation using two sets of antibodies; however, we were still unable to detect any signal using our samples. We attribute this to the low levels of SIRT1 in our samples, where the kit requires SIRT1 to be in the +100µg range, while our samples could not reach that level.

PERSPECTIVE

SIRT1 plays an important role in limiting the pathological response to hypoxic stress through modulation of the activity of hypoxia inducible factors. This makes activation of SIRT1 an attractive therapeutic option for modulation of hypoxia-driven vascular remodeling and vasodilation in HAPH and PAH. Future studies should focus on development and rigorous validations of SIRT1 activators (or mimics), subsequent validation in HAPH/PAH models and eventually testing in patients.

Development of SIRT1 activity kits: The field is in dire need for kits capable of accurately determining SIRT1 activity, both *in vitro* and *in vivo*. Since SIRT1 mRNA and protein levels do not correlate with activity, such kits would allow accurate assessment of SIRT1 activation in health and disease states. In PAH, these kits would further determine the degree of SIRT1 dysregulation and provide compelling evidence for its role in PAH pathology. Those kits would also assist in confirming the efficacy of SIRT1 activators.

Rigorous testing of SIRT1 activators in vivo: There is a large body of contradicting literature about the abilities of inhibitors and activators of SIRT1. We believe this is mostly due to lack of SIRT1 activity kits and absence of rigorous *in vivo* testing. Indeed, *in vivo* testing of these drugs, especially in SIRT1 mutant or knockout mice, would allow better understanding of their function and confirmation of their role in SIRT1 activation. This would also clarify contradictions and limit the waste of time, money and resources. Successful activators can then be subsequently tested in models of disease.

SIRT1 in the SUCH model: Due to its progressive nature and similar pathological and histological presentation, the SUCH model is by far the most representative model

for human PAH. Future studies should focus on utilizing the SUCH model to determine the efficacy of RSV treatment, SIRT1 overexpression or SIRT1 activators in preventing the pathological development of PAH. This could set the stage for subsequent clinical testing for SIRT1 activators/mimics in PAH patients. Indeed, since previous studies of dose safety have been undertaken, RSV can easily progress to clinical trial testing in PAH patients who show SIRT1 dysfunction or strong hypoxic pathway activation.

***SIRT1 in human pulmonary ECs*:** Future studies could further explore the role of SIRT1 in the human pulmonary ECs *in vitro*. This could be achieved by using siRNA to knockdown SIRT1 in hypoxia in human PAECs or pulmonary microvascular ECs. This might help provide further mechanistic insight into the role of SIRT1 in the human EC population, and might allow assessment of HIFα units abundance and acetylation levels. However, care must be taken when performing these studies since they will rely on transient SIRT1 knockdown rather than genetic deletion/inactivation. In addition, studies of human cells *in vitro* might not reflect the same findings of our *in vivo* mouse studies in CH. Therefore, while they might provide good insight into the mechanism of action, one should be careful when interpreting these findings.

SIRT1 in SMCs: SMCs play a crucial role in PH pathogenesis and the hypoxic response, including vasoconstriction, invading smaller arterioles and proliferating in medium/larger arteries. While we determined the role of EC-SIRT1 in CH-induced pathology, future studies in SMC targeted SIRT1 knockout mice will help better elucidate the role of SIRT1 in SMC response to hypoxia.

Appendix - Supplemental Figures:

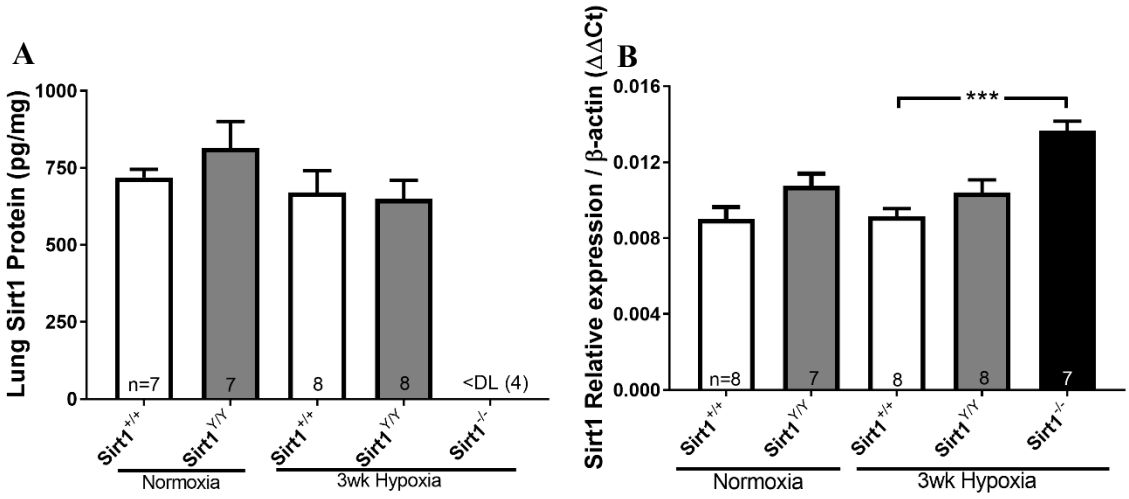

Supplemental Figure 1: **Protein and mRNA levels of SIRT1 in lung tissue from *Sirt1*$^{+/+}$, *Sirt1*$^{Y/Y}$ and *Sirt1*$^{-/-}$ in normoxia or chronic hypoxia for 3 weeks**. **A**) SIRT1 protein levels as assessed by SIRT1 ELISA (ab206983) were not affected by hypoxia treatment in *Sirt1*$^{+/+}$ lungs. Our antibodies bound and detected the mutant SIRT1 protein in *Sirt1*$^{Y/Y}$ lungs and confirmed absence of SIRT1 protein in *Sirt1*$^{-/-}$ lungs. **B**) *Sirt1* mRNA levels were not affected by hypoxic exposure in *Sirt1*$^{+/+}$ or *Sirt1*$^{Y/Y}$ lungs. Our primers can amplify a region that is outside exon 5/6, which seems to be increased in absence of SIRT1 protein in CH. ***p<0.001. n number indicated on bars.

A) Non-muscularized: 0 -50% muscularization

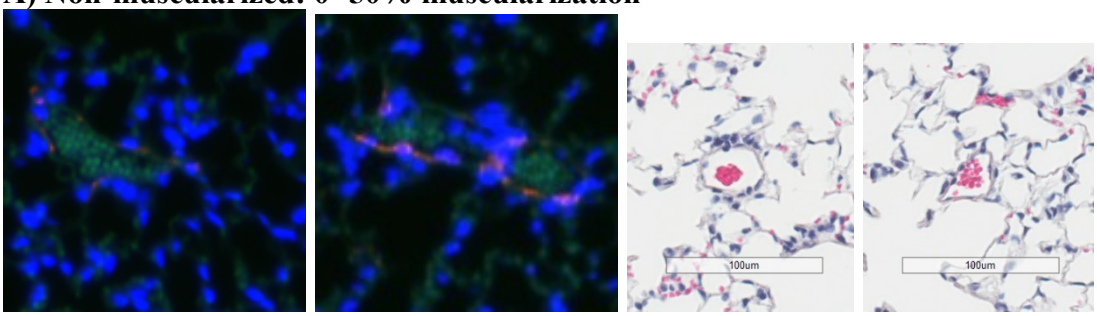

B) Partially muscularized: +50% muscularization, break in muscular layer

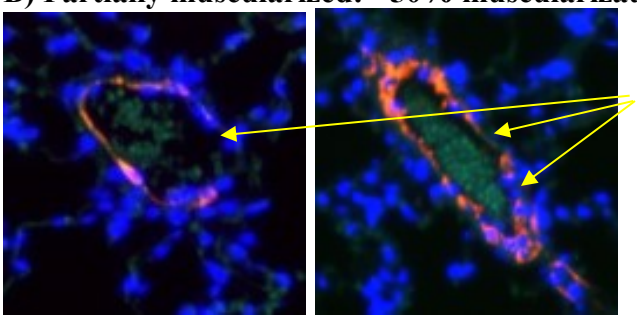

C) Fully muscularized: 100% muscular, no clear break in muscular layer

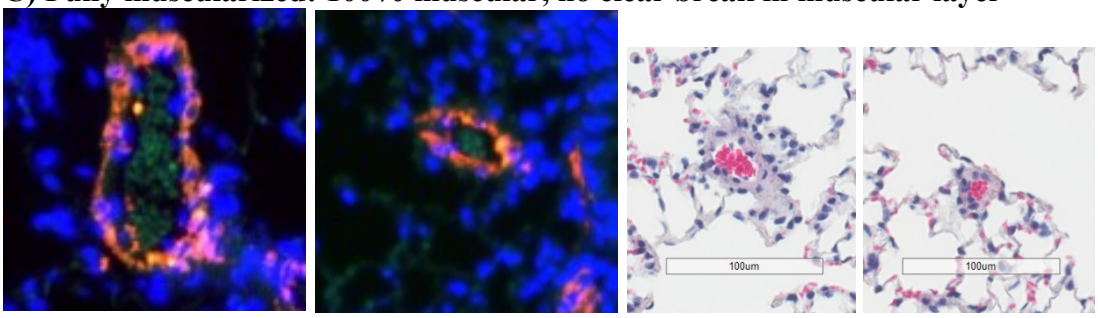

Supplemental Figure 2: Representative photomicrograph of lung tissue showing muscularized vessels stained using α-smooth muscle actin (Red) and counterstained with DAPI (Blue). Quantification of non-muscularized (**A**), partially muscularized (**B**) or fully muscularized (**C**) vessels using α-smooth muscle actin staining.

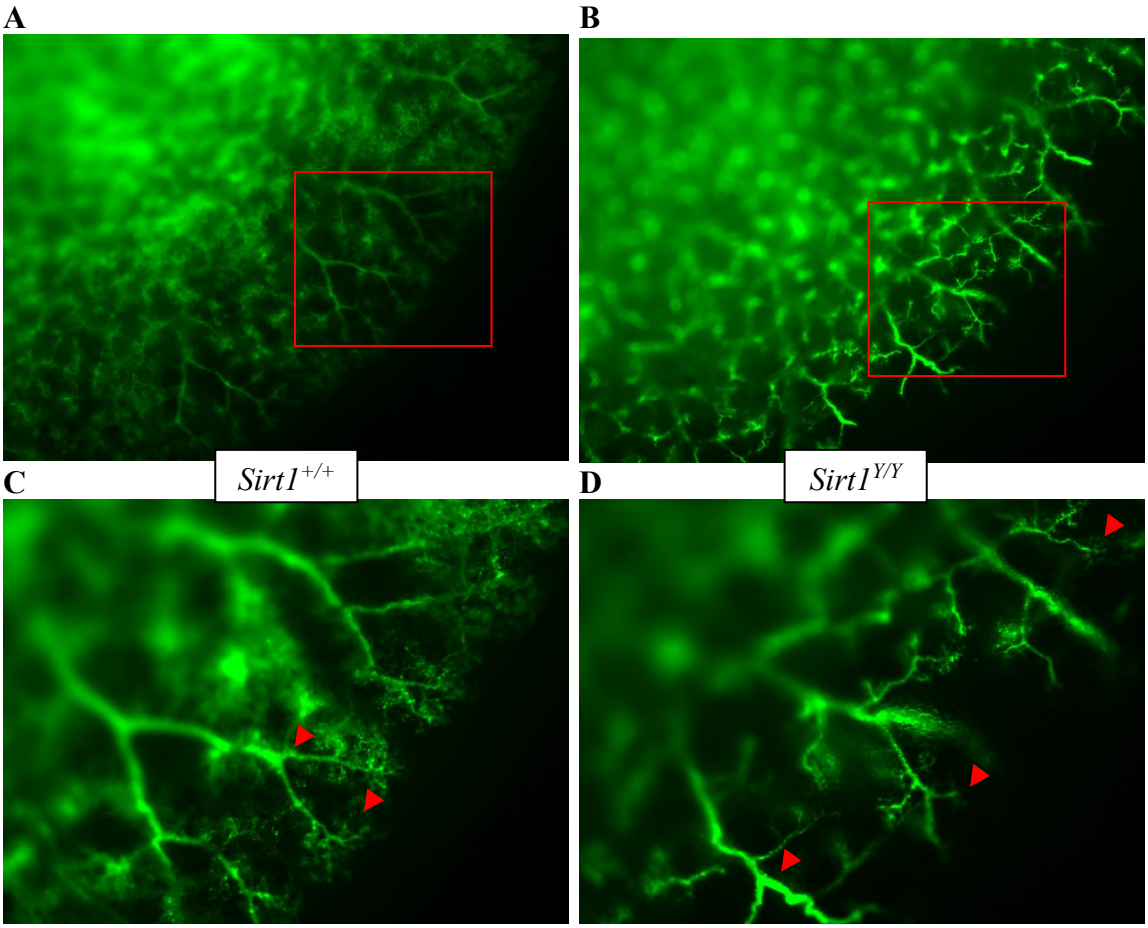

Supplemental Figure 3: **Fluorescent microangiography of a *Sirt1*$^{+/+}$ and *Sirt1*$^{Y/Y}$ mouse after three weeks of chronic hypoxia exposure**. **A**) *Sirt1*$^{+/+}$ female mouse lung with RVSP of 35mmHg. **B**) *Sirt1*$^{Y/Y}$ female mouse lung with RVSP of 40mmHg. **C, D**) Higher magnification images showing proper arterial and capillary vasculature in the *Sirt1*$^{+/+}$ mouse but abnormal vessels in the *Sirt1*$^{Y/Y}$ (Red arrows).

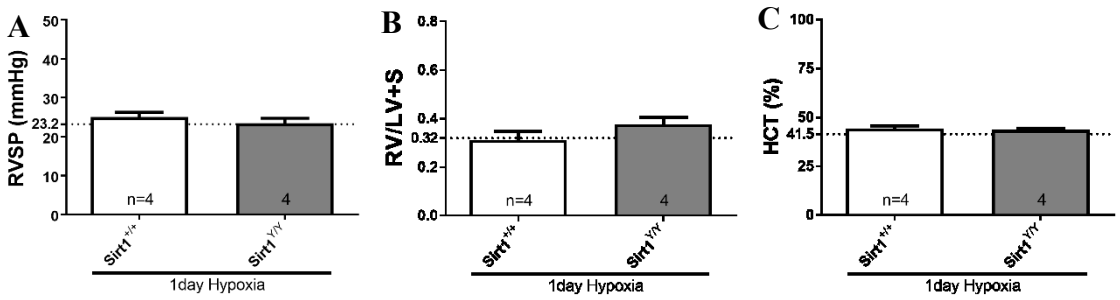

Supplemental Figure 4: Hemodynamic and hematocrit assessment of *Sirt1*$^{+/+}$ and *Sirt1*$^{Y/Y}$ mice after one day of normoxia or hypoxia. **A**) Right ventricle systolic pressure (RVSP). **B**) The weight ratio of the right ventricle (RV) to the left ventricle and septum (LV+S). **C**) Hematocrit levels (HCT). *The dotted line* indicates normal average values from our normoxic wildtype mice. n number indicated on bars. No differences in any hemodynamic parameters of HCT were observed at one day of hypoxia. Statistical analysis was performed using a students' t-test.

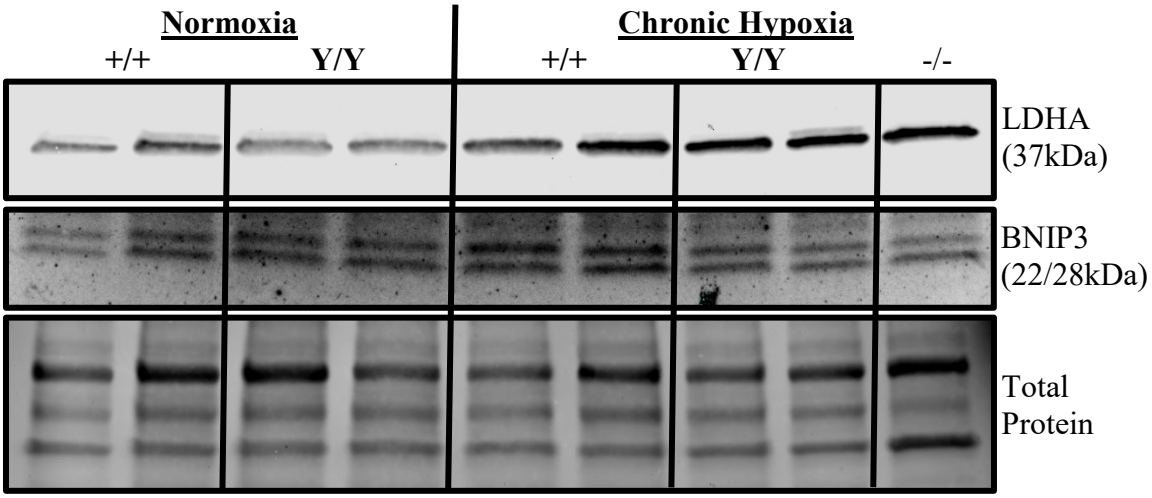

Supplemental Figure 5: **Representative western blot for protein expression of selective HIF1α targets BNIP3 and LDHA in lung tissue from *Sirt1*$^{+/+}$, *Sirt1*$^{Y/Y}$ and *Sirt1*$^{-/-}$ in normoxia or chronic hypoxia for 3 weeks**. LDHA: Lactate dehydrogenase A. BNIP3: BCL-2 and adenovirus E1B 19-kDa-interacting protein 3. Total protein levels were used for normalization.

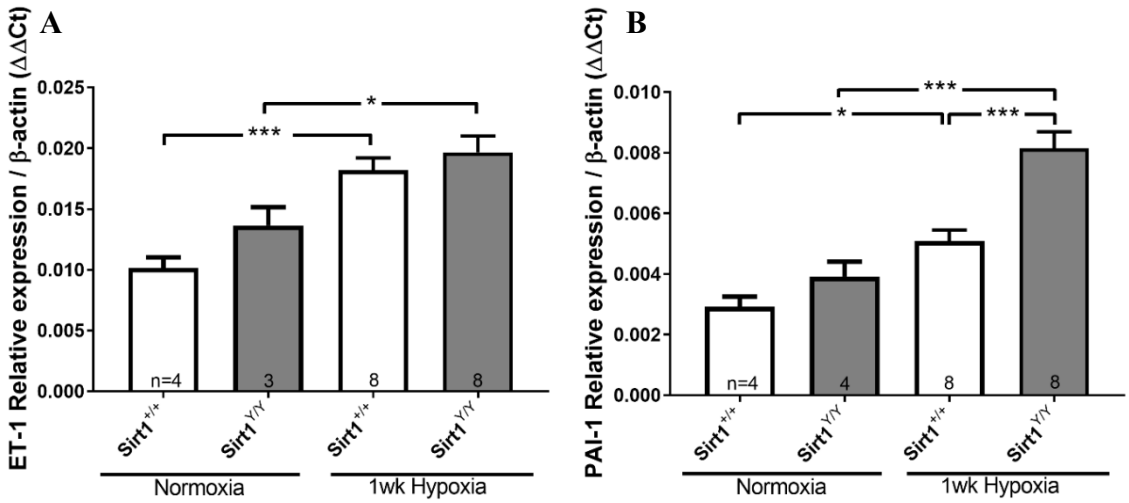

Supplemental Figure 6: **Endothelin-1 (ET-1, A) and plasminogen activator inhibitor 1 (PAI-1, B) mRNA levels in lung tissue from *Sirt1*$^{+/+}$, *Sirt1*$^{Y/Y}$ in normoxia or chronic hypoxia for 1 week**. n number indicated on bars. *p<0.05, **p<0.01, ***p<0.001.

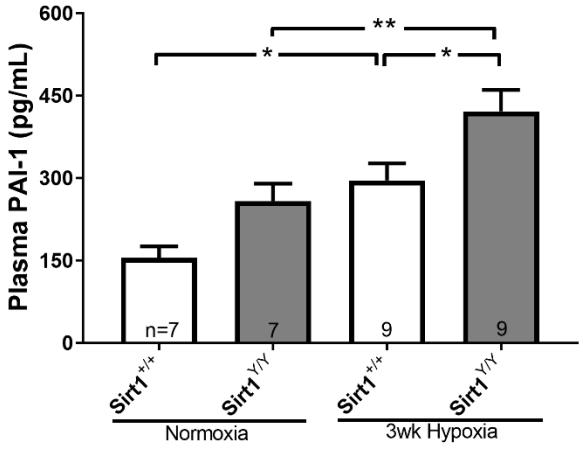

Supplemental Figure 7: **Plasminogen activator inhibitor 1 (PAI-1) plasma levels from *Sirt1*$^{+/+}$, *Sirt1*$^{Y/Y}$ in normoxia or chronic hypoxia for 3 weeks**. n number indicated on bars. *p<0.05, **p<0.01.

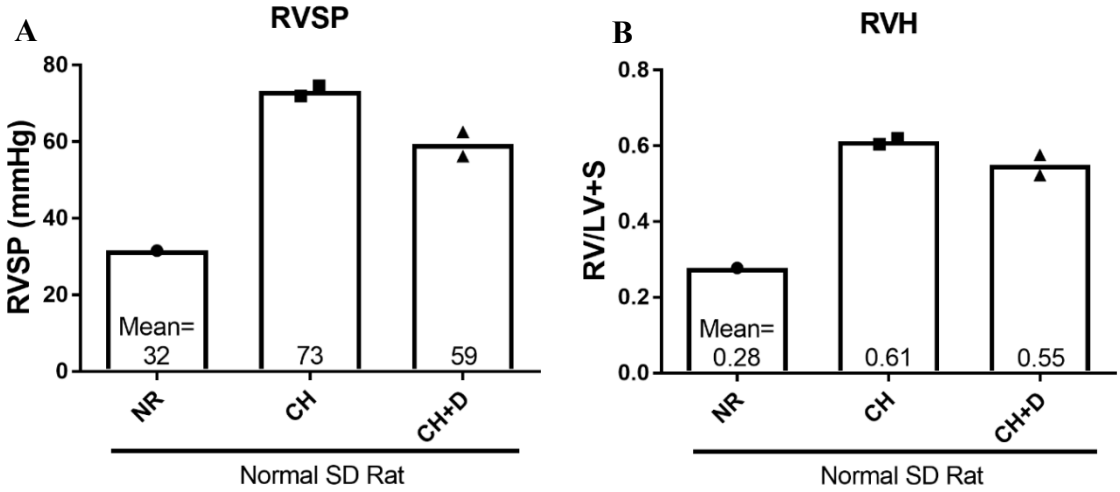

Supplemental Figure 8: Hemodynamic assessment in normal SD rats at 3 weeks of normoxia or chronic hypoxia, with or without Dichloroacetate (D) in drinking water. **A**) Right ventricle systolic pressure (RVSP). **B**) The weight ratio of the right ventricle (RV) to the left ventricle and septum (LV+S). NR= Normoxia, CH=Chronic hypoxia for three weeks, D=Dichloroacetate (70mg/kg/day). ***Mean value indicated on bars***. One animal in the CH+D group died before the end of the three-week hypoxic exposure. The CH protocol used was a replicate of literature which uses gradual decrease in hypoxia to 10% over a week rather than a rapid decrease within a couple of hours like our mouse model.

Appendix - Supplemental Tables:

Supplemental Table 1: **Right ventricle and body weight measurement in normoxic and hypoxic mice**

		N number	RV (mg)	Basal BW (g)	Final BW (g)	RV/ Final BW (mg/g)
Normoxia	*Sirt1*$^{+/+}$	13	28.5±1.8	27.2±1.2	28.6±1.25	1.00±0.04
	Sirt1$^{Y/Y}$	12	24.2±1.3	22.3±1.27^{+}	24.3±1.29^{+}	1.01±0.03
3wk	*Sirt1*$^{+/+}$	38	36.1±1.3*	25.7±0.59	24.6±0.51^{+}	1.46±0.04*
Hypoxia	*Sirt1*$^{Y/Y}$	27	41.1±1.2*,$^{+}$	21.2±0.53^{+}	21.6±0.57^{+}	1.93±0.07*,$^{+}$
	Sirt1$^{-/-}$	10	40.8±3.6	20.1±0.97^{+}	19.8±0.80^{+}	2.11±0.24^{+}

RV: Right ventricle; BW: Body Weight; Final body weight: Body weight measured at end of study before sacrifice. *p<0.05 vs. normoxia; +p<0.05 vs. *Sirt1*$^{+/+}$ in same condition

Supplemental Table 2: Spleen weight measurements in normoxic and hypoxic mice

		N number	Spleen (mg)	Spleen/ Final BW (mg/g)
Normoxia	*Sirt1*$^{+/+}$	11	105.8±5.5	3.7±0.3
	Sirt1$^{Y/Y}$	10	71.19±5.5	3.0±0.2
3wk Hypoxia	*Sirt1*$^{+/+}$	25	97.6±5.8	3.9±0.2
	Sirt1$^{Y/Y}$	18	129.8±13.9*	6.0±0.6*,$^{+}$
	Sirt1$^{-/-}$	8	156.7±29.1^{+}	8.0±1.5^{+}

*p<0.05 vs. normoxia; +p<0.05 vs. CH-*Sirt1*$^{+/+}$

Appendix - Solutions and Reagents (prepared and not purchased)

4% PFA
40g Paraformaldehyde (Sigma, P6148-500G)
1L 1XPBS
Heat slightly to dissolve
Adjust pH to 7.4

Acid alcohol
2.5 mL 12N HC1
500 mL 70% EtOH

Scott's solution
6 g MgSO4
1.05gNaHCO3
Fill to 300 mL with ddH_2O

BCA Reagent Mix
1 mL Bicinchoninic acid (Sigma, B9643)
1 mL dH2O
40 uL 4%CuSO4

References:

Abdalla, M., Sabbineni, H., Prakash, R., Ergul, A., Fagan, S. C., & Somanath, P. R. (2015). The Akt inhibitor, triciribine, ameliorates chronic hypoxia-induced vascular pruning and TGFβ-induced pulmonary fibrosis. *British Journal of Pharmacology*, *172*(16), 4173–4188. https://doi.org/10.1111/bph.13203

Abe, K., Toba, M., Alzoubi, A., Ito, M., Fagan, K. A., Cool, C. D., … Oka, M. (2010). Formation of plexiform lesions in experimental severe pulmonary arterial hypertension. *Circulation*, *121*(25), 2747–2754. https://doi.org/10.1161/CIRCULATIONAHA.109.927681

Akhavein, F., St-Michel, E. J., Seifert, E., & Rohlicek, C. V. (2007). Decreased left ventricular function, myocarditis, and coronary arteriolar medial thickening following monocrotaline administration in adult rats. *Journal of Applied Physiology (Bethesda, Md. : 1985)*, *103*(1), 287–95. https://doi.org/10.1152/japplphysiol.01509.2005

Alberts, G. F., Peifley, K. A., Johns, A., Kleha, J. F., & Winkles, J. A. (1994). Constitutive endothelin-1 overexpression promotes smooth muscle cell proliferation via an external autocrine loop. *The Journal of Biological Chemistry*, *269*(13), 10112–8. Retrieved from http://www.ncbi.nlm.nih.gov/pubmed/8144511

Armour, S. M., Bennett, E. J., Braun, C. R., Zhang, X.-Y., McMahon, S. B., Gygi, S. P., … Sinclair, D. A. (2013). A high-confidence interaction map identifies SIRT1 as a mediator of acetylation of USP22 and the SAGA coactivator complex. *Molecular and Cellular Biology*, *33*(8), 1487–502. https://doi.org/10.1128/MCB.00971-12

Austin, E. D., Loyd, J. E., & Phillips, J. A. (1993). *Heritable Pulmonary Arterial Hypertension*. *GeneReviews(®)*. University of Washington, Seattle. Retrieved from http://www.ncbi.nlm.nih.gov/pubmed/20301658

Autiero, I., Costantini, S., & Colonna, G. (2008). Human sirt-1: molecular modeling and structure-function relationships of an unordered protein. *PloS One*, *4*(10), e7350. https://doi.org/10.1371/journal.pone.0007350

Balaiya, S., Murthy, R. K., & Chalam, K. V. (2013). Resveratrol inhibits proliferation of hypoxic choroidal vascular endothelial cells. *Molecular Vision*, *19*(November), 2385–92. Retrieved from http://www.ncbi.nlm.nih.gov/pubmed/24319332

Ball, M. K., Waypa, G. B., Mungai, P. T., Nielsen, J. M., Czech, L., Dudley, V. J., … Schumacker, P. T. (2014). Regulation of hypoxia-induced pulmonary hypertension by vascular smooth muscle hypoxia-inducible factor-1α. *American Journal of Respiratory and Critical Care Medicine*, *189*(3), 314–24. https://doi.org/10.1164/rccm.201302-0302OC

Barst, R. J., Rubin, L. J., Long, W. A., McGoon, M. D., Rich, S., Badesch, D. B., … Primary Pulmonary Hypertension Study Group. (1996). A comparison of continuous intravenous epoprostenol (prostacyclin) with conventional therapy for primary pulmonary hypertension. *The New England Journal of Medicine*, *334*(5), 296–301. https://doi.org/10.1056/NEJM199602013340504

Barst, R. J., Rubin, L. J., McGoon, M. D., Caldwell, E. J., Long, W. A., & Levy, P. S. (1994). Survival in primary pulmonary hypertension with long-term continuous intravenous prostacyclin. *Annals of Internal Medicine*, *121*(6), 409–15. Retrieved from http://www.ncbi.nlm.nih.gov/pubmed/8053614

Baur, J. A. (2010a). Biochemical effects of SIRT1 activators. *Biochimica et Biophysica*

Acta, *1804*(8), 1626–34. https://doi.org/10.1016/j.bbapap.2009.10.025
Baur, J. A. (2010b). Resveratrol, sirtuins, and the promise of a DR mimetic. *Mechanisms of Ageing and Development*, *131*(4), 261–9. https://doi.org/10.1016/j.mad.2010.02.007
Baur, J. A., Pearson, K. J., Price, N. L., Jamieson, H. A., Lerin, C., Kalra, A., … Sinclair, D. A. (2006). Resveratrol improves health and survival of mice on a high-calorie diet. *Nature*, *444*(7117), 337–42. https://doi.org/10.1038/nature05354
Berman, A. Y., Motechin, R. A., Wiesenfeld, M. Y., & Holz, M. K. (2017). The therapeutic potential of resveratrol: a review of clinical trials. *Npj Precision Oncology*, *1*(1), 35. https://doi.org/10.1038/s41698-017-0038-6
Berra, E., Roux, D., Richard, D. E., & Pouysségur, J. (2001). Hypoxia-inducible factor-1 alpha (HIF-1 alpha) escapes O(2)-driven proteasomal degradation irrespective of its subcellular localization: nucleus or cytoplasm. *EMBO Reports*, *2*(7), 615–20. https://doi.org/10.1093/embo-reports/kve130
Boily, G., He, X. H., Pearce, B., Jardine, K., & McBurney, M. W. (2009). SirT1-null mice develop tumors at normal rates but are poorly protected by resveratrol. *Oncogene*, *28*(32), 2882–93. https://doi.org/10.1038/onc.2009.147
Bonnet, S., Michelakis, E. D., Porter, C. J., Andrade-Navarro, M. A., Thebaud, B., Haromy, A., … Archer, S. L. (2006). An abnormal mitochondrial-hypoxia inducible factor-1alpha-Kv channel pathway disrupts oxygen sensing and triggers pulmonary arterial hypertension in fawn hooded rats: similarities to human pulmonary arterial hypertension. *Circulation*, *113*(22), 2630–2641. https://doi.org/10.1161/CIRCULATIONAHA.105.609008
Borra, M. T., Smith, B. C., & Denu, J. M. (2005). Mechanism of human SIRT1 activation by resveratrol. *The Journal of Biological Chemistry*, *280*(17), 17187–95. https://doi.org/10.1074/jbc.M501250200
Boucherat, O., Chabot, S., Paulin, R., Trinh, I., Bourgeois, A., Potus, F., … Bonnet, S. (2017). HDAC6: A Novel Histone Deacetylase Implicated in Pulmonary Arterial Hypertension. *Scientific Reports*, *7*(1), 4546. https://doi.org/10.1038/s41598-017-04874-4
Brachmann, C. B., Sherman, J. M., Devine, S. E., Cameron, E. E., Pillus, L., & Boeke, J. D. (1995). The SIR2 gene family, conserved from bacteria to humans, functions in silencing, cell cycle progression, and chromosome stability. *Genes & Development*, *9*(23), 2888–902. Retrieved from http://www.ncbi.nlm.nih.gov/pubmed/7498786
Breitenstein, A., Stein, S., Holy, E. W., Camici, G. G., Lohmann, C., Akhmedov, A., … Tanner, F. C. (2011). Sirt1 inhibition promotes in vivo arterial thrombosis and tissue factor expression in stimulated cells. *Cardiovascular Research*, *89*(2), 464–72. https://doi.org/10.1093/cvr/cvq339
Bruick, R. K. (2000). Expression of the gene encoding the proapoptotic Nip3 protein is induced by hypoxia. *Proceedings of the National Academy of Sciences of the United States of America*, *97*(16), 9082–7. https://doi.org/10.1073/pnas.97.16.9082
Brusselmans, K., Compernolle, V., Tjwa, M., Wiesener, M. S., Maxwell, P. H., Collen, D., & Carmeliet, P. (2003). Heterozygous deficiency of hypoxia-inducible factor-2alpha protects mice against pulmonary hypertension and right ventricular dysfunction during prolonged hypoxia. *J Clin Invest*, *111*(10), 1519–1527. https://doi.org/10.1172/JCI15496

Burns, J., & Manda, G. (2017). Metabolic Pathways of the Warburg Effect in Health and Disease: Perspectives of Choice, Chain or Chance. *International Journal of Molecular Sciences*, *18*(12), 2755. https://doi.org/10.3390/ijms18122755

Burton, V. J., Holmes, A. M., Ciuclan, L. I., Robinson, A., Roger, J. S., Jarai, G., … Budd, D. C. (2011). Attenuation of leukocyte recruitment via CXCR1/2 inhibition stops the progression of PAH in mice with genetic ablation of endothelial BMPR-II. *Blood*, *118*(17), 4750–8. https://doi.org/10.1182/blood-2011-05-347393

Campagna, M., Herranz, D., Garcia, M. A., Marcos-Villar, L., González-Santamaría, J., Gallego, P., … Rivas, C. (2011). SIRT1 stabilizes PML promoting its sumoylation. *Cell Death and Differentiation*, *18*(1), 72–79. https://doi.org/10.1038/cdd.2010.77

Caron, A. Z., He, X., Mottawea, W., Seifert, E. L., Jardine, K., Dewar-Darch, D., … McBurney, M. W. (2014). The SIRT1 deacetylase protects mice against the symptoms of metabolic syndrome. *FASEB Journal : Official Publication of the Federation of American Societies for Experimental Biology*, *28*(3), 1306–16. https://doi.org/10.1096/fj.13-243568

Carreau, A., El Hafny-Rahbi, B., Matejuk, A., Grillon, C., & Kieda, C. (2011). Why is the partial oxygen pressure of human tissues a crucial parameter? Small molecules and hypoxia. *Journal of Cellular and Molecular Medicine*, *15*(6), 1239–53. https://doi.org/10.1111/j.1582-4934.2011.01258.x

Cavasin, M. A., Demos-Davies, K., Horn, T. R., Walker, L. A., Lemon, D. D., Birdsey, N., … McKinsey, T. A. (2012). Selective class I histone deacetylase inhibition suppresses hypoxia-induced cardiopulmonary remodeling through an antiproliferative mechanism. *Circulation Research*, *110*(5), 739–48. https://doi.org/10.1161/CIRCRESAHA.111.258426

Cesari, M., Pahor, M., & Incalzi, R. A. (2010). Plasminogen activator inhibitor-1 (PAI-1): A key factor linking fibrinolysis and age-related subclinical and clinical conditions. *Cardiovascular Therapeutics*, *28*(5), 72–91. https://doi.org/10.1111/j.1755-5922.2010.00171.x

Chandra, S. M., Razavi, H., Kim, J., Agrawal, R., Kundu, R. K., De Jesus Perez, V., … Chun, H. J. (2011). Disruption of the apelin-APJ system worsens hypoxia-induced pulmonary hypertension. *Arteriosclerosis, Thrombosis, and Vascular Biology*, *31*(4), 814–820. https://doi.org/10.1161/ATVBAHA.110.219980

Channick, R. N., Simonneau, G., Sitbon, O., Robbins, I. M., Frost, A., Tapson, V. F., … Rubin, L. J. (2001). Effects of the dual endothelin-receptor antagonist bosentan in patients with pulmonary hypertension: a randomised placebo-controlled study. *Lancet*, *358*(9288), 1119–1123. https://doi.org/S0140-6736(01)06250-X [pii]10.1016/S0140-6736(01)06250-X

Chaudhary, K. R., Taha, M., Cadete, V. J. J., Godoy, R. S., & Stewart, D. J. (2017). Proliferative Versus Degenerative Paradigms in Pulmonary Arterial Hypertension: Have We Put the Cart Before the Horse? *Circulation Research*, *120*(8), 1237–1239. https://doi.org/10.1161/CIRCRESAHA.116.310097

Chen, B., Xue, J., Meng, X., Slutzky, J. L., Calvert, A. E., & Chicoine, L. G. (2014). Resveratrol prevents hypoxia-induced arginase II expression and proliferation of human pulmonary artery smooth muscle cells via Akt-dependent signaling. *American Journal of Physiology. Lung Cellular and Molecular Physiology*, *307*(4), L317-25. https://doi.org/10.1152/ajplung.00285.2013

Chen, H. Z., Wan, Y. Z., Zhou, S., Lu, Y. B., Zhang, Z. Q., Zhang, R., … Liang, C. C. (2012). Endothelium-specific SIRT1 overexpression inhibits hyperglycemia-induced upregulation of vascular cell senescence. *Science China Life Sciences*, *55*(6), 467–473. https://doi.org/10.1007/s11427-012-4329-4

Chen, P.-I., Cao, A., Miyagawa, K., Tojais, N. F., Hennigs, J. K., Li, C. G., … Rabinovitch, M. (2017). Amphetamines promote mitochondrial dysfunction and DNA damage in pulmonary hypertension. *JCI Insight*, *2*(2), e90427. https://doi.org/10.1172/jci.insight.90427

Chen, R., Xu, M., Hogg, R. T., Li, J., Little, B., Gerard, R. D., & Garcia, J. A. (2012). The acetylase/deacetylase couple CREB-binding protein/sirtuin 1 controls hypoxia-inducible factor 2 signaling. *Journal of Biological Chemistry*, *287*(36), 30800–30811. https://doi.org/10.1074/jbc.M111.244780

Chen, R., Xu, M., Nagati, J. S., Hogg, R. T., Das, A., Gerard, R. D., & Garcia, J. A. (2015). The acetate/ACSS2 switch regulates HIF-2 stress signaling in the tumor cell microenvironment. *PLoS ONE*, *10*(2). https://doi.org/10.1371/journal.pone.0116515

Chen, Y., Zhao, W., Yang, J. S., Cheng, Z., Luo, H., Lu, Z., … Zhao, Y. (2012). Quantitative acetylome analysis reveals the roles of SIRT1 in regulating diverse substrates and cellular pathways. *Molecular & Cellular Proteomics : MCP*, *11*(10), 1048–62. https://doi.org/10.1074/mcp.M112.019547

Cheng, H.-L., Mostoslavsky, R., Saito, S., Manis, J. P., Gu, Y., Patel, P., … Chua, K. F. (2003). Developmental defects and p53 hyperacetylation in Sir2 homolog (SIRT1)-deficient mice. *Proceedings of the National Academy of Sciences of the United States of America*, *100*(19), 10794–10799. https://doi.org/10.1073/pnas.1934713100

Cheng, J., Liu, C., Hu, K., Greenberg, A., Wu, D., Ausman, L. M., … Wang, X. D. (2017). Ablation of systemic SIRT1 activity promotes nonalcoholic fatty liver disease by affecting liver-mesenteric adipose tissue fatty acid mobilization. *Biochimica et Biophysica Acta - Molecular Basis of Disease*, *1863*(11), 2783–2790. https://doi.org/10.1016/j.bbadis.2017.08.004

Chinnadurai, G., Vijayalingam, S., & Gibson, S. B. (2008). BNIP3 subfamily BH3-only proteins: Mitochondrial stress sensors in normal and pathological functions. *Oncogene*, *27*(S1), S114–S127. https://doi.org/10.1038/onc.2009.49

Cho, Y. K., Eom, G. H., Kee, H. J., Kim, H.-S., Choi, W.-Y., Nam, K.-I., … Kook, H. (2010). Sodium valproate, a histone deacetylase inhibitor, but not captopril, prevents right ventricular hypertrophy in rats. *Circulation Journal : Official Journal of the Japanese Circulation Society*, *74*(4), 760–70. https://doi.org/10.1253/circj.CJ-09-0580

Choudhary, C., Kumar, C., Gnad, F., Nielsen, M. L., Rehman, M., Walther, T. C., … Mann, M. (2009). Lysine acetylation targets protein complexes and co-regulates major cellular functions. *Science (New York, N.Y.)*, *325*(5942), 834–40. https://doi.org/10.1126/science.1175371

Christman, B. W., McPherson, C. D., Newman, J. H., King, G. A., Bernard, G. R., Groves, B. M., & Loyd, J. E. (1992). An imbalance between the excretion of thromboxane and prostacyclin metabolites in pulmonary hypertension. *The New England Journal of Medicine*, *327*(2), 70–5. https://doi.org/10.1056/NEJM199207093270202

Chu, F., Chou, P. M., Zheng, X., Mirkin, B. L., & Rebbaa, A. (2005). Control of

multidrug resistance gene mdr1 and cancer resistance to chemotherapy by the longevity gene sirt1. *Cancer Research*, *65*(22), 10183–7. https://doi.org/10.1158/0008-5472.CAN-05-2002

Ciuclan, L., Bonneau, O., Hussey, M., Duggan, N., Holmes, A. M., Good, R., … Thomas, M. (2011). A novel murine model of severe pulmonary arterial hypertension. *Am J Respir Crit Care Med*, *184*(10), 1171–82. https://doi.org/10.1164/rccm.201103-0412OC

Cool, C. D., Groshong, S. D., Oakey, J., & Voelkel, N. F. (2005). Pulmonary hypertension: cellular and molecular mechanisms. *Chest*, *128*(6 Suppl), 565S–571S. https://doi.org/128/6_suppl/565S [pii]10.1378/chest.128.6_suppl.565S

Cowburn, A. S., Crosby, A., Macias, D., Branco, C., Colaço, R. D. D. R., Southwood, M., … Johnson, R. S. (2016). HIF2α–arginase axis is essential for the development of pulmonary hypertension. *Proceedings of the National Academy of Sciences*, *113*(31), 8801–8806. https://doi.org/10.1073/pnas.1602978113

Csiszar, A., Labinskyy, N., Olson, S., Pinto, J. T., Gupte, S., Wu, J. M., … Ungvari, Z. (2009). Resveratrol prevents monocrotaline-induced pulmonary hypertension in rats. *Hypertension (Dallas, Tex. : 1979)*, *54*(3), 668–75. https://doi.org/10.1161/HYPERTENSIONAHA.109.133397

D'Onofrio, N., Vitiello, M., Casale, R., Servillo, L., Giovane, A., & Balestrieri, M. L. (2015). Sirtuins in vascular diseases: Emerging roles and therapeutic potential. *Biochimica et Biophysica Acta*, *1852*(7), 1311–22. https://doi.org/10.1016/j.bbadis.2015.03.001

da Cunha, F. M., Demasi, M., & Kowaltowski, A. J. (2011). Aging and calorie restriction modulate yeast redox state, oxidized protein removal, and the ubiquitin-proteasome system. *Free Radical Biology & Medicine*, *51*(3), 664–70. https://doi.org/10.1016/j.freeradbiomed.2011.05.035

Dai, Z., Li, M., Wharton, J., Zhu, M. M., & Zhao, Y.-Y. (2016). Prolyl-4 Hydroxylase 2 (PHD2) Deficiency in Endothelial Cells and Hematopoietic Cells Induces Obliterative Vascular Remodeling and Severe Pulmonary Arterial Hypertension in Mice and Humans Through Hypoxia-Inducible Factor-2α. *Circulation*, *133*(24), 2447–58. https://doi.org/10.1161/CIRCULATIONAHA.116.021494

Dai, Z., & Zhao, Y.-Y. (2017). Discovery of a murine model of clinical PAH: Mission impossible? *Trends in Cardiovascular Medicine*, *27*(4), 229–236. https://doi.org/10.1016/j.tcm.2016.12.003

Daitoku, H., Hatta, M., Matsuzaki, H., Aratani, S., Ohshima, T., Miyagishi, M., … Fukamizu, A. (2004). Silent information regulator 2 potentiates Foxo1-mediated transcription through its deacetylase activity. *Proceedings of the National Academy of Sciences of the United States of America*, *101*(27), 10042–7. https://doi.org/10.1073/pnas.0400593101

Dang, W. (2014). The controversial world of sirtuins. *Drug Discovery Today. Technologies*, *12*(18), e9–e17. https://doi.org/10.1016/j.ddtec.2012.08.003

Davie, N., Haleen, S. J., Upton, P. D., Polak, J. M., Yacoub, M. H., Morrell, N. W., & Wharton, J. (2002). ET(A) and ET(B) receptors modulate the proliferation of human pulmonary artery smooth muscle cells. *American Journal of Respiratory and Critical Care Medicine*, *165*(3), 398–405. https://doi.org/10.1164/ajrccm.165.3.2104059

De Raaf, M. A., Hussaini, A. Al, Gomez-Arroyo, J., Kraskaukas, D., Farkas, D., Happé, C., … Bogaard, H. J. (2014). Histone deacetylase inhibition with trichostatin A does not reverse severe angioproliferative pulmonary hypertension in rats (2013 Grover Conference series). *Pulmonary Circulation*, *4*(2), 237–43. https://doi.org/10.1086/675986

Deng, Y., Wu, W., Guo, S., Chen, Y., Liu, C., Gao, X., & Wei, B. (2017). Altered mTOR and Beclin-1 mediated autophagic activation during right ventricular remodeling in monocrotaline-induced pulmonary hypertension. *Respiratory Research*, *18*(1), 1–15. https://doi.org/10.1186/s12931-017-0536-7

Dengler, V. L., Galbraith, M. D., & Espinosa, J. M. (2008). Transcriptional regulation by hypoxia inducible factors. *Critical Reviews in Biochemistry and Molecular Biology*, *49*(1), 1–15. https://doi.org/10.3109/10409238.2013.838205

Diebold, I., Hennigs, J. K., Miyagawa, K., Li, C. G., Nickel, N. P., Kaschwich, M., … Rabinovitch, M. (2015). BMPR2 preserves mitochondrial function and DNA during reoxygenation to promote endothelial cell survival and reverse pulmonary hypertension. *Cell Metabolism*, *21*(4), 596–608. https://doi.org/10.1016/j.cmet.2015.03.010

Dimova, E. Y., Samoylenko, A., & Kietzmann, T. (2004). Oxidative stress and hypoxia: implications for plasminogen activator inhibitor-1 expression. *Antioxidants & Redox Signaling*, *6*(4), 777–91. https://doi.org/10.1089/1523086041361596

Dioum, E. M., Chen, R., Alexander, M. S., Zhang, Q., Hogg, R. T., Gerard, R. D., & Garcia, J. A. (2009). Regulation of hypoxia-inducible factor 2alpha signaling by the stress-responsive deacetylase sirtuin 1. *Science (New York, N.Y.)*, *324*(5932), 1289–93. https://doi.org/10.1126/science.1169956

Dong, S.-Y., Guo, Y.-J., Feng, Y., Cui, X.-X., Kuo, S.-H., Liu, T., & Wu, Y.-C. (2016). The epigenetic regulation of HIF-1α by SIRT1 in MPP(+) treated SH-SY5Y cells. *Biochemical and Biophysical Research Communications*, *470*(2), 453–459. https://doi.org/10.1016/j.bbrc.2016.01.013

Duan, C. (2016). Hypoxia-inducible factor 3 biology: complexities and emerging themes. *Am J Physiol Cell Physiol*, *310*(4), C260-9. https://doi.org/10.1152/ajpcell.00315.2015

Dunham-Snary, K. J., Wu, D., Sykes, E. A., Thakrar, A., Parlow, L. R. G., Mewburn, J. D., … Archer, S. L. (2017). Hypoxic Pulmonary Vasoconstriction: From Molecular Mechanisms to Medicine. *Chest*, *151*(1), 181–192. https://doi.org/10.1016/j.chest.2016.09.001

Dunwoodie, S. L. (2009). The role of hypoxia in development of the Mammalian embryo. *Developmental Cell*, *17*(6), 755–73. https://doi.org/10.1016/j.devcel.2009.11.008

Dutly, A. E., Kugathasan, L., Trogadis, J. E., Keshavjee, S. H., Stewart, D. J., & Courtman, D. W. (2006). Fluorescent microangiography (FMA): an improved tool to visualize the pulmonary microvasculature. *Laboratory Investigation; a Journal of Technical Methods and Pathology*, *86*(4), 409–16. https://doi.org/10.1038/labinvest.3700399

Ellen, T. P., Ke, Q., Zhang, P., & Costa, M. (2007). NDRG1, a growth and cancer related gene: regulation of gene expression and function in normal and disease states. *Carcinogenesis*, *29*(1), 2–8. https://doi.org/10.1093/carcin/bgm200

Fagan, K. A., Fouty, B. W., Tyler, R. C., Morris, K. G., Hepler, L. K., Sato, K., … Rodman, D. M. (1999). The pulmonary circulation of homozygous or heterozygous eNOS-null mice is hyperresponsive to mild hypoxia. *The Journal of Clinical Investigation*, *103*(2), 291–9. https://doi.org/10.1172/JCI3862

Farber, H. W., Miller, D. P., Poms, A. D., Badesch, D. B., Frost, A. E., Muros-Le Rouzic, E., … Benza, R. L. (2015). Five-Year outcomes of patients enrolled in the REVEAL Registry. *Chest*, *148*(4), 1043–1054. https://doi.org/10.1378/chest.15-0300

Feige, J. N., Lagouge, M., Canto, C., Strehle, A., Houten, S. M., Milne, J. C., … Auwerx, J. (2008). Specific SIRT1 activation mimics low energy levels and protects against diet-induced metabolic disorders by enhancing fat oxidation. *Cell Metabolism*, *8*(5), 347–58. https://doi.org/10.1016/j.cmet.2008.08.017

Fetalvero, K. M., Martin, K. A., & Hwa, J. (2007). Cardioprotective prostacyclin signaling in vascular smooth muscle. *Prostaglandins & Other Lipid Mediators*, *82*(1–4), 109–118. https://doi.org/10.1016/j.prostaglandins.2006.05.011

Foster, W., Suen, C., & Stewart D. J. (2014) Regenerative Cell and tissue-based therapies for pulmonary arterial hypertension. *Canadian Journal of Cardiology*, *30*, 1350-1360.

Frye, R. A. (2000). Phylogenetic classification of prokaryotic and eukaryotic Sir2-like proteins. *Biochemical and Biophysical Research Communications*, *273*(2), 793–8. https://doi.org/10.1006/bbrc.2000.3000

Fukuroda, T., Fujikawa, T., Ozaki, S., Ishikawa, K., Yano, M., & Nishikibe, M. (1994). Clearance of Circulating Endothelin-1 by ETB Receptors in Rats. *Biochemical and Biophysical Research Communications*, *199*(3), 1461–1465. https://doi.org/10.1006/bbrc.1994.1395

Galie, N., Brundage, B. H., Ghofrani, H. A., Oudiz, R. J., Simonneau, G., Safdar, Z., … Barst, R. J. (2009). Tadalafil therapy for pulmonary arterial hypertension. *Circulation*, *119*(22), 2894–2903. https://doi.org/10.1161/CIRCULATIONAHA.108.839274

Galie, N., Olschewski, H., Oudiz, R. J., Torres, F., Frost, A., Ghofrani, H. A., … Rubin, L. J. (2008). Ambrisentan for the treatment of pulmonary arterial hypertension: results of the ambrisentan in pulmonary arterial hypertension, randomized, double-blind, placebo-controlled, multicenter, efficacy (ARIES) study 1 and 2. *Circulation*, *117*(23), 3010–3019. https://doi.org/CIRCULATIONAHA.107.742510 [pii]10.1161/CIRCULATIONAHA.107.742510

Gao, R., Ma, Z., Hu, Y., Chen, J., Shetty, S., & Fu, J. (2015). Sirt1 restrains lung inflammasome activation in a murine model of sepsis. *American Journal of Physiology. Lung Cellular and Molecular Physiology*, *308*(8), L847-53. https://doi.org/10.1152/ajplung.00274.2014

Garcia-Rivas, G., Jerjes-Sánchez, C., Rodriguez, D., Garcia-Pelaez, J., & Trevino, V. (2017). A systematic review of genetic mutations in pulmonary arterial hypertension. *BMC Medical Genetics*, *18*(1), 82. https://doi.org/10.1186/s12881-017-0440-5

Garg, U. C., & Hassid, A. (1989). Nitric oxide-generating vasodilators and 8-bromo-cyclic guanosine monophosphate inhibit mitogenesis and proliferation of cultured rat vascular smooth muscle cells. *The Journal of Clinical Investigation*, *83*(5), 1774–7. https://doi.org/10.1172/JCI114081

Geng, J., Fan, F.-L., He, S., Liu, Y., Meng, Y., Tian, H., … Tian, H.-Y. (2016). The effects of the 5-HT2A receptor antagonist sarpogrelate hydrochloride on chronic hypoxic pulmonary hypertension in rats. *Experimental Lung Research*, *42*(4), 190–8. https://doi.org/10.1080/01902148.2016.1181122

Geraci, M. W., Gao, B., Shepherd, D. C., Moore, M. D., Westcott, J. Y., Fagan, K. A., … Voelkel, N. F. (1999). Pulmonary prostacyclin synthase overexpression in transgenic mice protects against development of hypoxic pulmonary hypertension. *The Journal of Clinical Investigation*, *103*(11), 1509–15. https://doi.org/10.1172/JCI5911

Gertz, M., Fischer, F., Nguyen, G. T. T., Lakshminarasimhan, M., Schutkowski, M., Weyand, M., & Steegborn, C. (2013). Ex-527 inhibits Sirtuins by exploiting their unique NAD+-dependent deacetylation mechanism. *Proceedings of the National Academy of Sciences*, *110*(30), E2772–E2781. https://doi.org/10.1073/pnas.1303628110

Ghosh, H. S., Spencer, J. V., Ng, B., McBurney, M. W., & Robbins, P. D. (2007). Sirt1 interacts with transducin-like enhancer of split-1 to inhibit nuclear factor κB-mediated transcription. *Biochemical Journal*, *408*(1), 105–111. https://doi.org/10.1042/BJ20070817

Giaid, A., & Saleh, D. (1995). Reduced expression of endothelial nitric oxide synthase in the lungs of patients with pulmonary hypertension. *The New England Journal of Medicine*, *333*(4), 214–21. https://doi.org/10.1056/NEJM199507273330403

Giaid, A., Yanagisawa, M., Langleben, D., Michel, R. P., Levy, R., Shennib, H., … Stewart, D. J. (1993). Expression of endothelin-1 in the lungs of patients with pulmonary hypertension. *The New England Journal of Medicine*, *328*(24), 1732–9. https://doi.org/10.1056/NEJM199306173282402

Ginouvès, A., Ilc, K., Macías, N., Pouysségur, J., & Berra, E. (2008). PHDs overactivation during chronic hypoxia "desensitizes" HIFalpha and protects cells from necrosis. *Proceedings of the National Academy of Sciences of the United States of America*, *105*(12), 4745–50. https://doi.org/10.1073/pnas.0705680105

Goldthorpe, H., Jiang, J.-Y., Taha, M., Deng, Y., Sinclair, T., Ge, C. X., … Stewart, D. J. (2015). Occlusive lung arterial lesions in endothelial-targeted, fas-induced apoptosis transgenic mice. *American Journal of Respiratory Cell and Molecular Biology*, *53*(5), 712–8. https://doi.org/10.1165/rcmb.2014-0311OC

Gomez-Arroyo, J. G., Farkas, L., Alhussaini, A. A., Farkas, D., Kraskauskas, D., Voelkel, N. F., & Bogaard, H. J. (2012). The monocrotaline model of pulmonary hypertension in perspective. *American Journal of Physiology. Lung Cellular and Molecular Physiology*, *302*(4), L363-9. https://doi.org/10.1152/ajplung.00212.2011

Gomez-Arroyo, J., Saleem, S. J., Mizuno, S., Syed, A. A., Bogaard, H. J., Abbate, A., … Voelkel, N. F. (2012). A brief overview of mouse models of pulmonary arterial hypertension: problems and prospects. *Am J Physiol Lung Cell Mol Physiol*, *302*(10), L977-91. https://doi.org/10.1152/ajplung.00362.2011

Gorenne, I., Kumar, S., Gray, K., Figg, N., Yu, H., Mercer, J., & Bennett, M. (2013). Vascular smooth muscle cell sirtuin 1 protects against DNA damage and inhibits atherosclerosis. *Circulation*, *127*(3), 386–96. https://doi.org/10.1161/CIRCULATIONAHA.112.124404

Groth, A., Vrugt, B., Brock, M., Speich, R., Ulrich, S., & Huber, L. C. (2014).

Inflammatory cytokines in pulmonary hypertension. *Respiratory Research*, *15*(1), 47. https://doi.org/10.1186/1465-9921-15-47

Guan, Z., Shen, L., Liang, H., Yu, H., Hei, B., Meng, X., & Yang, L. (2017). Resveratrol inhibits hypoxia-induced proliferation and migration of pulmonary artery vascular smooth muscle cells by inhibiting the phosphoinositide 3-kinase/protein kinase B signaling pathway. *Molecular Medicine Reports*, *16*(2), 1653–1660. https://doi.org/10.3892/mmr.2017.6814

Guarani, V., & Potente, M. (2010). SIRT1 - a metabolic sensor that controls blood vessel growth. *Current Opinion in Pharmacology*, *10*(2), 139–45. https://doi.org/10.1016/j.coph.2010.01.001

Guignabert, C., Tu, L., Izikki, M., Dewachter, L., Zadigue, P., Humbert, M., … Eddahibi, S. (2009). Dichloroacetate treatment partially regresses established pulmonary hypertension in mice with SM22alpha-targeted overexpression of the serotonin transporter. *FASEB Journal : Official Publication of the Federation of American Societies for Experimental Biology*, *23*(12), 4135–47. https://doi.org/10.1096/fj.09-131664

Guo, Y., Xu, A., & Wang, Y. (2016). SIRT1 in Endothelial Cells as a Novel Target for the Prevention of Early Vascular Aging. *Journal of Cardiovascular Pharmacology*, *67*(6), 465–73. https://doi.org/10.1097/FJC.0000000000000344

Hall, S. M., Davie, N., Klein, N., & Haworth, S. G. (2011). Endothelin receptor expression in idiopathic pulmonary arterial hypertension: effect of bosentan and epoprostenol treatment. *The European Respiratory Journal*, *38*(4), 851–60. https://doi.org/10.1183/09031936.00167010

Hickey, M. M., Richardson, T., Wang, T., Mosqueira, M., Arguiri, E., Yu, H., … Simon, M. C. (2010). The von Hippel-Lindau Chuvash mutation promotes pulmonary hypertension and fibrosis in mice. *The Journal of Clinical Investigation*, *120*(3), 827–39. https://doi.org/10.1172/JCI36362

Hitchon, C., Wong, K., Ma, G., Reed, J., Lyttle, D., & El-Gabalawy, H. (2002). Hypoxia-induced production of stromal cell-derived factor 1 (CXCL12) and vascular endothelial growth factor by synovial fibroblasts. *Arthritis and Rheumatism*, *46*(10), 2587–97. https://doi.org/10.1002/art.10520

Hong, K.-H., Lee, Y. J., Lee, E., Park, S. O., Han, C., Beppu, H., … Oh, S. P. (2008). Genetic ablation of the BMPR2 gene in pulmonary endothelium is sufficient to predispose to pulmonary arterial hypertension. *Circulation*, *118*(7), 722–30. https://doi.org/10.1161/CIRCULATIONAHA.107.736801

Hoshikawa, Y., Nana-Sinkam, P., Moore, M. D., Sotto-Santiago, S., Phang, T., Keith, R. L., … Geraci, M. W. (2003). Hypoxia induces different genes in the lungs of rats compared with mice. *Physiological Genomics*, *12*(3), 209–219. https://doi.org/10.1152/physiolgenomics.00081.2001

Howell, K., Preston, R. J., & McLoughlin, P. (2003). Chronic hypoxia causes angiogenesis in addition to remodelling in the adult rat pulmonary circulation. *The Journal of Physiology*, *547*(Pt 1), 133–45. https://doi.org/10.1113/jphysiol.2002.030676

Howitz, K. T., Bitterman, K. J., Cohen, H. Y., Lamming, D. W., Lavu, S., Wood, J. G., … Sinclair, D. A. (2003). Small molecule activators of sirtuins extend Saccharomyces cerevisiae lifespan. *Nature*, *425*(6954), 191–6.

https://doi.org/10.1038/nature01960
Hu, C. J., Wang, L. Y., Chodosh, L. A., Keith, B., & Simon, M. C. (2003). Differential roles of hypoxia-inducible factor 1alpha (HIF-1alpha) and HIF-2alpha in hypoxic gene regulation. *Mol Cell Biol*, *23*(24), 9361–9374. Retrieved from http://www.ncbi.nlm.nih.gov/pubmed/14645546
Hu, E.-C., He, J.-G., Liu, Z.-H., Ni, X.-H., Zheng, Y.-G., Gu, Q., … Xiong, C.-M. (2015). High levels of serum lactate dehydrogenase correlate with the severity and mortality of idiopathic pulmonary arterial hypertension. *Experimental and Therapeutic Medicine*, *9*(6), 2109–2113. https://doi.org/10.3892/etm.2015.2376
Huber, J. L., McBurney, M. W., Distefano, P. S., & McDonagh, T. (2010). SIRT1-independent mechanisms of the putative sirtuin enzyme activators SRT1720 and SRT2183. *Future Medicinal Chemistry*, *2*(12), 1751–9. https://doi.org/10.4155/fmc.10.257
Huertas, A., Tu, L., Thuillet, R., Le Hiress, M., Phan, C., Ricard, N., … Guignabert, C. (2015). Leptin signalling system as a target for pulmonary arterial hypertension therapy. *European Respiratory Journal*, *45*(4), 1066–1080. https://doi.org/10.1183/09031936.00193014
Humbert, M., Morrell, N. W., Archer, S. L., Stenmark, K. R., MacLean, M. R., Lang, I. M., … Rabinovitch, M. (2004). Cellular and molecular pathobiology of pulmonary arterial hypertension. *J Am Coll Cardiol*, *43*(12 Suppl S), 13S–24S. https://doi.org/10.1016/j.jacc.2004.02.029
Humbert, M., Sitbon, O., & Simonneau, G. (2004). Treatment of pulmonary arterial hypertension. *N Engl J Med*, *351*(14), 1425–1436. https://doi.org/10.1056/NEJMra040291
Iglarz, M., Binkert, C., Morrison, K., Fischli, W., Gatfield, J., Treiber, A., … Clozel, M. (2008). Pharmacology of macitentan, an orally active tissue-targeting dual endothelin receptor antagonist. *J Pharmacol Exp Ther*, *327*(3), 736–745. https://doi.org/10.1124/jpet.108.142976
Imai, S., Armstrong, C. M., Kaeberlein, M., & Guarente, L. (2000). Transcriptional silencing and longevity protein Sir2 is an NAD-dependent histone deacetylase. *Nature*, *403*(6771), 795–800. https://doi.org/10.1038/35001622
International, P. P. H. C., Lane, K. B., Machado, R. D., Pauciulo, M. W., Thomson, J. R., Phillips 3rd, J. A., … Trembath, R. C. (2000). Heterozygous germline mutations in BMPR2, encoding a TGF-beta receptor, cause familial primary pulmonary hypertension. *Nat Genet*, *26*(1), 81–84. https://doi.org/10.1038/79226
Ivy, C. M., & Scott, G. R. (2015). Control of breathing and the circulation in high-altitude mammals and birds. *Comparative Biochemistry and Physiology -Part A : Molecular and Integrative Physiology*, *186*, 66–74. https://doi.org/10.1016/j.cbpa.2014.10.009
James, M. O., Jahn, S. C., Zhong, G., Smeltz, M. G., Hu, Z., & Stacpoole, P. W. (2017). Therapeutic applications of dichloroacetate and the role of glutathione transferase zeta-1. *Pharmacology and Therapeutics*, *170*, 166–180. https://doi.org/10.1016/j.pharmthera.2016.10.018
Jeffery, T. K., & Morrell, N. W. (2002). Molecular and cellular basis of pulmonary vascular remodeling in pulmonary hypertension. *Prog Cardiovasc Dis*, *45*(3), 173–202. https://doi.org/10.1053/pcad.2002.130041S0033062002500475 [pii]

Jiang, B., Deng, Y., Suen, C., Taha, M., Chaudhary, K. R., Courtman, D. W., & Stewart, D. J. (2016). Marked strain-specific differences in the SU5416 rat model of severe pulmonary arterial hypertension. *American Journal of Respiratory Cell and Molecular Biology*, *54*(4), 461–8. https://doi.org/10.1165/rcmb.2014-0488OC

Jin, Q., Yan, T., Ge, X., Sun, C., Shi, X., & Zhai, Q. (2007). Cytoplasm-localized SIRT1 enhances apoptosis. *Journal of Cellular Physiology*, *213*(1), 88–97. https://doi.org/10.1002/jcp.21091

Jochmans-Lemoine, A., Shahare, M., Soliz, J., & Joseph, V. (2016). HIF1α and physiological responses to hypoxia are correlated in mice but not in rats. *The Journal of Experimental Biology*, *219*(24), 3952–3961. https://doi.org/10.1242/jeb.142869

Jochmans-Lemoine, A., Villalpando, G., Gonzales, M., Valverde, I., Soria, R., & Joseph, V. (2015). Divergent physiological responses in laboratory rats and mice raised at high altitude. *The Journal of Experimental Biology*, *218*(Pt 7), 1035–43. https://doi.org/10.1242/jeb.112862

Jonigk, D., Golpon, H., Bockmeyer, C. L., Maegel, L., Hoeper, M. M., Gottlieb, J., … Laenger, F. (2011). Plexiform lesions in pulmonary arterial hypertension composition, architecture, and microenvironment. *The American Journal of Pathology*, *179*(1), 167–79. https://doi.org/10.1016/j.ajpath.2011.03.040

Joo, H. Y., Yun, M., Jeong, J., Park, E. R., Shin, H. J., Woo, S. R., … Lee, K. H. (2015). SIRT1 deacetylates and stabilizes hypoxia-inducible factor-1α (HIF-1α) via direct interactions during hypoxia. *Biochemical and Biophysical Research Communications*, *462*(4), 294–300. https://doi.org/10.1016/j.bbrc.2015.04.119

Jurasz, P., Courtman, D., Babaie, S., & Stewart, D. J. (2010). Role of apoptosis in pulmonary hypertension: from experimental models to clinical trials. *Pharmacology & Therapeutics*, *126*(1), 1–8. https://doi.org/10.1016/j.pharmthera.2009.12.006

Kaeberlein, M., McDonagh, T., Heltweg, B., Hixon, J., Westman, E. A., Caldwell, S. D., … Kennedy, B. K. (2005). Substrate-specific activation of sirtuins by resveratrol. *The Journal of Biological Chemistry*, *280*(17), 17038–45. https://doi.org/10.1074/jbc.M500655200

Kaneko, F. T., Arroliga, a C., Dweik, R. a, Comhair, S. a, Laskowski, D., Oppedisano, R., … Erzurum, S. C. (1998). Biochemical reaction products of nitric oxide as quantitative markers of primary pulmonary hypertension. *American Journal of Respiratory and Critical Care Medicine*, *158*(3), 917–23. https://doi.org/10.1164/ajrccm.158.3.9802066

Kang, H., Suh, J.-Y., Jung, Y.-S., Jung, J.-W., Kim, M. K., & Chung, J. H. (2011). Peptide switch is essential for Sirt1 deacetylase activity. *Molecular Cell*, *44*(2), 203–13. https://doi.org/10.1016/j.molcel.2011.07.038

Kapitsinou, P. P., Rajendran, G., Astleford, L., Michael, M., Schonfeld, M. P., Fields, T., … Haase, V. H. (2016). The Endothelial Prolyl-4-Hydroxylase Domain 2/Hypoxia-Inducible Factor 2 Axis Regulates Pulmonary Artery Pressure in Mice. *Molecular and Cellular Biology*, *36*(10), 1584–94. https://doi.org/10.1128/MCB.01055-15

Kato, M., Li, J., Chuang, J. L., & Chuang, D. T. (2007). Distinct structural mechanisms for inhibition of pyruvate dehydrogenase kinase isoforms by AZD7545, dichloroacetate, and radicicol. *Structure (London, England : 1993)*, *15*(8), 992–1004. https://doi.org/10.1016/j.str.2007.07.001

Kay, J. M., Harris, P., & Heath, D. (1967). Pulmonary hypertension produced in rats by ingestion of Crotalaria spectabilis seeds. *Thorax*, *22*(2), 176–179. Retrieved from http://www.ncbi.nlm.nih.gov/pmc/articles/PMC471603/

Keith, B., Johnson, R. S., & Simon, M. C. (2012). HIF1alpha and HIF2alpha: sibling rivalry in hypoxic tumour growth and progression. *Nat Rev Cancer*, *12*(1), 9–22. https://doi.org/10.1038/nrc3183

Kennedy, B. E., Sharif, T., Martell, E., Dai, C., Kim, Y., Lee, P. W. K., & Gujar, S. A. (2016). NAD+ salvage pathway in cancer metabolism and therapy. *Pharmacological Research*, *114*, 274–283. https://doi.org/10.1016/j.phrs.2016.10.027

Kenneth, N. S., & Rocha, S. (2008). Regulation of gene expression by hypoxia. *Biochemical Journal*, *414*(1), 19–29. https://doi.org/10.1042/BJ20081055

Kim, J., Tchernyshyov, I., Semenza, G. L., & Dang, C. V. (2006). HIF-1-mediated expression of pyruvate dehydrogenase kinase: a metabolic switch required for cellular adaptation to hypoxia. *Cell Metabolism*, *3*(3), 177–85. https://doi.org/10.1016/j.cmet.2006.02.002

Kim, S. Y., Sim, C. K., Tang, H., Han, W., Zhang, K., & Xu, F. (2015). Acetylome analysis identifies SIRT1 targets in mRNA-processing and chromatin-remodeling in mouse liver. *PLoS ONE*, *10*(10), 1–16. https://doi.org/10.1371/journal.pone.0140619

Knight, J. R. P., & Milner, J. (2012). SIRT1, metabolism and cancer. *Current Opinion in Oncology*, *24*(1), 68–75. https://doi.org/10.1097/CCO.0b013e32834d813b

Kobayashi, S., Yamashita, T., Ohneda, K., Nagano, M., Kimura, K., Nakai, H., … Ohneda, O. (2015). Hypoxia-inducible factor-3alpha promotes angiogenic activity of pulmonary endothelial cells by repressing the expression of the VE-cadherin gene. *Genes Cells*, *20*(3), 224–241. https://doi.org/10.1111/gtc.12215

Koh, M. Y., & Powis, G. (2012). Passing the baton: The HIF switch. *Trends in Biochemical Sciences*, *37*(9), 364–372. https://doi.org/10.1016/j.tibs.2012.06.004

Kokkonen, P., Rahnasto-Rilla, M., Mellini, P., Jarho, E., Lahtela-Kakkonen, M., & Kokkola, T. (2014). Studying SIRT6 regulation using H3K56 based substrate and small molecules. *European Journal of Pharmaceutical Sciences*, *63*, 71–76. https://doi.org/10.1016/j.ejps.2014.06.015

Kugathasan, L., Ray, J. B., Deng, Y., Rezaei, E., Dumont, D. J., & Stewart, D. J. (2009). The angiopietin-1-Tie2 pathway prevents rather than promotes pulmonary arterial hypertension in transgenic mice. *The Journal of Experimental Medicine*, *206*(10), 2221–34. https://doi.org/10.1084/jem.20090389

Kylhammar, D., & Rådegran, G. (2016). The principal pathways involved in the in vivo modulation of hypoxic pulmonary vasoconstriction, pulmonary arterial remodelling and pulmonary hypertension. *Acta Physiologica*, (1946), 1–29. https://doi.org/10.1111/apha.12749

Labrousse-Arias, D., Castillo-González, R., Rogers, N. M., Torres-Capelli, M., Barreira, B., Aragonés, J., … Calzada, M. J. (2016). HIF-2α-mediated induction of pulmonary thrombospondin-1 contributes to hypoxia-driven vascular remodelling and vasoconstriction. *Cardiovascular Research*, *109*(1), 115–30. https://doi.org/10.1093/cvr/cvv243

Laemmle, A., Lechleiter, A., Roh, V., Schwarz, C., Portmann, S., Furer, C., … Stroka, D. (2012). Inhibition of SIRT1 impairs the accumulation and transcriptional activity of HIF-1alpha protein under hypoxic conditions. *PLoS One*, *7*(3), e33433.

https://doi.org/10.1371/journal.pone.0033433
Lan, B., Hayama, E., Kawaguchi, N., Furutani, Y., & Nakanishi, T. (2015). Therapeutic efficacy of valproic acid in a combined monocrotaline and chronic hypoxia rat model of severe pulmonary hypertension. *PloS One*, *10*(1), e0117211. https://doi.org/10.1371/journal.pone.0117211
Landry, J., Sutton, A., Tafrov, S. T., Heller, R. C., Stebbins, J., Pillus, L., & Sternglanz, R. (2000). The silencing protein SIR2 and its homologs are NAD-dependent protein deacetylases. *Proc Natl Acad Sci U S A*, *97*(11), 5807–5811. https://doi.org/10.1073/pnas.110148297
Langleben, D., & Orfanos, S. (2017). Vasodilator responsiveness in idiopathic pulmonary arterial hypertension: identifying a distinct phenotype with distinct physiology and distinct prognosis. *Pulmonary Circulation*, 2045893217714231. https://doi.org/10.1177/2045893217714231
Lara, E., Mai, A., Calvanese, V., Altucci, L., Lopez-Nieva, P., Martinez-Chantar, M. L., … Fraga, M. F. (2009). Salermide, a Sirtuin inhibitor with a strong cancer-specific proapoptotic effect. *Oncogene*, *28*(6), 781–91. https://doi.org/10.1038/onc.2008.436
Lau, E. M. T., Giannoulatou, E., Celermajer, D. S., & Humbert, M. (2017). Epidemiology and treatment of pulmonary arterial hypertension. *Nature Reviews. Cardiology*. https://doi.org/10.1038/nrcardio.2017.84
Lee, C. S., Choi, E. Y., Lee, S. C., Koh, H. J., Lee, J. H., & Chung, J. H. (2015). Resveratrol Inhibits Hypoxia-Induced Vascular Endothelial Growth Factor Expression and Pathological Neovascularization. *Yonsei Med J*, *56*(6), 1678–1685. https://doi.org/10.3349/ymj.2015.56.6.1678
Lemieux, M. E., Yang, X., Jardine, K., He, X., Jacobsen, K. X., Staines, W. A., … McBurney, M. W. (2005). The Sirt1 deacetylase modulates the insulin-like growth factor signaling pathway in mammals. *Mechanisms of Ageing and Development*, *126*(10), 1097–105. https://doi.org/10.1016/j.mad.2005.04.006
León-Velarde, F., & Mejía, O. (2008). Gene expression in chronic high altitude diseases. *High Altitude Medicine & Biology*, *9*(2), 130–9. https://doi.org/10.1089/ham.2007.1077
Li, B., Yan, J., Shen, Y., Liu, Y., & Ma, Z. (2014). Dichloroacetate prevents but not reverses the formation of neointimal lesions in a rat model of severe pulmonary arterial hypertension. *Molecular Medicine Reports*, *10*(4), 2144–2152. https://doi.org/10.3892/mmr.2014.2432
Li, C., Issa, R., Kumar, P., Hampson, I. N., Lopez-Novoa, J. M., Bernabeu, C., & Kumar, S. (2003). CD105 prevents apoptosis in hypoxic endothelial cells. *Journal of Cell Science*, *116*(Pt 13), 2677–85. https://doi.org/10.1242/jcs.00470
Li, H., Rajendran, G. K., Liu, N., Ware, C., Rubin, B. P., & Gu, Y. (2007). SirT1 modulates the estrogen-insulin-like growth factor-1 signaling for postnatal development of mammary gland in mice. *Breast Cancer Research*, *9*(1), 1–12. https://doi.org/10.1186/bcr1632
Li, L., Zhang, H.-N., Chen, H.-Z., Gao, P., Zhu, L.-H., Li, H.-L., … Liang, C.-C. (2011). SIRT1 acts as a modulator of neointima formation following vascular injury in mice. *Circulation Research*, *108*(10), 1180–9. https://doi.org/10.1161/CIRCRESAHA.110.237875
Liang, R., & Ghaffari, S. (2016). Advances in understanding the mechanisms of

erythropoiesis in homeostasis and disease. *British Journal of Haematology*, *174*(5), 661–73. https://doi.org/10.1111/bjh.14194

Lim, J. H., Lee, Y. M., Chun, Y. S., Chen, J., Kim, J. E., & Park, J. W. (2010). Sirtuin 1 modulates cellular responses to hypoxia by deacetylating hypoxia-inducible factor 1alpha. *Mol Cell*, *38*(6), 864–878. https://doi.org/10.1016/j.molcel.2010.05.023

Lorenzo, F. R., Yang, C., Ng Tang Fui, M., Vankayalapati, H., Zhuang, Z., Huynh, T., … Prchal, J. T. (2013). A novel EPAS1/HIF2A germline mutation in a congenital polycythemia with paraganglioma. *Journal of Molecular Medicine (Berlin, Germany)*, *91*(4), 507–12. https://doi.org/10.1007/s00109-012-0967-z

Luo, J., Nikolaev, A. Y., Imai, S., Chen, D., Su, F., Shiloh, A., … Gu, W. (2001). Negative control of p53 by Sir2alpha promotes cell survival under stress. *Cell*, *107*(2), 137–48. https://doi.org/10.1016/S0092-8674(01)00524-4

Machado, R. D., Southgate, L., Eichstaedt, C. A., Aldred, M. A., Austin, E. D., Best, D. H., … Grünig, E. (2015). Pulmonary Arterial Hypertension: A Current Perspective on Established and Emerging Molecular Genetic Defects. *Human Mutation*, *36*(12), 1113–27. https://doi.org/10.1002/humu.22904

Maizel, J., Xavier, S., Chen, J., Lin, C. H. S., Vasko, R., & Goligorsky, M. S. (2014). Sirtuin 1 ablation in endothelial cells is associated with impaired angiogenesis and diastolic dysfunction. *American Journal of Physiology. Heart and Circulatory Physiology*, *307*(12), H1691-704. https://doi.org/10.1152/ajpheart.00281.2014

Makino, Y., Cao, R., Svensson, K., Bertilsson, G., Asman, M., Tanaka, H., … Poellinger, L. (2001). Inhibitory PAS domain protein is a negative regulator of hypoxia-inducible gene expression. *Nature*, *414*(6863), 550–554. https://doi.org/10.1038/35107085

Makino, Y., Kanopka, A., Wilson, W. J., Tanaka, H., & Poellinger, L. (2002). Inhibitory PAS domain protein (IPAS) is a hypoxia-inducible splicing variant of the hypoxia-inducible factor-3alpha locus. *The Journal of Biological Chemistry*, *277*(36), 32405–8. https://doi.org/10.1074/jbc.C200328200

Marxsen, J. H., Stengel, P., Doege, K., Heikkinen, P., Jokilehto, T., Wagner, T., … Metzen, E. (2004). Hypoxia-inducible factor-1 (HIF-1) promotes its degradation by induction of HIF-alpha-prolyl-4-hydroxylases. *The Biochemical Journal*, *381*(Pt 3), 761–7. https://doi.org/10.1042/BJ20040620

Masri, F. A., Xu, W., Comhair, S. A., Asosingh, K., Koo, M., Vasanji, A., … Erzurum, S. C. (2007). Hyperproliferative apoptosis-resistant endothelial cells in idiopathic pulmonary arterial hypertension. *Am J Physiol Lung Cell Mol Physiol*, *293*(3), L548-54. https://doi.org/00428.2006 [pii]10.1152/ajplung.00428.2006

McBurney, M. W., Clark-Knowles, K. V, Caron, A. Z., & Gray, D. A. (2013). SIRT1 is a Highly Networked Protein That Mediates the Adaptation to Chronic Physiological Stress. *Genes & Cancer*, *4*(3–4), 125–34. https://doi.org/10.1177/1947601912474893

McBurney, M. W., Yang, X., Jardine, K., Hixon, M., Boekelheide, K., Webb, J. R., … Lemieux, M. (2003). The mammalian SIR2alpha protein has a role in embryogenesis and gametogenesis. *Molecular and Cellular Biology*, *23*(1), 38–54. Retrieved from http://www.ncbi.nlm.nih.gov/pubmed/12482959

McMurtry, M. S., Bonnet, S., Wu, X., Dyck, J. R. B., Haromy, A., Hashimoto, K., & Michelakis, E. D. (2004). Dichloroacetate prevents and reverses pulmonary

hypertension by inducing pulmonary artery smooth muscle cell apoptosis. *Circulation Research*, *95*(8), 830–40. https://doi.org/10.1161/01.RES.0000145360.16770.9f

Medarov, B. I., & Judson, M. A. (2015). The role of calcium channel blockers for the treatment of pulmonary arterial hypertension: How much do we actually know and how could they be positioned today? *Respiratory Medicine*, *109*(5), 557–64. https://doi.org/10.1016/j.rmed.2015.01.004

Medina, R. J., O'Neill, C. L., O'Doherty, T. M., Knott, H., Guduric-Fuchs, J., Gardiner, T. A., & Stitt, A. W. (2011). Myeloid angiogenic cells act as alternative M2 macrophages and modulate angiogenesis through interleukin-8. *Mol Med*, *17*(9–10), 1045–1055. https://doi.org/10.2119/molmed.2011.00129

Michelakis, E. D., Gurtu, V., Webster, L., Barnes, G., Watson, G., Howard, L., … Wilkins, M. R. (2017). Inhibition of pyruvate dehydrogenase kinase improves pulmonary arterial hypertension in genetically susceptible patients. *Science Translational Medicine*, *9*(413), 1–13. https://doi.org/10.1126/scitranslmed.aao4583

Michelakis, E. D., McMurtry, M. S., Wu, X.-C., Dyck, J. R. B., Moudgil, R., Hopkins, T. A., … Archer, S. L. (2002). Dichloroacetate, a metabolic modulator, prevents and reverses chronic hypoxic pulmonary hypertension in rats: role of increased expression and activity of voltage-gated potassium channels. *Circulation*, *105*(2), 244–50. Retrieved from http://www.ncbi.nlm.nih.gov/pubmed/11790708

Michelakis, E. D., Tymchak, W., Noga, M., Webster, L., Wu, X. C., Lien, D., … Archer, S. L. (2003). Long-term treatment with oral sildenafil is safe and improves functional capacity and hemodynamics in patients with pulmonary arterial hypertension. *Circulation*, *108*(17), 2066–2069. https://doi.org/10.1161/01.CIR.0000099502.17776.C2

Michelakis, E. D., Webster, L., & Mackey, J. R. (2008). Dichloroacetate (DCA) as a potential metabolic-targeting therapy for cancer. *British Journal of Cancer*, *99*(7), 989–94. https://doi.org/10.1038/sj.bjc.6604554

Michelakis, E. D., Wilkins, M. R., & Rabinovitch, M. (2008). Emerging concepts and translational priorities in pulmonary arterial hypertension. *Circulation*, *118*(14), 1486–1495. https://doi.org/118/14/1486 [pii]10.1161/CIRCULATIONAHA.106.673988

Milne, J. C., Lambert, P. D., Schenk, S., Carney, D. P., Smith, J. J., Gagne, D. J., … Westphal, C. H. (2007). Small molecule activators of SIRT1 as therapeutics for the treatment of type 2 diabetes. *Nature*, *450*(7170), 712–6. https://doi.org/10.1038/nature06261

Minor, R. K., Baur, J. A., Gomes, A. P., Ward, T. M., Csiszar, A., Mercken, E. M., … de Cabo, R. (2011). SRT1720 improves survival and healthspan of obese mice. *Scientific Reports*, *1*(2011 SRC-GoogleScholar FG-0), 70. https://doi.org/10.1038/srep00070

Mirrakhimov, A. E., & Strohl, K. P. (2016). High-altitude Pulmonary Hypertension: an Update on Disease Pathogenesis and Management. *The Open Cardiovascular Medicine Journal*, *10*(1), 19–27. https://doi.org/10.2174/1874192401610010019

Moledina, S., de Bruyn, A., Schievano, S., Owens, C. M., Young, C., Haworth, S. G., … Muthurangu, V. (2011). Fractal branching quantifies vascular changes and predicts survival in pulmonary hypertension: a proof of principle study. *Heart (British*

Cardiac Society), *97*(15), 1245–9. https://doi.org/10.1136/hrt.2010.214130
Morimatsu, Y., Sakashita, N., Komohara, Y., Ohnishi, K., Masuda, H., Dahan, D., … Marthan, R. (2012). Development and characterization of an animal model of severe pulmonary arterial hypertension. *Journal of Vascular Research*, *49*(1), 33–42. https://doi.org/10.1159/000329594
Morrell, N. W. (2006). Pulmonary Hypertension Due to BMPR2 Mutation: A New Paradigm for Tissue Remodeling? *Proceedings of the American Thoracic Society*, *3*(8), 680–686. https://doi.org/10.1513/pats.200605-118SF
Mortuza, R., Feng, B., & Chakrabarti, S. (2015). SIRT1 reduction causes renal and retinal injury in diabetes through endothelin 1 and transforming growth factor β1. *Journal of Cellular and Molecular Medicine*, *19*(8), 1857–67. https://doi.org/10.1111/jcmm.12557
Mubarak, K. K. (2010). A review of prostaglandin analogs in the management of patients with pulmonary arterial hypertension. *Respiratory Medicine*, *104*(1), 9–21. https://doi.org/10.1016/j.rmed.2009.07.015
Naeije, R. (2015). Pulmonary Circulation. In M. A. Grippi, J. A. Elias, J. A. Fishman, R. M. Kotloff, A. I. Pack, R. M. Senior, & M. D. Siegel (Eds.), *Fishman's Pulmonary Diseases and Disorders, 5e*. New York, NY: McGraw-Hill Education. https://doi.org/10.1016/B978-1-4557-0792-8.00004-0
Nagaya, N. (2004). Drug therapy of primary pulmonary hypertension. *Am J Cardiovasc Drugs*, *4*(2), 75–85. https://doi.org/422 [pii]
Nakahata, N. (2008). Thromboxane A2: physiology/pathophysiology, cellular signal transduction and pharmacology. *Pharmacology & Therapeutics*, *118*(1), 18–35. https://doi.org/10.1016/j.pharmthera.2008.01.001
Nakata, R., Takahashi, S., & Inoue, H. (2012). Recent advances in the study on resveratrol. *Biological & Pharmaceutical Bulletin*, *35*(3), 273–9. https://doi.org/JST.JSTAGE/bpb/35.273 [pii]
Nakayama Wong, L. S., Lamé, M. W., Jones, A. D., & Wilson, D. W. (2010). Differential cellular responses to protein adducts of naphthoquinone and monocrotaline pyrrole. *Chemical Research in Toxicology*, *23*(9), 1504–13. https://doi.org/10.1021/tx1002436
Newman, J. H., Holt, T. N., Cogan, J. D., Womack, B., Phillips, J. A., Li, C., … Hamid, R. (2015). Increased prevalence of EPAS1 variant in cattle with high-altitude pulmonary hypertension. *Nature Communications*, *6*, 6863. https://doi.org/10.1038/ncomms7863
O'Hagan, H. M., Mohammad, H. P., & Baylin, S. B. (2008). Double strand breaks can initiate gene silencing and SIRT1-dependent onset of DNA methylation in an exogenous promoter CpG island. *PLoS Genetics*, *4*(8), e1000155. https://doi.org/10.1371/journal.pgen.1000155
Ochs, M., & Weibel, E. R. (2008). Functional design of the human lung for gas exchange. In M. A. Grippi, J. A. Elias, J. A. Fishman, R. M. Kotloff, A. I. Pack, R. M. Senior, & M. D. Siegel (Eds.), *Fishman´s Pulmonary Disease and Disorders*. New York, NY: McGraw-Hill Education. Retrieved from accessmedicine.mhmedical.com/content.aspx?aid=1122354263
Ortmann, B., Druker, J., & Rocha, S. (2014). Cell cycle progression in response to oxygen levels. *Cell Mol Life Sci*, *71*(18), 3569–3582.

https://doi.org/10.1007/s00018-014-1645-9
Ota, H., Akishita, M., Eto, M., Iijima, K., Kaneki, M., & Ouchi, Y. (2007). Sirt1 modulates premature senescence-like phenotype in human endothelial cells. *Journal of Molecular and Cellular Cardiology*, *43*(5), 571–9. https://doi.org/10.1016/j.yjmcc.2007.08.008
Pacholec, M., Bleasdale, J. E., Chrunyk, B., Cunningham, D., Flynn, D., Garofalo, R. S., … Ahn, K. (2010). SRT1720, SRT2183, SRT1460, and resveratrol are not direct activators of SIRT1. *The Journal of Biological Chemistry*, *285*(11), 8340–51. https://doi.org/10.1074/jbc.M109.088682
Paffett, M. L., Lucas, S. N., & Campen, M. J. (2012). Resveratrol reverses monocrotaline-induced pulmonary vascular and cardiac dysfunction: a potential role for atrogin-1 in smooth muscle. *Vascular Pharmacology*, *56*(1–2), 64–73. https://doi.org/10.1016/j.vph.2011.11.002
Pan, M., Yuan, H., Brent, M., Ding, E. C., & Marmorstein, R. (2012). SIRT1 contains N- and C-terminal regions that potentiate deacetylase activity. *The Journal of Biological Chemistry*, *287*(4), 2468–76. https://doi.org/10.1074/jbc.M111.285031
Park, S.-J., Ahmad, F., Philp, A., Baar, K., Williams, T., Luo, H., … Chung, J. H. (2012). Resveratrol ameliorates aging-related metabolic phenotypes by inhibiting cAMP phosphodiesterases. *Cell*, *148*(3), 421–33. https://doi.org/10.1016/j.cell.2012.01.017
Patel, S. A., & Simon, M. C. (2008). Biology of hypoxia-inducible factor-2α in development and disease. *Cell Death and Differentiation*, *15*(4), 628–634. https://doi.org/10.1038/cdd.2008.17
Paulin, R., Dromparis, P., Sutendra, G., Gurtu, V., Zervopoulos, S., Bowers, L., … Michelakis, E. D. (2014). Sirtuin 3 deficiency is associated with inhibited mitochondrial function and pulmonary arterial hypertension in rodents and humans. *Cell Metab*, *20*(5), 827–839. https://doi.org/10.1016/j.cmet.2014.08.011
Pfister, J. A., Ma, C., Morrison, B. E., & D'Mello, S. R. (2008). Opposing effects of sirtuins on neuronal survival: SIRT1-mediated neuroprotection is independent of its deacetylase activity. *PLoS ONE*, *3*(12), 1–8. https://doi.org/10.1371/journal.pone.0004090
Pfluger, P. T., Herranz, D., Velasco-Miguel, S., Serrano, M., & Tschop, M. H. (2008). Sirt1 protects against high-fat diet-induced metabolic damage. *Proc Natl Acad Sci U S A*, *105*(28), 9793–9798. https://doi.org/10.1073/pnas.0802917105
Piao, L., Fang, Y.-H., Cadete, V. J. J., Wietholt, C., Urboniene, D., Toth, P. T., … Archer, S. L. (2010). The inhibition of pyruvate dehydrogenase kinase improves impaired cardiac function and electrical remodeling in two models of right ventricular hypertrophy: resuscitating the hibernating right ventricle. *Journal of Molecular Medicine (Berlin, Germany)*, *88*(1), 47–60. https://doi.org/10.1007/s00109-009-0524-6
Piao, L., Sidhu, V. K., Fang, Y. H., Ryan, J. J., Parikh, K. S., Hong, Z., … Archer, S. L. (2013). FOXO1-mediated upregulation of pyruvate dehydrogenase kinase-4 (PDK4) decreases glucose oxidation and impairs right ventricular function in pulmonary hypertension: therapeutic benefits of dichloroacetate. *J Mol Med (Berl)*, *91*(3), 333–346. https://doi.org/10.1007/s00109-012-0982-0
Pinsky, D. J., Liao, H., Lawson, C. A., Yan, S. F., Chen, J., Carmeliet, P., … Stern, D. M. (1998). Coordinated induction of plasminogen activator inhibitor-1 (PAI-1) and

inhibition of plasminogen activator gene expression by hypoxia promotes pulmonary vascular fibrin deposition. *The Journal of Clinical Investigation*, *102*(5), 919–28. https://doi.org/10.1172/JCI307

Planavila, A., Dominguez, E., Navarro, M., Vinciguerra, M., Iglesias, R., Giralt, M., … Villarroya, F. (2012). Dilated cardiomyopathy and mitochondrial dysfunction in Sirt1-deficient mice: a role for Sirt1-Mef2 in adult heart. *Journal of Molecular and Cellular Cardiology*, *53*(4), 521–31. https://doi.org/10.1016/j.yjmcc.2012.07.019

Potente, M., Ghaeni, L., Baldessari, D., Mostoslavsky, R., Rossig, L., Dequiedt, F., … Dimmeler, S. (2007). SIRT1 controls endothelial angiogenic functions during vascular growth. *Genes & Development*, *21*(20), 2644–58. https://doi.org/10.1101/gad.435107

Prabhakar, N. R., & Semenza, G. L. (2012). Adaptive and maladaptive cardiorespiratory responses to continuous and intermittent hypoxia mediated by hypoxia-inducible factors 1 and 2. *Physiological Reviews*, *92*(3), 967–1003. https://doi.org/10.1152/physrev.00030.2011

Pruitt, K., Zinn, R. L., Ohm, J. E., McGarvey, K. M., Kang, S.-H. L., Watkins, D. N., … Baylin, S. B. (2006). Inhibition of SIRT1 reactivates silenced cancer genes without loss of promoter DNA hypermethylation. *PLoS Genetics*, *2*(3), e40. https://doi.org/10.1371/journal.pgen.0020040

Qureshi, S. M., & Mustafa, R. (2018). Measurement of respiratory function: Gas exchange and its clinical applications. *Anaesthesia and Intensive Care Medicine*, 1–7. https://doi.org/10.1016/j.mpaic.2017.11.006

Rankin, E. B., Biju, M. P., Liu, Q., Unger, T. L., Rha, J., Johnson, R. S., … Haase, V. H. (2007). Hypoxia-inducible factor-2 (HIF-2) regulates hepatic erythropoietin in vivo. *The Journal of Clinical Investigation*, *117*(4), 1068–77. https://doi.org/10.1172/JCI30117

Rauh, D., Fischer, F., Gertz, M., Lakshminarasimhan, M., Bergbrede, T., Aladini, F., … Steegborn, C. (2013). An acetylome peptide microarray reveals specificities and deacetylation substrates for all human sirtuin isoforms. *Nature Communications*, *4*, 2327. https://doi.org/10.1038/ncomms3327

Ravenna, L., Salvatori, L., & Russo, M. A. (2016). HIF3α: the little we know. *The FEBS Journal*, *283*(6), 993–1003. https://doi.org/10.1111/febs.13572

Rehman, J., & Archer, S. L. (2010). A proposed mitochondrial-metabolic mechanism for initiation and maintenance of pulmonary arterial hypertension in fawn-hooded rats: the Warburg model of pulmonary arterial hypertension. *Adv Exp Med Biol*, *661*, 171–185. https://doi.org/10.1007/978-1-60761-500-2_11

Renaud, S., & de Lorgeril, M. (1992). Wine, alcohol, platelets, and the French paradox for coronary heart disease. *Lancet (London, England)*, *339*(8808), 1523–6. Retrieved from http://www.ncbi.nlm.nih.gov/pubmed/1351198

Richter, A., Yeager, M. E., Zaiman, A., Cool, C. D., Voelkel, N. F., & Tuder, R. M. (2004). Impaired transforming growth factor-beta signaling in idiopathic pulmonary arterial hypertension. *Am J Respir Crit Care Med*, *170*(12), 1340–1348. https://doi.org/10.1164/rccm.200311-1602OC200311-1602OC [pii]

Ritman, E. L. (2005). Micro-computed tomography of the lungs and pulmonary-vascular system. *Proceedings of the American Thoracic Society*, *2*(6), 477–80, 501. https://doi.org/10.1513/pats.200508-080DS

Ryan, J. J., Marsboom, G., & Archer, S. L. (2013). Rodent models of group 1 pulmonary hypertension. *Handb Exp Pharmacol*, *218*, 105–149. https://doi.org/10.1007/978-3-642-38664-0_5

Sacconnay, L., Carrupt, P.-A., & Nurisso, A. (2016). Human sirtuins: Structures and flexibility. *Journal of Structural Biology*, *196*(3), 534–542. https://doi.org/10.1016/j.jsb.2016.10.008

Sander, M. (2016). *Does the Sympathetic Nervous System Adapt to Chronic Altitude Exposure?* (Vol. 903). https://doi.org/10.1007/978-1-4899-7678-9

Sato, K., Webb, S., Tucker, A., Rabinovitch, M., O'Brien, R. F., McMurtry, I. F., & Stelzner, T. J. (1992). Factors influencing the idiopathic development of pulmonary hypertension in the fawn hooded rat. *The American Review of Respiratory Disease*, *145*(4 Pt 1), 793–7. https://doi.org/10.1164/ajrccm/145.4_Pt_1.793

Schlosser, K., Taha, M., Deng, Y., Jiang, B., McIntyre, L. A., Mei, S. H., & Stewart, D. J. (2017). Lack of elevation in plasma levels of pro-inflammatory cytokines in common rodent models of pulmonary arterial hypertension: questions of construct validity for human patients. *Pulmonary Circulation*, *7*(2), 476–485. https://doi.org/10.1177/2045893217705878

Schmitt, C. A., Heiss, E. H., & Dirsch, V. M. (2010). Effect of resveratrol on endothelial cell function: Molecular mechanisms. *BioFactors*, *36*(5), 342–349. https://doi.org/10.1002/biof.109

Schölz, C., Weinert, B. T., Wagner, S. A., Beli, P., Miyake, Y., Qi, J., … Choudhary, C. (2015). Acetylation site specificities of lysine deacetylase inhibitors in human cells. *Nature Biotechnology*, *33*(4), 415–23. https://doi.org/10.1038/nbt.3130

Schuliga, M., Westall, G., Xia, Y., & Stewart, A. G. (2013). The plasminogen activation system: new targets in lung inflammation and remodeling. *Current Opinion in Pharmacology*, *13*(3), 386–93. https://doi.org/10.1016/j.coph.2013.05.014

Seifert, E. L., Caron, A. Z., Morin, K., Coulombe, J., He, X. H., Jardine, K., … McBurney, M. W. (2012). SirT1 catalytic activity is required for male fertility and metabolic homeostasis in mice. *FASEB Journal : Official Publication of the Federation of American Societies for Experimental Biology*, *26*(2), 555–66. https://doi.org/10.1096/fj.11-193979

Semenza, G., Jiang, B., Leung, S., Passantino, R., Concordet, J., Maire, P., & Giallongo, A. (1996). Hypoxia Response Elements in the Aldolase A, Enolase 1,and Lactate Dehydrogenase A Gene Promoters Contain Essential Binding Sites for Hypoxia-inducible Factor 1. *Journal of Biological Chemistry*, *271*(51), 32529–32537. https://doi.org/10.1074/jbc.271.51.32529

Simonneau, G., Gatzoulis, M. A., Adatia, I., Celermajer, D., Denton, C., Ghofrani, A., … Souza, R. (2013). Updated clinical classification of pulmonary hypertension. *Journal of the American College of Cardiology*, *62*(25 Suppl), D34-41. https://doi.org/10.1016/j.jacc.2013.10.029

Sitbon, O., Channick, R., Chin, K. M., Frey, A., Gaine, S., Galiè, N., … GRIPHON Investigators. (2015). Selexipag for the Treatment of Pulmonary Arterial Hypertension. *The New England Journal of Medicine*, *373*(26), 2522–33. https://doi.org/10.1056/NEJMoa1503184

Skoro-Sajer, N., & Lang, I. (2008). Treprostinil for the treatment of pulmonary hypertension. *Expert Opinion on Pharmacotherapy*, *9*(8), 1415–20.

https://doi.org/10.1517/14656566.9.8.1415
Smith, J. S., Brachmann, C. B., Celic, I., Kenna, M. A., Muhammad, S., Starai, V. J., … Boeke, J. D. (2000). A phylogenetically conserved NAD+-dependent protein deacetylase activity in the Sir2 protein family. *Proc Natl Acad Sci U S A*, *97*(12), 6658–6663. Retrieved from http://www.ncbi.nlm.nih.gov/pubmed/10841563
Stacher, E., Graham, B. B., Hunt, J. M., Gandjeva, A., Groshong, S. D., McLaughlin, V. V, … Tuder, R. M. (2012). Modern age pathology of pulmonary arterial hypertension. *Am J Respir Crit Care Med*, *186*(3), 261–272. https://doi.org/10.1164/rccm.201201-0164OC
Stacpoole, P. W. (2017). Therapeutic Targeting of the Pyruvate Dehydrogenase Complex/Pyruvate Dehydrogenase Kinase (PDC/PDK) Axis in Cancer. *Journal of the National Cancer Institute*, *109*(11), 1–14. https://doi.org/10.1093/jnci/djx071
Steiner, M. K., Syrkina, O. L., Kolliputi, N., Mark, E. J., Hales, C. A., & Waxman, A. B. (2009). Interleukin-6 overexpression induces pulmonary hypertension. *Circ Res*, *104*(2), 236–44, 28p following 244. https://doi.org/10.1161/CIRCRESAHA.108.182014
Stenmark, K. R., Fagan, K. A., & Frid, M. G. (2006). Hypoxia-induced pulmonary vascular remodeling: Cellular and molecular mechanisms. *Circulation Research*, *99*(7), 675–691. https://doi.org/10.1161/01.RES.0000243584.45145.3f
Stenmark, K. R., & Mecham, R. P. (1997). Cellular and molecular mechanisms of pulmonary vascular remodeling. *Annual Review of Physiology*, *59*, 89–144. https://doi.org/10.1146/annurev.physiol.59.1.89
Stenmark, K. R., Meyrick, B., Galie, N., Mooi, W. J., & McMurtry, I. F. (2009). Animal models of pulmonary arterial hypertension: the hope for etiological discovery and pharmacological cure. *American Journal of Physiology. Lung Cellular and Molecular Physiology*, *297*(6), L1013-32. https://doi.org/10.1152/ajplung.00217.2009
Stewart, D. J., Levy, R. D., Cernacek, P., & Langleben, D. (1991). Increased plasma endothelin-1 in pulmonary hypertension: marker or mediator of disease? *Annals of Internal Medicine*, *114*(6), 464–9. https://doi.org/10.7326/0003-4819-114-6-464
Stratton, M. S., & McKinsey, T. A. (2015). Acetyl-lysine erasers and readers in the control of pulmonary hypertension and right ventricular hypertrophy. *Biochemistry and Cell Biology = Biochimie et Biologie Cellulaire*, *93*(2), 149–57. https://doi.org/10.1139/bcb-2014-0119
Sugden, M. C., & Holness, M. J. (2003). Recent advances in mechanisms regulating glucose oxidation at the level of the pyruvate dehydrogenase complex by PDKs. *American Journal of Physiology - Endocrinology And Metabolism*, *284*(5), E855–E862. https://doi.org/10.1152/ajpendo.00526.2002
Sylvester, J. T., Shimoda, L. A., Aaronson, P. I., & Ward, J. P. T. (2012). Hypoxic pulmonary vasoconstriction. *Physiological Reviews*, *92*(1), 367–520. https://doi.org/10.1152/physrev.00041.2010
Tada, Y., Laudi, S., Harral, J., Carr, M., Ivester, C., Tanabe, N., … West, J. (2008). Murine pulmonary response to chronic hypoxia is strain specific. *Experimental Lung Research*, *34*(6), 313–23. https://doi.org/10.1080/01902140802093204
Taha, M., Jiang, B., Deng, Y., & Stewart, D. (2012). Abstract 16372: Effect of T-Cell Activity on Susceptibility of Mice for Development of Severe Pulmonary Arterial

Hypertension in Response to SU5416 and Chronic Hypoxia. *Circulation*, *126*(Suppl 21). Retrieved from http://circ.ahajournals.org/content/126/Suppl_21/A16372

Taichman, D. B., Mandel, J., Smith, K. A., Yuan, J. X.-J., & Taichman DB, Mandel J, Smith KA, Yuan JJ. Pulmonary Arterial Hypertension. In: Grippi MA, Elias JA, Fishman JA, Kotloff RM, Pack AI, Senior RM, S. M. (2015). Pulmonary Arterial Hypertension. In M. A. Grippi, J. A. Elias, J. A. Fishman, R. M. Kotloff, A. I. Pack, R. M. Senior, & M. D. Siegel (Eds.), *Fishman's Pulmonary Diseases and Disorders, 5e*. New York, NY: McGraw-Hill Education. Retrieved from accessmedicine.mhmedical.com/content.aspx?aid=1122362559

Tan, Q., Kerestes, H., Percy, M. J., Pietrofesa, R., Chen, L., Khurana, T. S., … Lee, F. S. (2013). Erythrocytosis and pulmonary hypertension in a mouse model of human HIF2A gain of function mutation. *The Journal of Biological Chemistry*, *288*(24), 17134–44. https://doi.org/10.1074/jbc.M112.444059

Tang, H., Babicheva, A., McDermott, K. M., Gu, Y., Ayon, R. J., Song, S., … Yuan, J. X.-J. (2017). Endothelial HIF-2α Contributes to Severe Pulmonary Hypertension by Inducing Endothelial-to-Mesenchymal Transition. *American Journal of Physiology. Lung Cellular and Molecular Physiology*, (520), ajplung.00096.2017. https://doi.org/10.1152/ajplung.00096.2017

Taraseviciene-Stewart, L., Kasahara, Y., Alger, L., Hirth, P., Mc Mahon, G., Waltenberger, J., … Tuder, R. M. (2001). Inhibition of the VEGF receptor 2 combined with chronic hypoxia causes cell death-dependent pulmonary endothelial cell proliferation and severe pulmonary hypertension. *FASEB J*, *15*(2), 427–438. https://doi.org/10.1096/fj.00-0343com

Teichert-Kuliszewska, K., Kutryk, M. J. B., Kuliszewski, M. A., Karoubi, G., Courtman, D. W., Zucco, L., … Stewart, D. J. (2006). Bone morphogenetic protein receptor-2 signaling promotes pulmonary arterial endothelial cell survival: implications for loss-of-function mutations in the pathogenesis of pulmonary hypertension. *Circulation Research*, *98*(2), 209–17. https://doi.org/10.1161/01.RES.0000200180.01710.e6

Teixidó, J., Martínez-Moreno, M., Díaz-Martínez, M., & Sevilla-Movilla, S. (2017). The good and bad faces of the CXCR4 chemokine receptor. *The International Journal of Biochemistry & Cell Biology*, *95*(December 2017), 121–131. https://doi.org/10.1016/j.biocel.2017.12.018

Thompson, A. M., Wagner, R., & Rzucidlo, E. M. (2014). Age-related loss of SirT1 expression results in dysregulated human vascular smooth muscle cell function. *American Journal of Physiology. Heart and Circulatory Physiology*, *307*(4), H533-41. https://doi.org/10.1152/ajpheart.00871.2013

Tozzi, C. A., Christiansen, D. L., Poiani, G. J., & Riley, D. J. (1994). Excess collagen in hypertensive pulmonary arteries decreases vascular distensibility. *American Journal of Respiratory and Critical Care Medicine*, *149*(5), 1317–26. https://doi.org/10.1164/ajrccm.149.5.8173773

Tuder, R. M., Cool, C. D., Geraci, M. W., Wang, J., Abman, S. H., Wright, L., … Voelkel, N. F. (1999). Prostacyclin synthase expression is decreased in lungs from patients with severe pulmonary hypertension. *American Journal of Respiratory and Critical Care Medicine*, *159*(6), 1925–32. https://doi.org/10.1164/ajrccm.159.6.9804054

Tuder, R. M., Groves, B., Badesch, D. B., & Voelkel, N. F. (1994). Exuberant endothelial cell growth and elements of inflammation are present in plexiform lesions of pulmonary hypertension. *The American Journal of Pathology*, *144*(2), 275–85. Retrieved from http://www.ncbi.nlm.nih.gov/entrez/query.fcgi?cmd=Retrieve&db=PubMed&dopt=Citation&list_uids=7508683

Uversky, V. N., & Redwan, E. M. (2016). Erythropoietin and co.: intrinsic structure and functional disorder. *Molecular bioSystems*, *13*(1), 56–72. https://doi.org/10.1039/c6mb00657d

Vaid, H. M., Camacho, X., Granton, J. T., Mamdani, M. M., Yao, Z., Singh, S., … Gomes, T. (2016). The Characteristics of Treated Pulmonary Arterial Hypertension Patients in Ontario. *Canadian Respiratory Journal*, *2016*, 6279250. https://doi.org/10.1155/2016/6279250

Valvona, C. J., Fillmore, H. L., Nunn, P. B., & Pilkington, G. J. (2016). The Regulation and Function of Lactate Dehydrogenase A: Therapeutic Potential in Brain Tumor. *Brain Pathology*, *26*(1), 3–17. https://doi.org/10.1111/bpa.12299

Vaquero, A., Scher, M., Erdjument-Bromage, H., Tempst, P., Serrano, L., & Reinberg, D. (2007). SIRT1 regulates the histone methyl-transferase SUV39H1 during heterochromatin formation. *Nature*, *450*(7168), 440–4. https://doi.org/10.1038/nature06268

Vasko, R., Xavier, S., Chen, J., Lin, C. H. S., Ratliff, B., Rabadi, M., … Goligorsky, M. S. (2014). Endothelial sirtuin 1 deficiency perpetrates nephrosclerosis through downregulation of matrix metalloproteinase-14: relevance to fibrosis of vascular senescence. *Journal of the American Society of Nephrology : JASN*, *25*(2), 276–91. https://doi.org/10.1681/ASN.2013010069

Vaziri, H., Dessain, S. K., Ng Eaton, E., Imai, S. I., Frye, R. A., Pandita, T. K., … Weinberg, R. A. (2001). hSIR2(SIRT1) functions as an NAD-dependent p53 deacetylase. *Cell*, *107*(2), 149–59. https://doi.org/10.1016/S0092-8674(01)00527-X

Verdin, E., & Ott, M. (2015). 50 years of protein acetylation: from gene regulation to epigenetics, metabolism and beyond. *Nat Rev Mol Cell Biol*, *16*(4), 258–264. https://doi.org/10.1038/nrm3931

Vitali, S. H., Hansmann, G., Rose, C., Fernandez-Gonzalez, A., Scheid, A., Mitsialis, S. A., & Kourembanas, S. (2014). The Sugen 5416/hypoxia mouse model of pulmonary hypertension revisited: long-term follow-up. *Pulmonary Circulation*, *4*(4), 619–29. https://doi.org/10.1086/678508

Vogel, J., Kiessling, I., Heinicke, K., Stallmach, T., Ossent, P., Vogel, O., … Gassmann, M. (2003). Transgenic mice overexpressing erythropoietin adapt to excessive erythrocytosis by regulating blood viscosity. *Blood*, *102*(6), 2278–2284. https://doi.org/10.1182/blood-2003-01-0283

Wan, Y.-Z. Z., Gao, P., Zhou, S., Zhang, Z.-Q. Q., Hao, D.-L. L., Lian, L.-S. S., … Liu, D.-P. P. (2014). SIRT1-mediated epigenetic downregulation of plasminogen activator inhibitor-1 prevents vascular endothelial replicative senescence. *Aging Cell*, *13*(5), 890–899. https://doi.org/10.1111/acel.12247

Wang, S., Zeng, H., Xie, X.-J., Tao, Y.-K., He, X., Roman, R. J., … Chen, J.-X. (2016). Loss of prolyl hydroxylase domain protein 2 in vascular endothelium increases pericyte coverage and promotes pulmonary arterial remodeling. *Oncotarget*, *7*(37),

58848–58861. https://doi.org/10.18632/oncotarget.11585
Wapenaar, H., & Dekker, F. J. (2016). Histone acetyltransferases: challenges in targeting bi-substrate enzymes. *Clinical Epigenetics*, *8*(1), 59. https://doi.org/10.1186/s13148-016-0225-2
Waypa, G. B., Osborne, S. W., Marks, J. D., Berkelhamer, S. K., Kondapalli, J., & Schumacker, P. T. (2013). Sirtuin 3 deficiency does not augment hypoxia-induced pulmonary hypertension. *Am J Respir Cell Mol Biol*, *49*(6), 885–891. https://doi.org/10.1165/rcmb.2013-0191OC
Wedgwood, S., Dettman, R. W., & Black, S. M. (2001). ET-1 stimulates pulmonary arterial smooth muscle cell proliferation via induction of reactive oxygen species. *American Journal of Physiology. Lung Cellular and Molecular Physiology*, *281*(5), L1058-67. Retrieved from http://www.ncbi.nlm.nih.gov/entrez/query.fcgi?cmd=Retrieve&db=PubMed&dopt=Citation&list_uids=11597896
Weisel, F. C., Kloepping, C., Pichl, A., Sydykov, A., Kojonazarov, B., Wilhelm, J., … Kwapiszewska, G. (2014). Impact of S-adenosylmethionine decarboxylase 1 on pulmonary vascular remodeling. *Circulation*, *129*(14), 1510–1523. https://doi.org/10.1161/CIRCULATIONAHA.113.006402
Weissmann, N., Manz, D., Buchspies, D., Keller, S., Mehling, T., Voswinckel, R., … Grimminger, F. (2005). Congenital erythropoietin over-expression causes "anti-pulmonary hypertensive" structural and functional changes in mice, both in normoxia and hypoxia. *Thrombosis and Haemostasis*, *94*(3), 630–8. https://doi.org/10.1160/TH05-02-0104
Wharton, J., Strange, J. W., Moller, G. M., Growcott, E. J., Ren, X., Franklyn, A. P., … Wilkins, M. R. (2005). Antiproliferative effects of phosphodiesterase type 5 inhibition in human pulmonary artery cells. *Am J Respir Crit Care Med*, *172*(1), 105–113. https://doi.org/10.1164/rccm.200411-1587OC
Wilson, D. W., Segall, H. J., Pan, L. C., & Dunston, S. K. (1989). Progressive inflammatory and structural changes in the pulmonary vasculature of monocrotaline-treated rats. *Microvascular Research*, *38*(1), 57–80. Retrieved from http://www.ncbi.nlm.nih.gov/pubmed/2503687
Wood, J. G., Rogina, B., Lavu, S., Howitz, K., Helfand, S. L., Tatar, M., & Sinclair, D. (2004). Sirtuin activators mimic caloric restriction and delay ageing in metazoans. *Nature*, *430*(7000), 686–9. https://doi.org/10.1038/nature02789
Wu, Z., Liu, M. C., Liang, M., & Fu, J. (2012). Sirt1 protects against thrombomodulin down-regulation and lung coagulation after particulate matter exposure. *Blood*, *119*(10), 2422–2429. https://doi.org/10.1182/blood-2011-04-350413
Xu, D., Li, Y., Zhang, B., Wang, Y., Liu, Y., Luo, Y., … Li, Z. (2016). Resveratrol alleviate hypoxic pulmonary hypertension via anti-inflammation and anti-oxidant pathways in rats. *International Journal of Medical Sciences*, *13*(12), 942–954. https://doi.org/10.7150/ijms.16810
Xu, F., Burk, D., Gao, Z., Yin, J., Zhang, X., Weng, J., & Ye, J. (2012). Angiogenic deficiency and adipose tissue dysfunction are associated with macrophage malfunction in SIRT1-/- mice. *Endocrinology*, *153*(4), 1706–16. https://doi.org/10.1210/en.2011-1667
Xu, W., Koeck, T., Lara, A. R., Neumann, D., DiFilippo, F. P., Koo, M., … Erzurum, S.

C. (2007). Alterations of cellular bioenergetics in pulmonary artery endothelial cells. *Proc Natl Acad Sci U S A*, *104*(4), 1342–1347. https://doi.org/10.1073/pnas.0605080104

Yamashita, T., Ohneda, O., Nagano, M., Iemitsu, M., Makino, Y., Tanaka, H., … Yamamoto, M. (2008). Abnormal heart development and lung remodeling in mice lacking the hypoxia-inducible factor-related basic helix-loop-helix PAS protein NEPAS. *Mol Cell Biol*, *28*(4), 1285–1297. https://doi.org/10.1128/MCB.01332-07

Yamazaki, Y. (2009). Treatment with SRT a SIRT1 Liver with Reduced Expression of Lipogenic Enzymes in Am Endocrinol. *Metab 297*, *1720 SRC*, E1179–E1186.

Yang, D.-L., Zhang, H.-G., Xu, Y.-L., Gao, Y.-H., Yang, X.-J., Hao, X.-Q., & Li, X.-H. (2010). Resveratrol inhibits right ventricular hypertrophy induced by monocrotaline in rats. *Clinical and Experimental Pharmacology & Physiology*, *37*(2), 150–5. https://doi.org/10.1111/j.1440-1681.2009.05231.x

Yang, S. R. (2007). Sirtuin regulates cigarette smoke induced pro-inflammatory mediators release via RelA/p65 NF-{kappa}B in macrophages in vitro and in rat lungs in vivo. *Am Lung Cell Mol Physiol*, *292 SRC*-, L567–L576.

Yao, H., Chung, S., Hwang, J., Rajendrasozhan, S., Sundar, I. K., Dean, D. A., … Rahman, I. (2012). SIRT1 protects against emphysema via FOXO3-mediated reduction of premature senescence in mice. *The Journal of Clinical Investigation*, *122*(6), 2032–45. https://doi.org/10.1172/JCI60132

Yao, H., Sundar, I. K., Ahmad, T., Lerner, C., Gerloff, J., Friedman, A. E., … Rahman, I. (2014). SIRT1 protects against cigarette smoke-induced lung oxidative stress via a FOXO3-dependent mechanism. *American Journal of Physiology. Lung Cellular and Molecular Physiology*, *306*(9), L816-28. https://doi.org/10.1152/ajplung.00323.2013

Yeager, M. E., Golpon, H. A., Voelkel, N. F., & Tuder, R. M. (2002). Microsatellite mutational analysis of endothelial cells within plexiform lesions from patients with familial, pediatric, and sporadic pulmonary hypertension. *Chest*, *121*(3 Suppl), 61S. Retrieved from http://www.ncbi.nlm.nih.gov/entrez/query.fcgi?cmd=Retrieve&db=PubMed&dopt=Citation&list_uids=11893687

Yoon, H., Shin, S. H., Shin, D. H., Chun, Y. S., & Park, J. W. (2014). Differential roles of Sirt1 in HIF-1alpha and HIF-2alpha mediated hypoxic responses. *Biochem Biophys Res Commun*, *444*(1), 36–43. https://doi.org/10.1016/j.bbrc.2014.01.001

Yoshida, M., Kudo, N., Kosono, S., & Ito, A. (2017). Chemical and structural biology of protein lysine deacetylases. *Proceedings of the Japan Academy. Series B, Physical and Biological Sciences*, *93*(5), 297–321. https://doi.org/10.2183/pjab.93.019

Yu, A. Y., Shimoda, L. A., Iyer, N. V, Huso, D. L., Sun, X., McWilliams, R., … Semenza, G. L. (1999). Impaired physiological responses to chronic hypoxia in mice partially deficient for hypoxia-inducible factor 1alpha. *J Clin Invest*, *103*(5), 691–696. https://doi.org/10.1172/JCI5912

Yu, L., Tu, Y., Jia, X., Fang, K., Liu, L., Wan, L., … Fan, Y. (2017). Resveratrol Protects Against Pulmonary Arterial Hypertension in Rats via Activation of Silent Information Regulator 1. *Cellular Physiology and Biochemistry : International Journal of Experimental Cellular Physiology, Biochemistry, and Pharmacology*, *42*(1), 55–67. https://doi.org/10.1159/000477115

Zhang, P., Yao, Q., Lu, L., Li, Y., Chen, P.-J., & Duan, C. (2014). Hypoxia-inducible

factor 3 is an oxygen-dependent transcription activator and regulates a distinct transcriptional response to hypoxia. *Cell Reports*, *6*(6), 1110–1121. https://doi.org/10.1016/j.celrep.2014.02.011

Zhang, Q. J., Wang, Z., Chen, H. Z., Zhou, S., Zheng, W., Liu, G., … Liang, C. C. (2008). Endothelium-specific overexpression of class III deacetylase SIRT1 decreases atherosclerosis in apolipoprotein E-deficient mice. *Cardiovascular Research*, *80*(2), 191–199. https://doi.org/10.1093/cvr/cvn224

Zhang, Y., Zhang, M., Dong, H., Yong, S., Li, X., Olashaw, N., … Zhang, X. (2009). Deacetylation of cortactin by SIRT1 promotes cell migration. *Oncogene*, *28*(3), 445–60. https://doi.org/10.1038/onc.2008.388

Zhao, L., Chen, C.-N., Hajji, N., Oliver, E., Cotroneo, E., Wharton, J., … Wilkins, M. R. (2012). Histone deacetylation inhibition in pulmonary hypertension: therapeutic potential of valproic acid and suberoylanilide hydroxamic acid. *Circulation*, *126*(4), 455–67. https://doi.org/10.1161/CIRCULATIONAHA.112.103176

Zhao, X., Allison, D., Condon, B., Zhang, F., Gheyi, T., Zhang, A., … Luz, J. G. (2013). The 2.5 Å crystal structure of the SIRT1 catalytic domain bound to nicotinamide adenine dinucleotide (NAD+) and an indole (EX527 analogue) reveals a novel mechanism of histone deacetylase inhibition. *Journal of Medicinal Chemistry*, *56*(3), 963–9. https://doi.org/10.1021/jm301431y

Zhao, Y. D., Courtman, D. W., Ng, D. S., Robb, M. J., Deng, Y. P., Trogadis, J., … Stewart, D. J. (2006). Microvascular regeneration in established pulmonary hypertension by angiogenic gene transfer. *American Journal of Respiratory Cell and Molecular Biology*, *35*(2), 182–9. https://doi.org/10.1165/rcmb.2005-0115OC

Zhong, L., D'Urso, A., Toiber, D., Sebastian, C., Henry, R. E., Vadysirisack, D. D., … Mostoslavsky, R. (2010). The Histone Deacetylase Sirt6 Regulates Glucose Homeostasis via Hif1α. *Cell*, *140*(2), 280–293. https://doi.org/10.1016/j.cell.2009.12.041

Zhou, S., Li, M.-T., Jia, Y.-Y., Liu, J.-J., Wang, Q., Tian, Z., … Zeng, X.-F. (2015). Regulation of Cell Cycle Regulators by SIRT1 Contributes to Resveratrol-Mediated Prevention of Pulmonary Arterial Hypertension. *BioMed Research International*, *2015*, 762349. https://doi.org/10.1155/2015/762349

Zhou, X., Guo, X., Chen, M., Xie, C., & Jiang, J. (2018). HIF-3α Promotes Metastatic Phenotypes in Pancreatic Cancer by Transcriptional Regulation of the RhoC–ROCK1 Signaling Pathway. *Molecular Cancer Research*, *16*(1), 124–134. https://doi.org/10.1158/1541-7786.MCR-17-0256

Zurlo, G., Piquereau, J., Moulin, M., Pires Da Silva, J., Gressette, M., Ranchoux, B., … Veksler, V. (2018). Sirtuin 1 regulates pulmonary artery smooth muscle cell proliferation. *Journal of Hypertension*, 1. https://doi.org/10.1097/HJH.0000000000001676